A FRAMEWORK FOR CONCEPT VALIDATION IN DESIGN USING DIGITAL PROTOTYPING

SOHEIL ARASTEHFAR

(B.Sc. (Hons.), M.Sc. (Hons.), Shahrood University of Technology)

A THESIS SUBMITTED

FOR THE DEGREE OF DOCTOR OF PHILOSOPHY

DEPARTMENT OF MECHANICAL ENGINEERING

NATIONAL UNIVERSITY OF SINGAPORE

2015

DECLARATION

I hereby declare that this thesis is my original work and it has been written by me in its entirety. I have duly acknowledged all the sources of information which have been used in the thesis.

This thesis has also not been submitted for any degree in any university previously.

SOHEIL ARASTEHFAR

12 November 2015

ACKNOWLEDGEMENTS

It has been my honor to be under the supervision of Associate Professor Wen-Feng Lu throughout the course of my research. While knowledge is the prerequisite to being a supervisor, Associate Professor Lu has been a supervisor who is not only knowledgeable but also abounds in wisdom. I have gained a lot from him, and I want to express my most sincere gratitude to him. His professional and constructive guidance has been of great help to me during my study. His depth of knowledge, insight, and untiring work ethic has been and will continue to be a source of inspiration to me. Despite his busy schedule, he always has time for his students.

Additional gratitude is offered to Associate Professor Ying Liu, my former supervisor, for his great advices, encouragements, and supports. He has been of immense help in forming a sound and solid basis of this research. His intensive discussions and many valuable suggestions throughout these years have been intense light in the darkness. I also thank him for all the lunch gathering and the social life we, including my wife and teammates, had with him. Moreover, I thank him for his advice on attending ICED13 in Korea, which was a great experience.

Very special thanks is due to my friends and colleagues in the research students and assistants' room, especially Mrs. Athena Jalalian, Mrs. Lan Lijun, and Miss Hu Huicong for their encouragement and supports during these years and in the group meetings. I also want to thank all of Advanced Manufacturing Laboratory staffs at NUS, especially Mr. Tan Choon Huat, who took time out of their busy schedules to provide me with the hardware and software required for my studies.

I especially thank my mother, father, and siblings. My hard-working parents have sacrificed their lives for my siblings and me, and provided unconditional love and care. I would not have made it this far without them.

Last, but most importantly, I wish to thank my best friend, soul mate, and wife Athena Jalalian for her patience, assistance, support, and faith in me. Athena has been a true and great supporter and has unconditionally stood by me during the good and bad times. She has been non-judgmental of me and instrumental in instilling confidence.

I could not have completed my research without the support of all these wonderful people.

Table of Contents

Summary

Validation of product concepts to fulfill user needs is of great importance to develop a successful product in a market. To develop a valid concept, users could be involved at conceptual design to give feedback on the produced design solutions. Digital prototyping and quantitative feedback have received a great attention for concept validation to render design solutions and collect user feedback on the solutions respectively. In general, users have been involved at late conceptual design; (1) when designers are dealing with development of a product concept from a few design solutions (e.g. after concept screening), and (2) when refining technical specification values of the developed product concept. Involving users at early conceptual design can help to generate a space of design solutions complying better with the user needs, and select the best solutions from the space for development of a better product concept. However, such early involvement of users is considerably lacking in the existing literature. One of the major issues relating to involving users at early conceptual design is user fatigue when users give quantitative feedback on a typically big design space. To prevent fatigue, it is required to reduce the number of solutions represented to users. This reduction could cause difficulty in identifying the best target specifications and design solutions. The other issue is that users can also encounter fatigue when reviewing design solutions through interactions with digital prototypes. The fatigue negatively affects users' feedback.

The objective of this thesis was to develop a framework for concept validation by using digital prototyping and quantitative feedback. The framework aimed to identify the best product concept by using user feedback on specification values and design solutions at early conceptual design. The framework involves users at two stages (1) before concept generation to identify the best target specifications from product design specification so as to produce better design solutions, and (2) at concept selection to identify the best solutions to develop a product concept complying better with user needs. For these two stages, two methodologies, namely specification solicitation and concept selection, were devised to deal with the large number of specification values and the big space of design solutions respectively. The methodologies utilized adaptive sampling and statistical hypothesis test. Adaptive sampling prevents user fatigue when giving feedback by effectively reducing the number of samples of specification values and solutions. The hypothesis test considers the variance of user feedback on the reduced samples as well as the mean,

to resolve the difficulty in identifying the best target specifications and solutions. Specification solicitation has not been done on large number of specifications. We showed that our methodology for specification solicitation could identify the targets for a large number of specifications, while the existing methods have not gone beyond two specifications because of user fatigue. The methodology for concept selection is based on a novel approach that allows users to produce a design solution within the boundary of the space of design solutions. It was shown that the methodology outperformed a recently revealed interactive evolutionary method in terms of identifying the best solutions and preventing user fatigue. To implement the methodologies, a tool was created. The tool communicates digital prototypes to users in a new interactive way in order to help users estimate the values of specifications correctly and quickly. A novel method was developed to build hand-prototype natural interactions in virtual environment. We showed that fatigue could be effectively reduced. Besides, users could understand design solutions correctly and quickly so as to collect helpful feedback. Overall, conclusive evidence was provided that the concept validation (based on the developed framework, methodologies, and tools) can deal with a large number of specifications and solutions, and yields the product concepts that effectively fulfill user needs. To validate the proposed framework and methodologies, hand-held electronic consumer products, such as smartphones were considered for the case studies with the focus on their form, size, weight, and talk-time.

List of Tables

List of Figures

List of Symbols

✓	null hypothesis is rejected
×	failed to reject null hypothesis
α	confidence level
β	angle measured for the bisector test
θ	joint variables
$\Delta\ \varepsilon\ \delta$	real numbers greater than 0
Δt	short period of time
d	value reflecting the dissimilarity between the values in **V**
D	distance between the visualized and estimated values in **V**
DT	demonstration time in an assessment stage
E	error
f	function mapping a solution to a score
f_y	function mapping a value of a metric to a score
$f_{\mathbf{Y}}$	function mapping a metric to a weight
f_{yy}	function mapping a value of a 2-combination to a score
$f_{\mathbf{YY}}$	function mapping a 2-combination of metrics to a weight
F	fingertips
F	function mapping user estimates to a score
F_{DC}	functions mapping user estimates to a score on degree-of-correctness
F_{HV}	functions mapping user estimates to a score on handling-of-variations
F_{TE}	functions mapping user estimates to a score on time-to-estimate
H_0	null hypothesis
L	length
m	total number of metrics
M	mean value of the scores of all users
M_{DC}	mean value of the scores of all users on degree-of-correctness
M_{HV}	mean value of the scores of all users on handling-of-variations
M_{TE}	mean value of the scores of all users on time-to-estimate
n	total number of values assessed by a user
N	number of solutions considered for handling-of-variations
Ω	weight of product
p	parameter of design solutions
P	palm
PDS	product design specification

q	quality
q_u	quality determined by a user
$\overline{q}_u$	mean of the quality determined by all users
Q	set of values for the quality
$\mathbf{Q}_u$	set of integer values for the quality
r	assessment stage number
R^2	coefficient of determination
RT	representation time in an assessment stage
s	solution
S	set of all solutions
SD	standard deviation
SDS	space of design solutions
SP	specification values of product
SV	set of v
t	time
T	thumb
Tr	effectiveness of DCC
$\mathbf{Tr}_{DC}$	effectiveness of DCC on degree-of-correctness
$\mathbf{Tr}_{HV}$	effectiveness of DCC on handling-of-variations
$\mathbf{Tr}_{TE}$	effectiveness of DCC on time-to-estimate
u	user
v	value assigned a score by a user
V	set of values considered for capturing user estimates
VV	Cartesian product of two **SV**
w	weight allocated to a metric
W	wrist
ww	weight allocated a 2-combination of metrics
w_{DC}	weights showing the relative importance of degree-of-correctness
w_{HV}	weights showing the relative importance of handling-of-variations
w_{TE}	weights showing the relative importance of time-to-estimate
y	value of a metric
Y	set of all metrics
yy	value of a 2-combination
YY	set of all 2-combinations of the metrics

Chapter 1 Introduction

1.1 Background

Early phase (or concept development phase [1]) of product design and development maps user needs into a product concept. This phase typically contains several interrelated processes that can be ordered as user need identification, setting target specifications, and conceptual design. Need identification gathers users' needs of the product (i.e. voice-of-customer) that are generally subjective, vague, ambiguous, and incomplete [2]. Setting target specification translates users' need statements into technical specifications[1] spelling out in precise, measurable detail what the product has to do. Conceptual design maps the technical specifications to product concepts approximately describing the appearance and function of the product. In conceptual design, designers decompose the product into features, produce design solutions for each feature, synthesize the solutions to generate a number of product concepts, and select a product concept (or a few ones) for further development [3]. Then, the final specifications of the selected product concept are established.

Validation of the product concept and its technical specification values to fulfill user needs is of great importance to develop a successful product in the market [4-7]. The validation determines the degree to which a design solution and its specification values fulfill the user needs [8]. One factor that affects the validation is the level of designers' understanding of the user needs [9, 10]. The understanding is surrounded with uncertainty caused by the users' need statements [11-13]. The statements are generally subjective, vague, ambiguous, and incomplete since the users may not know or may not be able to describe what they want exactly [14, 15]. It is important that the user needs are clarified to reduce the uncertainty so as to precisely determine the degree of fulfilling user needs for the validation. User feedback on design solutions and the specification values helps to provide information concerning clarification of the user needs [16, 17] because the feedback reflects the needs [18, 19]. Therefore, user feedback plays critical roles in the validation. In this thesis, the degree to which a design solution or a specification value fulfills the user needs is called its quality.

[1] Some literature uses the terms 'product specifications', 'product requirements', 'product characteristics', or 'engineering characteristics'.

1.2 Motivation

Digital prototyping and quantitative feedback has motivated researchers to involve users at different stages of conceptual design, e.g. concept scoring and setting final specifications, so as to perform the validation [19, 20]. Digital prototypes (DPs), as a form of communication media, render the technical specification values (e.g. color and size) and parameters of the design solutions (e.g. parameters defined for the form). DP effectively helps users understand the solutions and estimate the specification values [21-24]. It is effective because users can sense the solutions through vision, and vision in cooperation with their memory helps them understand the solutions [25]. In addition, DPs offer a degree of flexibility to render the changes in the specification values and the parameters of the design solutions. Therefore, users can understand several solutions correctly and quickly. This results in useful user feedback for determining the quality of the solutions [26, 27]. Moreover, DPs are typically low cost, and they are produced in a short period of time [28, 29]. Quantitative feedback is the answer to which, how many, or how often questions. It is easy-to-collect and easy-to-interpret. Besides, mathematical tools can be employed to analyze the feedback to determine the quality. Therefore, in this thesis, we adopt digital prototyping and quantitative feedback for the validation.

Designers have involved users in the validation process to collect the user feedback on the design solutions so as to determine the quality of the solutions [11, 30]. In general, users have been involved at late conceptual design; (1) when the designers are dealing with development of the best product concept from a few design solutions (e.g. after concept screening) [31, 32], and (2) when refining technical specification values of the developed product concept to better fulfill user needs [33]. The product concept and its specification values are chosen from the space of design solutions developed at concept generation. The input and output of concept generation are validated without involving users and based on the designers' understanding surrounded with the uncertainty [11]. User feedback at early conceptual design helps to (1) identify the best technical specifications to develop the space of better design solutions and (2) select the best solutions from the space to develop a better product concept. However, involving users at early conceptual design is considerably lacking in the existing literature.

User involvement at early conceptual design raises two major issues. One of the issues is user fatigue when users give quantitative feedback (1) on the large number of technical specifications before concept generation and (2) on the big space of generated design solutions [34]. User fatigue can stop user involvement, and even if users continue, it can affect the user's feedback [18]. To prevent fatigue, it is required to reduce the number of specifications and solutions represented to users [35]. This reduction could cause difficulty in identifying the best targets from the product design specification and the best solutions from the space of design solutions. Thus, we need to choose a number of specification values and solutions to achieve a balance between reducing the difficulty and preventing user fatigue. The other issue relates to analysis of the quantitative feedback. In previous studies, the mean of the users' quantitative feedback was chosen as the degree to which a specification value or a design solution fulfills the needs [36]. However, uncertainty on the mean has not been taken into account [35]. Therefore, there is a need to devise a methodology for each user involvement stage (i.e. before concept generation and at concept selection) to determine the best targets and solutions while preventing the fatigue and considering the uncertainty on the mean of quantitative feedback.

In early conceptual design, users also encounter fatigue when they review design solutions and specification values through interactions with DPs. The fatigue is encountered especially when users face difficulty in understanding design solutions and estimating specification values. One factor that causes this difficulty is the dissimilarity of user-DP interactions from the natural interactions (e.g. grasping and manipulation of physical objects) [37, 38]. Reducing the dissimilarity is essential to ease the understanding and estimating processes for users so as to prevent fatigue [2]. In this regard, hand-DP interactions, especially grasping and manipulating DPs in 3D space, play critical roles in easing the processes [39]. In design review process, to build natural hand-DP interactions, vision-based tools have come into interests because they are low cost, user-friendly, and nonintrusive [40]. Additionally, these tools obviate the need for wearing the devices that often inhibit the hand motions and distract users [41]. However, the existing vision-based tools are far from implementing real-time grasping and manipulation in virtual environment. Hence, to prevent fatigue in design review process, there is a need to create a tool for real-time virtual grasping and manipulation.

1.3 Objectives

The objective of this thesis is to develop a framework for concept validation by using digital prototyping and quantitative feedback. The framework aims to identify the best product concept by using user feedback on the specification values and design solutions at early conceptual design. The framework involves users at early conceptual design. It focuses on two critical stages of conceptual design for the involvement; before concept generation and at concept selection. The framework collects user feedback on the values of the technical specifications before concept generation to identify the best target values from product design specification. The framework identifies the best solutions from the space of generated design solutions by using user feedback at concept selection.

For the two stages in the framework, two methodologies, namely specification solicitation and concept selection, is devised to deal with the large number of specification values and the big space of design solutions respectively. Specification solicitation has not been done on large number of specifications. Concept selection is based on a novel approach that allows users to produce a design solution within the boundary of the space of design solutions. The methodologies should prevent user fatigue when giving feedback by effectively reducing the number of specification values and solutions. To do this, adaptive sampling method is used. Besides, the methodologies should reduce the uncertainty on the mean of user quantitative feedback to identify the best target specifications and solutions. To reduce the uncertainty, the variance of the feedback is considered by utilizing statistical hypothesis test.

To implement the methodologies, a tool was created. The tool communicates digital prototypes to users in a new interactive way in order to help users estimate the values of specifications and design solutions correctly and quickly. A novel method is developed to build real-time virtual grasping and manipulation of DPs in 3D space. The tool should help users understand design solutions and estimate specification values easily to prevent user fatigue.

The proposed work of this thesis may have significant impacts for development of a quality product concept at conceptual design. The framework may identify the higher quality product concept by using user feedback on the specification values and design solutions. Before concept generation, the framework can deal with a large number of specifications to identify the best targets from the product design specification. At

concept selection, the framework may resolve the difficulty in identification of best solutions from the big space of design solutions. As another important significance, the framework can prevent user fatigue by using the developed methodologies and tools. Besides, the framework may better determine the quality of the specification values and design solutions by considering the variance and mean of the user feedback.

Hand-held electronic consumer products, such as smartphones, are considered for the case studies to validate the proposed framework and methodologies. This thesis focuses on form, size, weight, and talk-time of the smartphones. The form, size, and weight of smartphones affect the ergonomic aspects and usability because smartphones are hand-held [42, 43]. They also influence the cognitive aspects of user experience of smartphones. For example, the ratio between the width and height is the factor that can elicit the aesthetic aspects of the product experience [44, 45]. In addition, the depth and weight are the other factors that can elicit the experience of meaning such as luxury and professional [46]. The size and weight also affect the battery capacity and some other technical aspects of smartphone design such as the screen size [47]. Talk-time is the other technical specification that influences users' purchasing decisions. In the last few years, it has been observed that users are carrying power banks, which are bulky, to have extra battery-life [48]. Therefore, identification of the best form, size, weight, and talk-time can be a key task to increase the chance of success of a smartphone in the market. In this thesis, the form and size are communicated to users using digital prototyping. Weight and talk-time are communicated through interviews. A possible complementary alternative for communication of weight is the use of haptic devices to render a vertical downward force equal to the weight. In this case, users experience the weight of a design and estimate the weight more correctly. Feeling of the weight helps users consider the weight more effectively when interacting with a design solution. This leads to collection of more helpful feedback from users.

1.4 Organization

A comprehensive literature review for the validation through digital prototyping and quantitative feedback is given in Chapter 2. Chapter 3 introduces the framework for concept validation. The term 'concept validation' is defined. Three critical steps for performing the validation process are identified. The steps are the representation and

communication of the design solutions and specifications to users, the collection and analysis of the user feedback on the represented solutions and specification values, and determining the quality of the solutions and values for the validation. Three critical validation tasks at conceptual design are identified and explained. Each task specifies when, why, and how the validation is undergone. The rest of the content of this thesis can be categorized into three parts. The first part, Chapter 4 and Chapter 5, discusses the validation steps. Chapter 4 proposes a methodology to build an effective design concept communication to users by using DPs. Chapter 5 describes the collection of user feedback and introduces a method to determine the quality by considering the mean and variance of the users' quantitative feedback. The second part, Chapter 6 and Chapter 7, introduces the methodologies for implementation of the validation tasks. The third part, Chapter 8 and Chapter 9, proposes the developed tool. Chapter 10 concludes the thesis, identifies the limitations of the work, and offers recommendations for future work.

Chapter 2 Literature review

Digital prototyping and quantitative feedback has motivated researchers to involve users at different stages of conceptual design, including concept selection and setting final specifications, so as to perform the validation. For example, Artacho et al. [33] adopted digital prototyping to render the forms of a loudspeaker at setting final specifications, and collected user feedback by using scoring. They showed that the user interactions with many forms lead to helpful feedback for identification of a higher quality form. Such studies can also be helpful in the early conceptual design. However, they are significantly limited in the existing literature [11].

This chapter reviews the studies used digital prototyping and quantitative feedback to involve users in the validation at conceptual design. It is categorized based on the steps of the validation process. The first step is to communicate design solutions to users. In this step, the level of the user understanding of the solutions through interaction with the DPs and the representation of the solutions to users are two major issues. The studies on resolving the former issue are reviewed in Section 2.1. The latter issue is critical because the number of the solutions is typically large and a user may not be able to give feedback on all of them [36]. IEC and sampling are two frequently employed approaches to the representation. They are comprehensively reviewed in Section 2.2. The second step of the validation process is to collect the users' quantitative feedback. Several types of quantitative feedback (e.g. pairwise comparison, ranking, and scoring) and their pros and cons are reviewed in Section 2.3. The third step is to determine the quality of the solutions by using the user quantitative feedback. Section 2.4 reviews the methods of determining the quality. In Section 2.5, we review the physical characteristics rendered to communicate the design solutions to users by using digital prototyping.

2.1 Communication of design solutions to users by using digital prototypes

DPs have been utilized to visualize a realistic 3D conceptual embodiment of design solutions by rendering some of the important physical characteristics (e.g. size, color, and texture) [5, 49]. One aspect of user understanding of the design solutions depends on how well users can estimate the values of the characteristics through interactions with DPs. The trend towards enhancing the user estimates suggests improving the

ability of DPs to render the characteristics [8, 50]. For this end, two criteria, fidelity [51] and flexibility [52], were developed to assess the ability of DPs.

The fidelity refers to the degree to which the rendered physical characteristics are realistic [53]. Virzi *et al*. [51] and Sauer *et al*. [53] proposed four dimensions to evaluate fidelity in terms of appearance and function. The dimensions (breadth of functions, depth of functions, physical similarity, and similarity of interaction) specify the degree to which a prototype of a physical object looks and works like that object. Fontana et al. [54] developed a high-fidelity DP of fabrics for representation of apparels so as to enhance user estimates of the appearance and softness of apparel designs. Gyi et al. [55] and Soderman [56] empirically studied the effects of the level of fidelity, and showed that high-fidelity DP can lead to better user estimates.

The flexibility is the degree to which a prototype can be changed in order to render different values of the physical characteristics [27]. For the validation, various studies [57, 58] have suggested increasing the level of flexibility of DPs to render more values of the characteristics [52, 56, 59]. Barbieri et al. [60] developed a flexible DP to represent possible changes in the interface of a washing machine (e.g. the position of the buttons and knobs) so as to enhance user estimates of the possible configurations of the interface. Zhang et al. [27] and Ford and Sobek [26] demonstrated that flexible prototypes can help designers to predict user perception better and quicker through exploring and evaluating more values of the physical characteristics.

According to the abovementioned benefits of the high fidelity and flexible DPs, a great deal of studies has adopted them for the communication of physical characteristics of the design solutions. Ren and Papalambros [18] and Poirson et al. [20] represented the appearance of a car and a wine glass respectively, and rendered their 3D geometrical form on a solid white background. Kim and Lee [61] developed a comprehensive digital model for the color to represent the appearance of digital hand-held products with different colors. They put each design on three different backgrounds, which were scenes of urban, and showed that user estimates of the color can be different for different backgrounds. As such, it may be concluded that the background can affect user estimates of color. Orzechowski et al. [62], through a study on the non-interactive communications of physical characteristics, found that the interactivity have no significant effect on user estimates of the values of the characteristics. Tovares et al. [19] also studied the effects of interactive and non-interactive communications. They asked users to estimate the geometrical form of a

represented mug. They also brought the form to users by using a DP in two different ways: non-interactive way and interactive way in which the users could explore the form (e.g. the diameter of the outer edge of the mug) in virtual environment by manipulating the DP through gesture-based commands. They compared the results of the studies with the DP and the real mug by using statistical hypothesis tests, and demonstrated that the interactive way of using a DP is superior to the non-interactive one. Artacho et al. [37] conducted similar study with a DP of a loudspeaker. They also found that interactive ways outperform the non-interactive ones. Consequently, apart from the ability of DPs, the way of using them is one of the factors affecting user estimates.

Overall, there is a need to study 'how to use a DP to help users estimate the values of the physical characteristics?' [46]. However, little attention has been given to the research into addressing the question. In our effort to address the question, we propose a methodology for evaluating the effectiveness of communication of physical characteristics by using DPs in Chapter 4. The effectiveness can be used to evaluate and compare the different ways of using a DP in order to select the effective combination of the background and input/output devices for the communication.

2.2 Representation of design solutions to users

Representing all the design solutions to users may be difficult because of user fatigue when collecting their feedback [36]. Poirson et al. [20] parameterized the form of a car dashboard by seven parameters with three values, and this resulted in 3^7=2187 solutions. As is clear, users can encounter fatigue when giving feedback on 2187 solutions. Two approaches have been proposed to represent the produced solutions to users; interactive evolutionary computation (IEC) [63, 64] and sampling [35].

IEC introduces a user in a loop to identify a high quality design solution for him/her [18]. In a loop, a number of solutions are chosen based on the user's feedback on the solutions in the previous loops. IEC, after several loops, may converge to a fitness function approximating the quality of the solutions [65, 66]. Poirson et al. [20], using IEC, searched 2187 solutions of the car dashboard for the French carmaker Renault to identify a quality dashboard. At the end, the algorithm converged towards a dashboard with better typology. IEC can identify a fitness function for a user at a time. After identifying the fitness function for all the users, it aggregates them to define a function estimating the quality of the design solutions. IEC typically requires

users to give feedback on a large number of solutions, which can cause user fatigue affecting the convergence of the fitness function [18, 34]. Another issue affecting the convergence is that the user feedback are typically intransitive (e.g. a user prefers solution s_1 to s_2, s_2 to s_3, and s_3 to s_1, i.e. $s_1 > s_2 > s_3 > s_1$) and inconsistent (e.g. a user strongly prefers s_1 to s_2 and s_2 to s_3, but he/she slightly prefers s_1 to s_3) [30]. Such properties of the user feedback introduce noise to the identification of the fitness function [35]. Overall, IEC suffers from several issues relating to the convergence of the fitness function.

In the sampling approach, the space of design solutions is sampled and the samples are represented to users. Kelly et al. [36] parameterized the solutions for the shape of a cola bottle to two parameters. They sampled 25 solutions (five values for each parameter) to collect user feedback. However, the number of samples grows exponentially by increasing the number of the parameters, which causes user fatigue. Besides, taking account of more than two parameters and the relationship between their values can cause user fatigue. Some studies adopted existing products as the samples. Kulok et al. [31] adopted 18 drills to elicit user preference for the drills with respect to three parameters; number of operations, price, and weight. Hsu et al. [15] used 24 available telephones to identify a quality telephone. Although these studies could deal with more than two parameters, the existing products may not be representative of the space of design solutions.

This thesis chooses sampling rather than IEC because more users give feedback on a solution. The total number of the samples is critical. Considering the typically large number of design solutions at early conceptual design, we need to grow the samples in number to be representative of the space of design solutions. From the other side, we need to reduce the number to prevent user fatigue when collecting user feedback. Therefore, there is a need to study how to sample the design solutions to collect useful user feedback for determining the quality of the solutions. To address this question, we aim to take the approach of adaptive sampling. A methodology was developed for the representation in each user involvement stage defined by the framework (Chapter 6 and Chapter 7).

2.3 Collection of user feedback on design solutions

Stewart [67] and Lim [68] discussed theoretical and empirical limitations of several types of feedback (e.g. pairwise comparison and ranking). Pairwise comparison

compares design solutions in a tournament. At each time, two solutions are compared with each other. The tournament continues until a winning solution is identified. Pairwise comparison can be easily administrated [30]. It has been widely used in the analytic hierarchy process to find relative importance of technical specifications [69] and to select a solution from the space of design solutions [70, 71]. However, pairwise comparison can cause the intransitive and inconsistent user feedback [30]. In contrast, ranking is slightly more elaborate [72, 73]. In ranking, each user ranks design solutions on an ordinal scale. However, when the number of solutions increases, ranking becomes difficult to adopt. In this case, users require taking account of several solutions at a time to sort them, and this can cause fatigue [67].

Scoring has also been used for collecting user feedback [15, 74]. Scores can be defined on the cardinal scales. The cardinal scores demonstrate the extent to which the qualities of the solutions are different. This can make decision-making easier at concept selection. To illustrate, we consider two solutions s_1 and s_2 with qualities of q and $0.9q$ and development costs of c and $0.5c$ respectively. Design group can choose one of the solutions by determining whether 10% higher quality is worth 50% higher costs. In contrast, the scores on the ordinal scales only show that the quality of s_1 is higher than s_2. Thus, they may not be as helpful as cardinal scores for the decision-makings. This thesis employs scoring on cardinal scales to collect user feedback. In previous studies, users assign a score to a solution at each time [19, 75]. This may cause intransitive or inconsistent feedback when the number of the solutions is large [30]. Two methodologies are proposed to represent the large number of specification values and design solutions to users before collection of feedback to prevent the intransitive and inconsistent feedback (Chapter 6 and Chapter 7).

2.4 Analysis of user feedback for concept validation

A represented solution is given numerical values (quantitative feedback) by a number of users. The values are bounded to a range. An important step is to allocate a value from the range to the solution as its quality. The arithmetic mean referring to the central value of the given values has generally been adopted. However, the mean may not list the solutions in order of their quality. To illustrate, the quantitative feedback of two solutions (s_1 and s_2) are shown in Table 2.1. The means show that the quality of s_2 is higher than s_1. We use paired student's *t*-test to test the hypothesis 'the

qualities of s_2 and s_1 are not equal'. The null hypothesis (H_0) stands for the equal quality. We failed to reject H_0, P-value<0.05. Therefore, the issue is that the mean value may not reflect the equality/inequality relations between the qualities of the solutions. As is shown, the mean can cause fixation with a design solution that may not have higher quality than the other solutions. Villa et al. [35] hypothesized that the variance of the feedback can be helpful to prevent the fixation. In our attempt to tackle the fixation issue, a method based on the statistical hypothesis test is proposed to include the variance in the analysis (Chapter 5).

Table 2.1 An example of user feedback and the conclusion drawn by considering the mean and variance of the feedback

solution	user feedback[1]					mean (SD[2])	results of the hypothesis test			
	u_1	u_2	u_3	u_4	u_5		df[3]	t-stat	P-value	H_0
s_1	5	10	7	6	5	6.6 (1.85)	4	-0.2325	0.8276	failed to reject
s_2	4	8	7	9	6	6.8 (1.72)				

[1] the data is adopted from the results of the case study in Section 5.2. User feedback is collected by assigning each solution a score between 1 and 10; where 10 and 1 correspond to the highest and lowest quality solutions respectively
[2] standard deviation
[3] degree-of-freedom

A mathematical relationship (f) is defined to estimate the quality of all design solutions in SDS by using the esitmated quality of the represented solutions so as to identify the highest quality solution. Depending on the type of the feedback, methods such as conjoint analysis [19, 49], vector field-based methods [30], utility function [76], and preference mapping (PREFMAP) [35, 36] have been used to identify f. Conjoint analysis is based on the notion that users try to maximize the utility of products [77]. Kelly et al. [36] and Tovares et al. [19] applied conjoint analysis to identify better geometrical forms of a cola bottle and a mug respectively. Kelly et al. [36] collected user feedback by using discrete choice analysis [78], and computed the utility of represented solutions by using logit models [79]. To form f, natural cubic splines were fitted to that utility. On the other hand, PREFMAP analysis typically uses potential existing products as samples of design solutions. Each user assigns each sample a numerical value as the feedback. Then, samples are decomposed to a space of parameters called 'stimuli space' [80]. For example, the feedback on potential smartphone products can be related to the size of smartphones. In this case,

the stimuli space is width×height×depth; where × denotes the Cartesian product. The mean of the assessments are considered as data points of the codomain (i.e. quality). PREFMAP typically fits a quadratic model to the means to define *f*. In both conjoint analysis and PREFMAP, fitting a function becomes difficult when the dimension (i.e. the number of parameters and the range of their values) of the stimuli space increases because the number of unknown coefficients of the function grows. In this case, estimation of *f* becomes very noise-sensitive [81, 82]. In Kelly's work [36], for the simple case of 2 parameters with 5 discrete values, there were 29 unknown coefficients. To reduce the sensitivity to noise, collection of user feedback on more solutions is effectively helpful [35], which may cause user fatigue.

Some other studies have utilized the approach of weighted scoring method (WSM) to define *f* [83-85]. WSM decomposes design solutions into several parameters. Each parameter is weighted to determine its relative importance in relation to the other parameters. The quality of the values of the parameter is determined and multiplied by the weight of the parameter. Then, the weighted qualities of a value of all the parameters are totaled to give *f*. Scott and Antonsson [86] recommended a modification to WSM, and used the i^{th} root of *f* to achieve better cardinality in the determined quality. Kulok et al. [31] utilized this modified WSM to identify a quality drill decomposed into three parameters. The method allocates a weight to a parameter by using the weights assigned by users, and designers give scores to the parameter values. WSM is simple and may not cause user fatigue because each user is only required to determine the level of importance of the parameters. This thesis adopts the approach of WSM to determine the quality because of its capability to reducing user fatigue. As a major limitation, WSM takes no correlation between the values of parameters into account. It assumes that the values are independent, which is not always true [87]. To address this limitation, we modify WSM to incorporate the correlations (Chapter 6).

2.5 Product characteristics rendered by using digital prototyping for concept validation

Several physical characteristics have been rendered by using digital prototyping (Figure 2.1). Some examples are form and size of loudspeaker [33], car dashboard [20], mug [19], and coffee maker [75]; form and color of digital hand-held devices

[61] and electric door lock [88]; form and texture [89]; form, size, color, and material of eyeglasses [90]; and form, size, color, material, and texture of apparels [54].

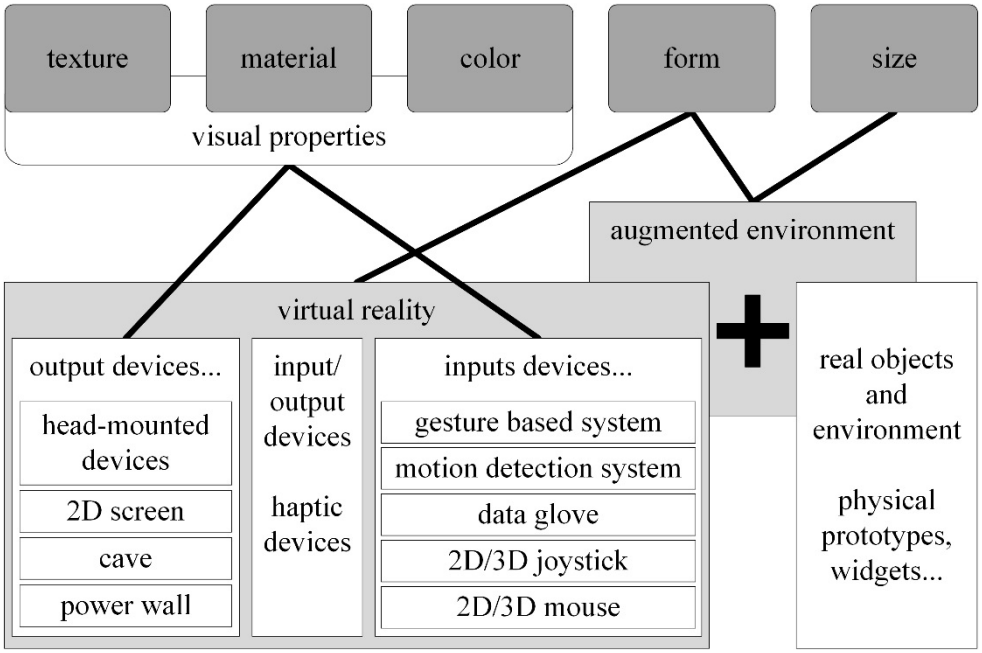

Figure 2.1 The physical characteristics and their corresponding input/output devices adopted for user-DP interactions

DPs have been projected in virtual/augmented environments. Users can interact with DPs by using variety of input/output devices. Virtual reality (VR) offers interactive and immersive virtual environment for creation, modification, manipulation (i.e. translation or rotation), and communication of design solutions. Augmented reality (AR, or mixed reality in some literature) mixes real and virtual objects and environments. In concept validation, virtual objects are augmented in real environment or virtual scenes are projected on real objects and in some cases, on physical prototypes [91]. VR and AR provide users with realistic rendering and stereo views to immerse them in the environment [29]. Huang et al. [90] developed a system augmenting DP of eyeglasses on the a user's face in a live environment. The user could change the form, color, and material of the frame. Kim and Lee [61] developed a comprehensive model for rendering color and coating materials in virtual environment. Haptic devices have been playing the role of input devices to receive users' commands and output devices to exert force on the hand. Bordegoni et al. [92] and Gironimo et al. [24] employed a haptic device for designing car dashboards. Projection of virtual environment to the users' eyes has been done through 2D screens

(e,g. PowerWall in [93]), head-mounted devices (HMD) [94, 95] such as stereoscopic devices [96] and lit eyes [97], and so on. Various 3D input devices such as mouse [94], pens [98], position sensors [99], data gloves [100-102] and several gesture-based systems [38, 97] have been offered.

Among the characteristics, form and size have received great attention [2]. HMD and data glove have been adopted to help users estimate the form and size. HMD illustrates DPs in the real perspective view and with the real size, and data gloves can build natural hand-object interactions. However, such intrusive devices are generally not user-friendly [39-41], and they are costly [103]. In comparison, vision-based methods for user-DP interactions can be better alternative because the users may not have to wear a device and the hardware requirement is typically low [104]. Besides, the users can be involved in the validation remotely. Thus, more users can be involved in the validation, since they can participate at the time and place of their convenient. Among the vision-based methods, gesture-based methods have become popular [38, 39]. However, users are required to remember the gestures. Forgetting a gesture for a command can distract the users from immersion in the environment, affecting user feedback. To render the form and size, building natural hand-object interactions in the virtual environments can be helpful because the users can interact with DPs in the way they interact with physical objects [39]. However, the existing literature considerably lacks a vision-based method for real-time natural interactions. We aim to develop a vision-based method for real-time virtual grasping and manipulation of DPs (Chapter 8 and Chapter 9).

2.6 Summary

Several studies on involving users at conceptual design by using digital prototyping and quantitative feedback were reviewed. We raised several issues relating to the design concept communication using DPs, the representation of design solutions to users, and the collection and analysis of user feedback. We also briefly outlined our approach to tackle the issues.

Chapter 3 A framework for concept validation

A framework is proposed for concept validation by using digital prototyping and quantitative feedback. The term 'concept validation' is defined, and the process of the validation is explained. The generic functionality of the validation is proposed. The size of the front face of smartphones is considered for a case study to show the capabilities of the framework to identify the highest quality specification values and design solutions.

3.1 Concept validation: what it means

Validation can be generally defined as quality assurance process [5, 8]. Several standard bodies have defined the term 'validation' (Table 3.1). Referring to Table 3.1, the validation is a process to confirm that the requirements of intended uses of a product are fulfilled through provision of objective evidence. The definitions assume that the requirements can be correctly and completely known, as emphasized by JCGM and SAE. Otherwise, the confirmation would be arguable [105-107].

Table 3.1 The definitions of the term 'validation' offered by the international and national standard bodies

standard body	definition
ISO[1] 9000	confirmation, through the provision of objective evidence, that the requirements for a specific intended use or application have been fulfilled [108].
IEEE[2]	the process of evaluating a system or component during or at the end of the development process to determine whether it satisfies specified requirements [109].
JCGM[3]	where the specified requirements are adequate for an intended use [110].
GHTF[4]	objective evidence that a process consistently produces a result or product meeting its predetermined requirements [111].
SAE[5]	validation of requirements and specific assumptions is the process of ensuring that the specified requirements are sufficiently correct and complete so that the product will meet applicable airworthiness requirements [112].

[1] International Organization for Standardization
[2] Institute of Electrical and Electronics Engineers
[3] Joint Committee for Guides in Metrology
[4] Global Harmonization Task Force
[5] Society of Automotive Engineers

In conceptual design, identification of requirements of the user needs is difficult because the available information about the needs is limited and surrounded by uncertainty. Such identification typically requires lengthy and considerable discussions between designers. Several researchers have collected user feedback on design solutions to provide evidence for the validation [16, 20, 33]. User feedback has been potentially helpful in developing a product concept complying with user needs [9, 10, 14, 17]. Therefore, we define 'concept validation' as 'the process to ensure whether a product concept complies with user needs, through provision of objective evidence from user feedback'.

The process of concept validation comprises three steps; two steps for provision of objective evidence and one step for determining the quality [2, 8]. To provide the evidence, the design solutions are represented to users, and then, their feedback on the solutions are collected and analyzed. The analyzed feedback is used to determine the quality of the solutions.

3.2 Conceptual design

Conceptual design translates specification values into a product concept in 'concept generation and selection' stages (Figure 3.1). It refines the specification values of the developed product concept at setting final specifications.

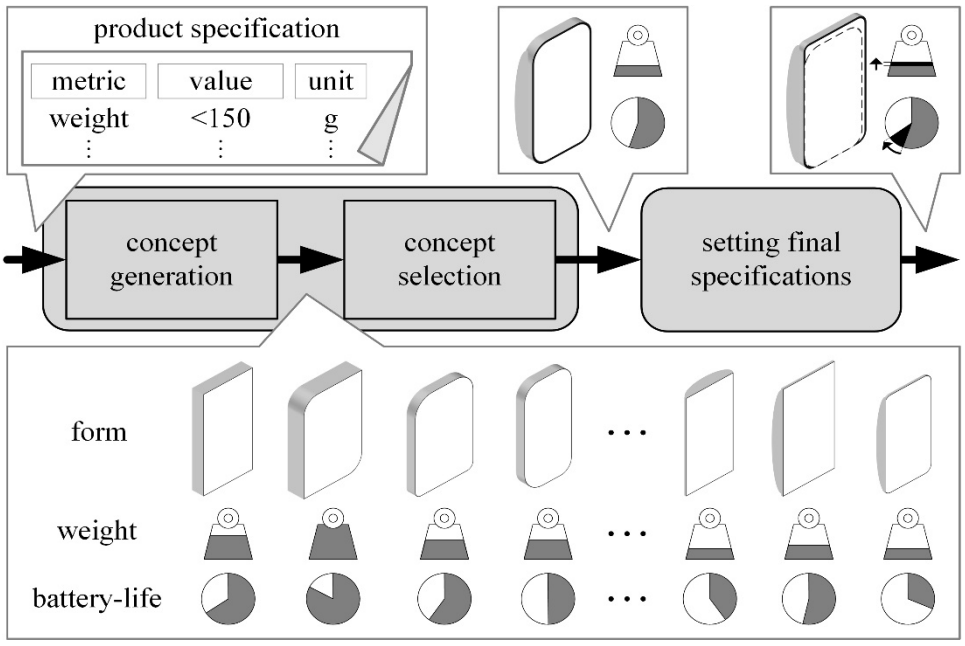

Figure 3.1 The stages at conceptual design and their inputs and outputs

At the first stage, the technical specification values are translated into a product concept represented by the forms and functions [3, 8]. During this stage, the design group deals with the specification values and the correlations between them to generate design solutions to meet user needs. Then, the group selects the highest quality design solutions. This is a critical stage because the design group needs to (1) choose the highest quality specification values for generating the solutions, (2) generate the highest quality solutions, and (3) select the highest quality ones in order to develop a more successful product concept. At setting final specifications, the specification values of the developed product concept are refined so as to improve its quality.

3.3 Concept validation: when and why?

The input to conceptual design is product design specification (PDS). PDS specifies the boundary of the technical specification values of a product [8, 113, 114]. Each specification is represented by a metric and numerical values. For example, for the specification 'talk-time is more than 10 h', 'talk-time' is the metric and 'more than 10 h' is the value defined on an interval. Target specification is the value that design group hopes to achieve, e.g. 15 h. Uncertainty surrounds the intervals and targets because of the subjective, vague, ambiguous, incomplete, and conflicting users' need statements. To reduce the uncertainty, concept validation contributes to discover a relationship between the quality of a product and its specification values (i.e. the values defined by the PDS) before starting concept generation. This is the first task of concept validation, and it is called 'specification solicitation'. Specification solicitation aims to identify the highest quality specification values and send them to concept generation so that higher quality design solutions can be produced.

Concept selection looks for the highest quality design solutions among the generated ones. The set of all the generated solutions is called space of design solutions (SDS) [115, 116]. Concept selection aims to identify the highest quality product concept from SDS. It plays critical roles in the success of a product because the selected concept defines the core of the product, including the form, function, and work flow [1, 74]. Concept validation contributes to explore SDS to identify the highest quality product concept. For this end, it decomposes SDS to a number of parameters and their values, and collects user feedback on the parameter values. This is the second task of concept validation, and it is called 'concept selection'.

3.4 Concept validation: how?

A framework is developed for concept validation to generate a good design concept from PDS at conceptual design of hand-held electronic consumer products (Figure 3.2). The framework involves users at conceptual design to use user feedback for concept validation. The framework utilizes digital prototyping to communicate design solutions to user, and quantitative feedback to collect user feedback about design solutions. Concept validation under the framework focuses on two tasks at conceptual design to map PDS to a good design concept, namely specification solicitation and concept selection. Specification solicitation takes PDS as the input and identifies the best target values for the product specifications from PDS. At concept generation, the framework draws designers' attention to translation of the best target values into design solutions. This leads to generation of a better SDS. Concept selection takes SDS as input and identifies the best design solutions from SDS for the product concept. To support the validation process, the framework focuses on two steps of the

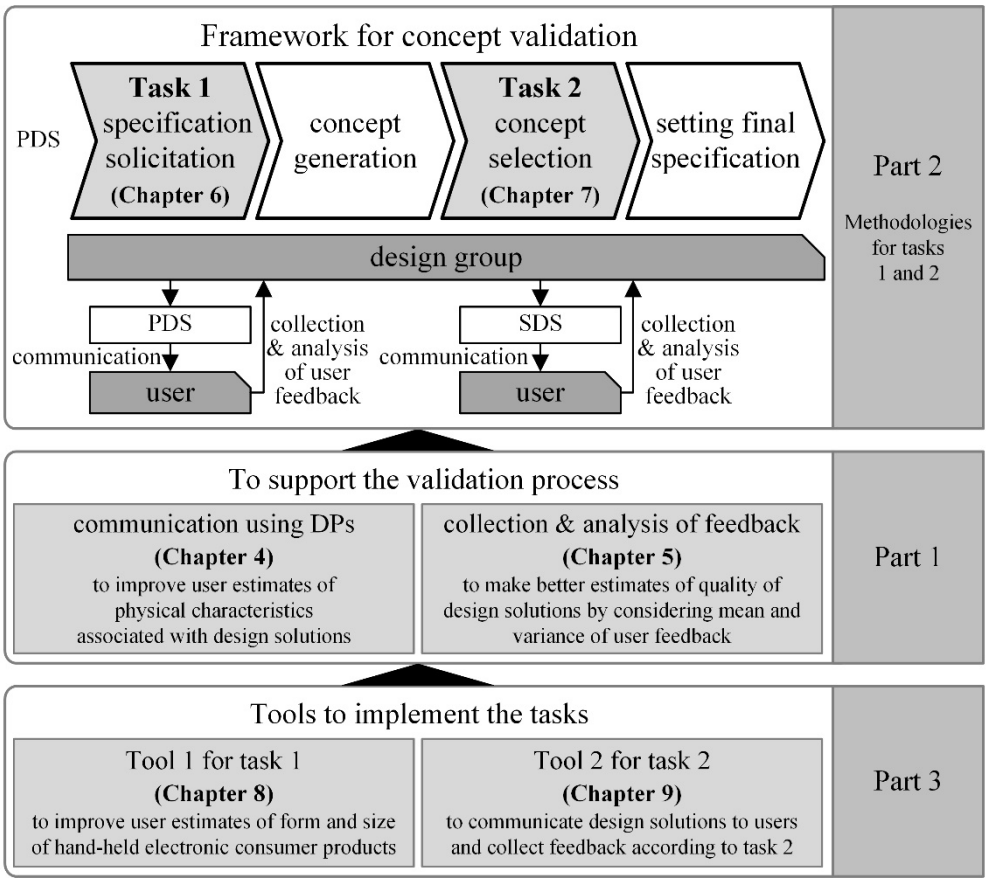

Figure 3.2 The framework for concept validation

validation, i.e. concept communication to users, and collection and analysis of user feedback. A method is devised to build an effective communication using DPs to help users understand design solutions through interactions with DPs. A process is developed to collect and analyze user feedback in order to reduce design fixation. The framework utilizes the method and process at both tasks 1 and 2 to support the validation. Two tools, based on digital prototyping and quantitative feedback, are developed to implement specification solicitation (task 1) and concept selection (task 2).

According to the framework (Figure 3.2), this thesis is categorized into three parts. In the first part, we devise a method to support the concept validation at design communication stage (Chapter 4), and develop a process at collection and analysis of user feedback (Chapter 5). In the second part, we introduce our methodologies, i.e. specification solicitation (Chapter 6) and concept selection (Chapter 7), to do tasks 1 and 2, respectively. The third part explains the development of the tools for implementing specification solicitation and concept selection in Chapter 8 and Chapter 9 respectively. The generic functionality of each part is described in the following.

The first part (Chapter 4 and Chapter 5). This part is to support the concept validation process to enhance the communication of design solutions to users by using digital prototypes, and collection and analysis of user feedback. In the validation process, at design communication, specification values and design solutions of hand-held electronic consumer products are communicated to users by rendering physical characteristics associated with the specifications and solutions. It is important that users be able to estimate the values of physical characteristics to make a good estimate of specification values and a good understanding of design solutions. Apart from the level of fidelity of a digital prototype, the way that the prototype is communicated to users is influential to users' estimates of the values of physical characteristics (for more details, please see Section 2.1). Users' good estimate of the values helps users estimate specification values better and understand design solutions better. This leads to collection of more helpful user feedback for concept validation because user feedback will be based on good estimates and understanding. Therefore, we develop a method to identify an effective way for using a prototype in a communication so that users can estimate the values of physical characteristics more correctly and quickly. This method is introduced in Chapter 4. Our framework utilizes the method (Chapter 4) to use a DP in a better way so that

users can estimate values of physical characteristics of hand-held electronic consumer products better. After making the good estimates in Chapter 4, we collect and analyze user feedback in Chapter 5.

In the validation process, after the communication, user feedback is collected and analyzed. In Section 2.3, we explained that scoring as a type of quantitative feedback is adopted for collection of user feedback in this thesis. In Section 2.4, it was shown that we might encounter design fixation when we take account of the mean values of user feedback to estimate the quality of specification values and design solutions. We developed a process to analyze the scores given by users in order to reduce the fixation in Chapter 5. The process estimates the quality by considering the variance of scores as well as the mean values of the scores. The process compares the scores of specification values and design solutions, and looks for statistical evidence to estimate their quality. Our framework utilizes this process to analyze user feedback to estimate the quality of specification values and design solutions.

Chapter 4 and Chapter 5 present our contributions to enhancement of the process of concept validation taking account of user feedback. These chapters describe how the framework builds an effective design communication with users, and how it analyzes user feedback to estimate the quality better.

The second part (Chapter 6 and Chapter 7). This part helps to produce a good design concept by involving users in the two tasks of concept validation. As described in Section 1.3, we involve users at two stages in conceptual design; before concept generation to identify the best target values for product specifications from PDS, and at concept selection to identify the best design solutions from SDS. In Section 2.2, we explained the issue ‘user fatigue’ that is encountered when PDS or SDS is large. Representation of a large PDS or SDS to users and collection of user feedback on a large number of specification values and design solutions can cause user fatigue. To reduce user fatigue, we devised two methodologies; one for PDS to involve users before concept generation (namely specification solicitation, Chapter 6), and the other for SDS to involves users at concept selection (namely concept selection, Chapter 7). These two methodologies were devised to implement our framework for concept validation using digital prototyping and quantitative feedback.

Task 1: specification solicitation. PDS consists of metrics and their values. An ordered list of single values for all metrics gives the Specification values of a Product

(SP[2]). PDS is typical big, and thus, the typical sampling, which has been used by many studies [31, 35, 36], may not be able to effectively reduce the number of samples for the representation of PDS and preventing user fatigue. Specification solicitation first screens PDS by taking the approach of WSM. It asks a user to assign a score to the values of each metric. This indicates that the quality of SPs is assessed against each metric. In addition, the user allocates a weight to each metric, showing its importance in relation to the other metrics. Then, the scores are weighed and totaled to give a score to SP. These scores can give an idea about the user's possible lowest and highest quality SPs (discussed in detail in Chapter 6). The scores are used to screen and sample the PDS for the user. To collect user feedback on the samples, specification solicitation asks a user to allocate a score to each sample. The scores of the samples are mapped in the domain of PDS. Triangulation method is utilized to interpolate the score of SPs in PDS. Statistical hypothesis test is utilized to aggregate the scores given by all the users to determine the quality. Statistical hypothesis test considers the variance of the scores as well as their mean. At the end, a relationship is determined between SPs and scores (quality of SPs). This is explained in detail in Chapter 5. A methodology is devised for specification solicitation to deal with large PDS in Chapter 6.

Task 2: concept selection. SDS is typically large, and users may not be able to give feedback on all design solutions in SDS. Concept selection (Chapter 7) decomposes design solutions to a number of parameters, and sets their values according to the best targets identified by specification solicitation. It adaptively samples the parameter values to represent the solutions to users. Concept selection introduces a user in a loop. In each loop, the user sets the value of a parameter. After setting the value, a number of design solutions are sampled, and the user select one of them. The selected sample is used for starting the next loop. Concept selection uses the relationship identified in specification solicitation (*f* between SPs and quality) as well as the user's choices to screen SDS in order to sample the solutions for the user. The loop is continued until the user reaches a design solution that complies with his/her needs. The relationship *f* is used to sample the higher quality solutions in each loop so that the user reaches his/her highest quality design solution more quickly. Concept selection identifies the best designs from SDS. The main part of this thesis ends here.

[2] Considering two specifications 'depth is less than 9 mm' and 'talk-time is more than 10 h', the ordered list is (depth, talk-time). An example of a SP is the 2-tuple (8 mm, 12 h).

The third part (Chapter 8 and Chapter 9). The third part develops two tools to implement the tasks of the framework. The tool for specification solicitation communicates the form and size of hand-held electronic consumer products to users in a new interactive way (Chapter 8). The tool builds the natural hand-product interactions to help users in the estimation of the form and size. It allows a user to grasp DP of a product and manipulate the DP in 3D space to explore its form and size. The tool augments the DP on the user's hand at the same scale and with the same perspective view as that of the hand. The tool for concept selection allows a user to produce a design solution by setting the values of parameters defined for design solutions (Chapter 9). It should be noted that at the end of Chapter 8 and Chapter 9, the effectiveness of the tools (in helping users estimate the values of physical characteristics correctly and quickly) is evaluated by using the evaluation method proposed in Chapter 4.

3.5 An Illustration Example

This section illustrates an example to demonstrate task 1 (specification solicitation) of the framework. This section demonstrates that we can effectively accomplish the objective of concept validation by using DPs and scoring. The size of the front face (width×height) of the smartphones was used for the case study. We attempted to identify the best size in an experiment (EXP-D). EXP-D is designed based on the first task of the framework; the details are presented in Section 3.5.1. The best size (OUT-D) was physically realized, and user feedback on it was collected to determine its quality. This was done to show how effectively the best size was identified.

Physical prototyping and qualitative feedback can also be the potential choices for performing the validation. We performed another experiment (EXP-P) utilizing these methods to identify the best size. The best size (OUT-P) was physically realized and its quality was determined by using the user feedback. The quality of OUT-D and OUT-P were compared to show whether DP and quantitative feedback are the better choices.

3.5.1 Study design

Fifteen subjects participated in this study. Their ages were between 25 to 31 years with the mean value of 27 years. They participated in both experiments, and were

informed that the prototypes illustrated the size of the front face of a smartphone. The size was defined in the interval of 60≤width≤70 mm and 125≤height≤135 mm. The initial size of the DP and the size of the physical prototype in EXP-P was 65×130.

Nine sizes were sampled in EXP-D; three samples for each of width and height. The samples of the width and height were {60,65,70} mm and {125,130,135} mm respectively. The DP was projected in the subjects' hand, and they could virtually grasp and manipulate it in 3D space (Figure 3.3). The DP was projected with the scale and in the perspective view of the hand. The background was the live environment behind the hand. The subjects could navigate between the samples of the size by using the left/right arrow keys on the computer keyboard. The subjects assigned a score to each sample. The scores were defined on a cardinal scale of integer values from 1 to 10, where 1 and 10 represented the lowest and highest quality sizes.

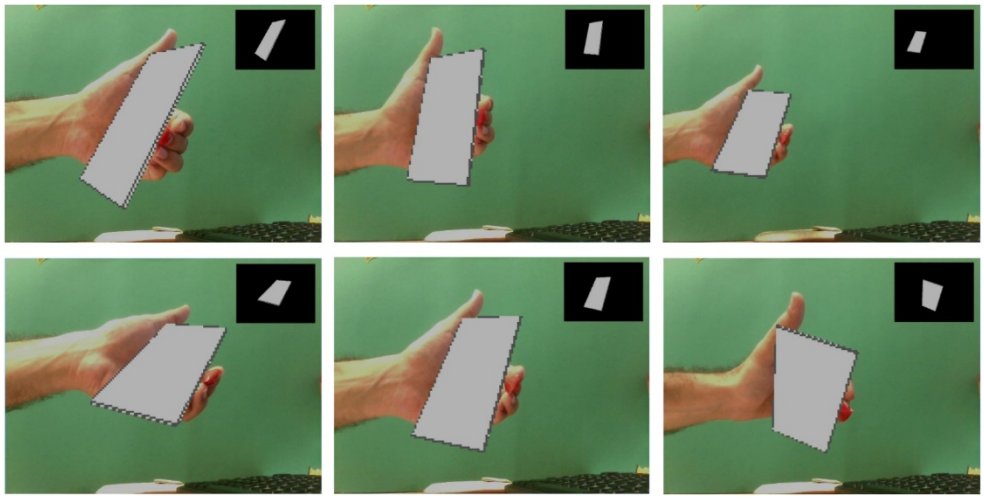

Figure 3.3 Several screenshots of the user interactions with the DP in EXP-D

To grasp the DP with the new size, the subjects only required changing the hand pose by moving their fingertips because the DP with the new size was projected at the same location and with the same orientation of the last DP (Figure 3.4). When the subjects thought that they grasped the DP, they pressed Enter to continue the interactions. In our experiments, no subject had difficulty with this. It should also be noted that we supervised and helped the subjects during their interactions with DPs.

In EXP-P, the subjects interacted with the physical prototype. The subjects were interviewed to collect their qualitative feedback on the size. After obtaining OUT-D and OUT-P, the subjects were recalled to allocate a score to them.

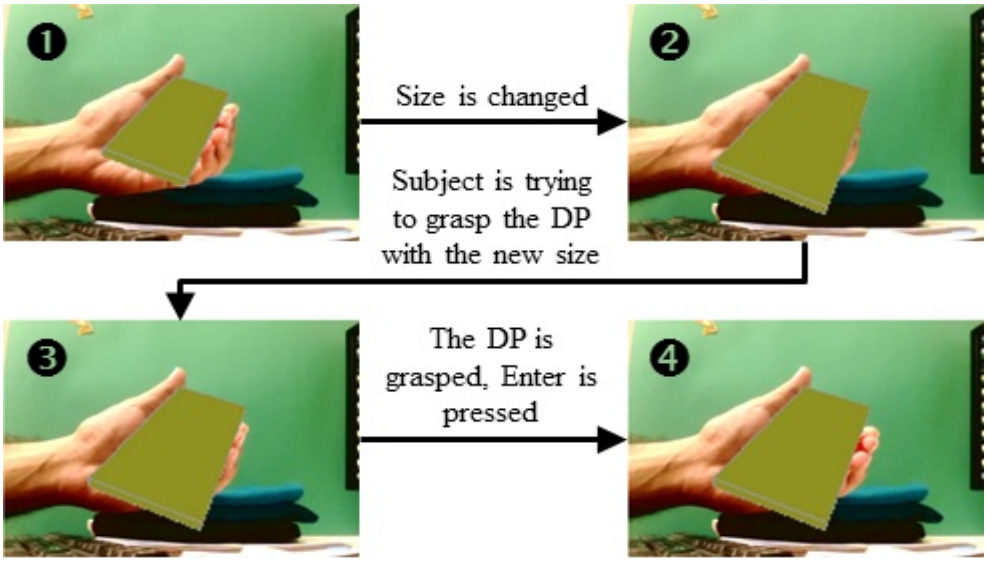

Figure 3.4 Screenshots of changing the size of the DP in EXP-D

3.5.2 Method

Statistical hypothesis test was utilized to determine the quality of the samples of the sizes. The mean of the scores of each 2 samples were compared by using the paired student's *t*-test. The hypothesis was: 'the mean values of the scores are not equal', *P*-value<0.05. H_0 stood for the equal quality. If we failed to reject H_0 for two samples, the populations of their scores were merged and the mean of the merged populations was considered as the quality of the samples. The samples, whose scores were not merged with the scores of the other samples, got the mean of their own scores as their quality. The hypothesis tests were done to not distinguish the same quality sizes because of the different mean values of their scores (this is illustrated in Section 2.4). The quality of the sizes in the domain [60,70]×[125,135] mm^2 was interpolated by using the triangulation method and the determined quality of the samples [117].

3.5.3 Results

The quality of the sizes in EXP-D is shown in Figure 3.5-a and b. The sizes (60 to 65,135) mm achieved 8.1 scores, and their median (63,135) mm was considered as OUT-D. In EXP-P, the subjects were provided with one physical prototype with the size of 65×130 mm^2. During the interactions with the physical prototype, the feedback of the majority of the subjects (11 out of 15) was that 'width should be a little greater than 65 mm'. According to the feedback, we considered 65+Δ mm (Δ is

real number>0) as the width guessed more suitable by the subjects. OUT-P was set to (67,130) mm. The physical realizations of OUT-D and OUT-P achieved 8.00±0.73 and 5.67±1.01 scores respectively (Figure 3.5-c). This shows that EXP-D that is designed based on the proposed framework selected a higher quality size than EXP-P.

3.6 Discussion

A framework was introduced for concept validation through digital prototyping and quantitative feedback. It targets two critical stages at conceptual design to involve users for the validation. The tasks for the validation at each stage and the generic functionality of each task were defined. To support the validation process, a method was devised to help communicating design solutions to users by using DPs, and a process was developed to collect and analyze user feedback about design solutions. Tools based on digital prototyping were developed to facilitate implementation of the tasks. Through an illustrated example for the size of smartphones, we showed that one of the highest quality sizes could be identified. This indicates that the framework is able to identify the best solutions by utilizing the developed methods (used for analysis of user feedback in the example), methodologies (task 1), and tools (used for communication of the size to users by using DPs in the example).

The scores of OUT-D and OUT-P are estimated by using Figure 3.5-b. OUT-D and OUT-P are given the scores of 8.1 and 5.94 respectively. The difference between the scores of OUT-D and OUT-P and the mean of the scores given to their physical realizations was 0.1 and 0.27 respectively. Such small differences can show that the scores obtained by EXP-D correctly estimate the quality of the sizes. The ratios between the qualities of OUT-D and OUT-P were calculated by using the results of EXP-D (Figure 3.5-b) and also by using the scores given by the subjects to the realizations. The former was 1.36 and the latter was 1.47±0.38 (Figure 3.6). Such small difference between the ratios shows that the estimated scores in EXP-D give the degree to which the quality of OUT-D is higher than OUT-P. Thus, it can be said that the cardinality is achieved in EXP-D. The cardinal scores can be helpful in decision-making as mentioned in Section 2.3. Overall, it can be concluded that EXP-D, defined based on the tasks of the framework, successfully determined the quality of the sizes.

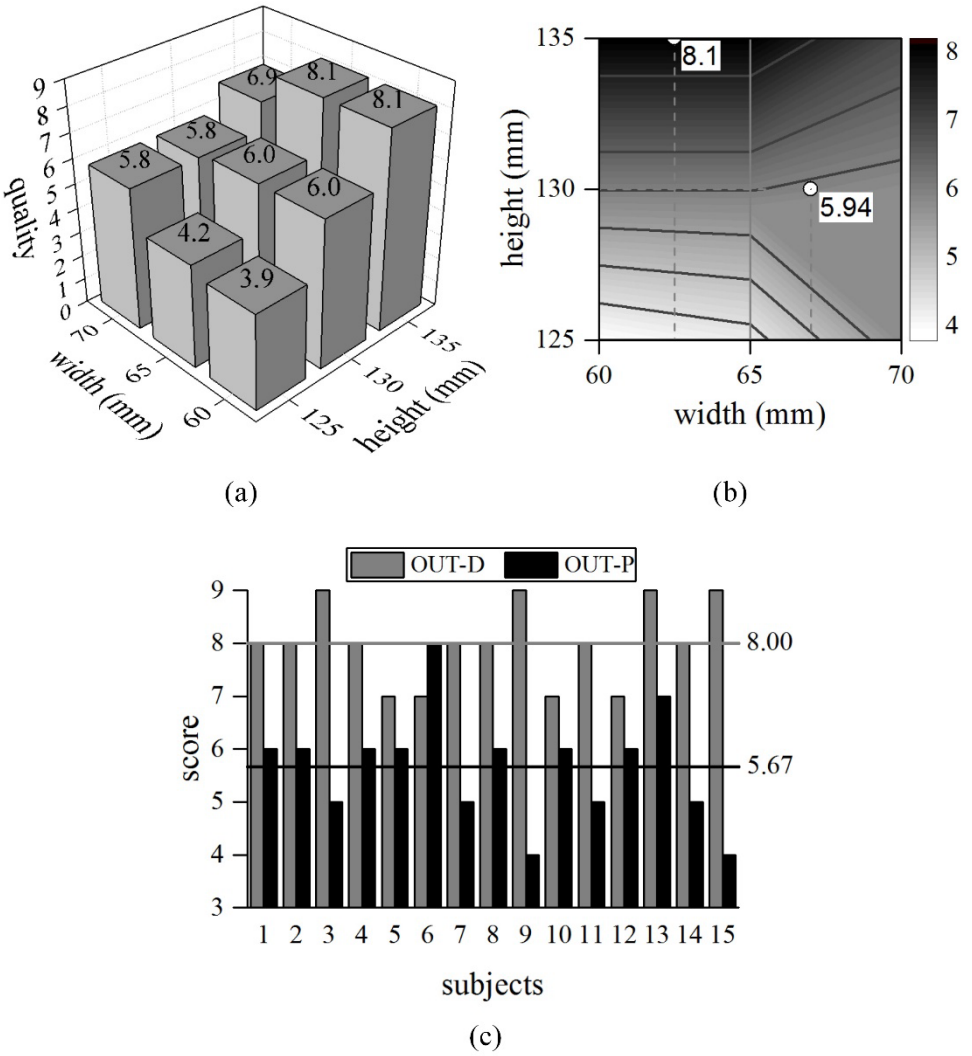

Figure 3.5 The subjects' feedback (a) the quality of the samples of the size, (b) the interpolated quality of the sizes in the domain, and (c) the scores of the outputs of the experiments and their mean values

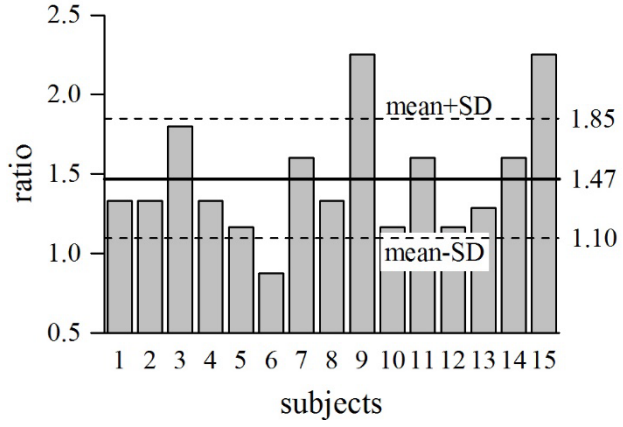

Figure 3.6 The ratio between the scores given by the subjects to the physical realization of OUT-D and OUT-P

The scores given by the subjects to the realizations of OUT-D and OUT-P were compared. One-tailed paired student's *t*-test was utilized to check the hypothesis 'OUT-D gets higher score than OUT-P'. The scores by each subject were paired. H_0 stood for the difference in the other direction. Significant statistical evidence was found to reject H_0, *P*-value≈0.0001. Therefore, it can be concluded that EXP-D selects the size with the higher quality than EXP-P, showing DP and scoring can be the better choices for the concept validation designed by our framework.

In EXP-D, we had objective evidence (i.e. the scores) to assess the quality of the sizes, whereas, in EXP-P, we had to interpret the subjective terms (e.g. larger and a little smaller in the subjects' feedback). For example, Figure 3.5-b shows that width should be less than 65 mm when height is more than 128 mm, and users are indifferent between the values between 60 and 65 mm. Besides, it illustrates that the quality increases by increasing the height, and the heights more than 134 mm are high quality. Such objective evidence could help us to identify a quality size. Therefore, the quantitative feedback can be superior to the qualitative one for our framework.

EXP-D helped users estimate the sizes by changing the length of the width and height, while users had to imagine the sizes in EXP-P. In the latter case, the estimates may not be correct. To illustrate, 11 subjects wanted the width 'a little greater' than 65 mm in EXP-P. The scores they gave to the samples in EXP-D (Figure 3.7) show that for only height of 125 mm, the statement 'a little greater' is valid. This can imply that in EXP-P, the subjects could not correctly estimate the sizes and their feedback was not useful. Therefore, digital prototyping can be the better choice for our framework.

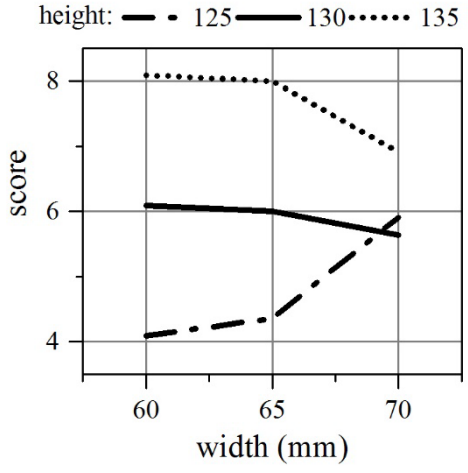

Figure 3.7 The mean of the scores in EXP-D against width

Chapter 4 Design concept communication by using digital prototypes

Design concept communication, in the context of this thesis, is a process in which critical information, such as design intents[3] [118] and user experience of design solutions [119] are exchanged through designer-user interactions via a medium[4] [121, 122]. The communication brings design concepts (as embodiments of design intents) to users and brings user feedback (as interpretations of design intents) back to designers [50, 123]. For example, Poirson et al. [20] elicited user perceptions of several geometrical forms of a wine glass on the sematic dimension 'elegant' in order to generate the most elegant wine glass. Elicited user perceptions can be useful for selecting a design solution that fulfills the intents if the users have a good level of understanding of the solutions before giving feedback on them [4, 33]. To help users understand the solutions, the communication medium plays a critical role [8, 124].

The proposed framework utilizes DP, as a form of communication media, to visualize a realistic 3D conceptual embodiment of design solutions and specification values by rendering some of the important physical characteristics (e.g. size, color, and texture) [5, 49]. One aspect of user understanding depends on how well users can estimate the values of the physical characteristics through interactions with DPs. The trend towards enhancing the user estimates of the physical characteristics suggests improving the ability of DPs to render the characteristics [8, 50] by increasing its level of fidelity [51] and flexibility [52] (Section 2.1). In addition to the ability of DPs, several studies [19, 60, 61] have argued that the environment in which a DP is projected and the input/output devices utilized for building user-DP interactions also have impacts on how well the physical characteristics can be sensed and estimated. For example, Kim and Lee [61] showed that user estimates of the color can be different when a DP is represented on different backgrounds. Tovares et al. [19] and Artacho et al. [37] studied the effects of the interactive communications (i.e. the communications in which users can manipulate DPs) on the user estimates, and

[3] Design intents refer to the designers' message embedded in the design concepts. The communication aims to send the message (e.g. 'elegant' embedded in the form of a wine glass) to users via the medium and elicit their perceptions (i.e. how elegant the form is).

[4] The medium is the representation of designer intents [120] of the future product and its features.

demonstrated that the interactive ways are superior to the non-interactive ones. These studies have emphasized that user estimates can be different when a DP is used in different ways.

In the communication of physical characteristics, DPs can be projected on different backgrounds (e.g. 2D instant images and live environment), and can be manipulated with different input devices (e.g. 2D/3D mouse and haptic devices). In addition, the response to the manipulations can be received by users with different output devices (e.g. head-mounted devices, 2D screen, and force feedback devices). Each way of using a DP in a communication has impacts on how correct the users can estimate the values of the physical characteristics. To identify the best way (background and input/output device) among the available ways for building the communication, we need to know how effective each way is in terms of the correctness of user estimates. However, little attention has been given to the research into the way of using DPs to enhance user estimates of the physical characteristics, especially the evaluation of the effectiveness of different ways of using a DP [46].

This chapter develops a methodology to evaluate the effectiveness of communication of physical characteristics of design solutions and specification values by using DPs. The effectiveness is obtained by measuring the degree of correctness of user estimates of the values of the physical characteristics during user-DP interactions. The measurements are assessed on three assessment dimensions to determine how correct and quick the users can estimates the values. The assessments are then evaluated on two evaluation criteria by using statistical analysis and hypothesis test to reveal the effectiveness of communication. The effectiveness shows the extent to which the communication can help users estimate the values of the characteristics correctly and quickly. Such evaluation helps designers compare different ways of using a DP in order to identify the most effective ways among the considered ones. For validating the proposed methodology, the size (width, height, and depth) of smartphones is used for a case study in this paper.

4.1 A methodology for evaluating the effectiveness of communication of physical characteristics

The effectiveness, in the context of this thesis, demonstrates how successfully the communication of physical characteristics by using a DP can help users correctly and quickly estimate the values of the characteristics. A methodology is proposed to

evaluate the effectiveness of the communication of physical characteristics (Figure 4.1) [46]. In the methodology, an experiment is designed for the evaluation (Step-1), users are involved in the communication (Step-2), and the users' estimates of the values of the characteristics are assessed and analyzed to reveal the effectiveness (Step-3). In Step-3, the users' estimates of the values are assessed several times during the users' interactions with the DP on three assessment dimensions (Step-3A). A relationship is identified between the degree of correctness of users' estimates and the time required to achieve that degree (Step-3B).

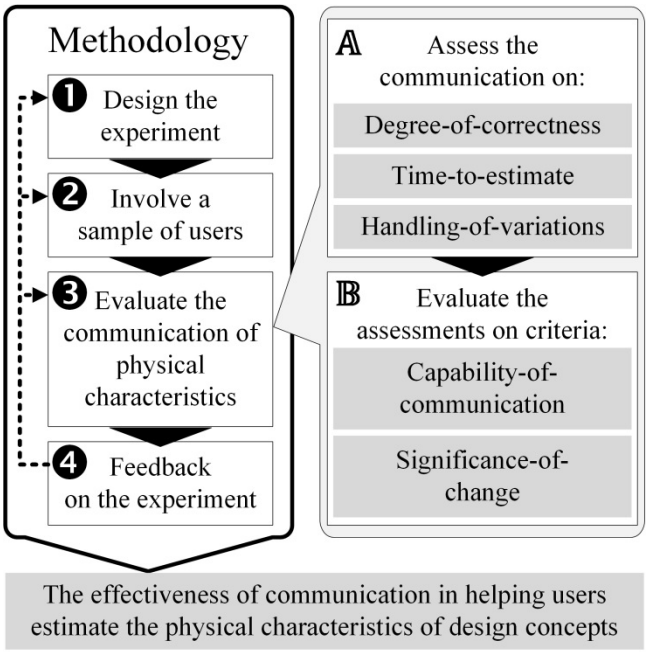

Figure 4.1 The evaluation methodology

Figure 4.2 shows an example of how a user's estimate of the color rendered by a DP can be assessed and evaluated. The user's estimates are assessed several times during the interaction with the DP. The degree of similarity between the user's estimates of the color and the rendered value is assessed at each assessment time to determine the degree of correctness of the estimates. By using the determined degree, we identify a relationship showing how correct the user's estimates are against the communication time. The relationships identified for all the involved users are analyzed and aggregated to reveal the effectiveness.

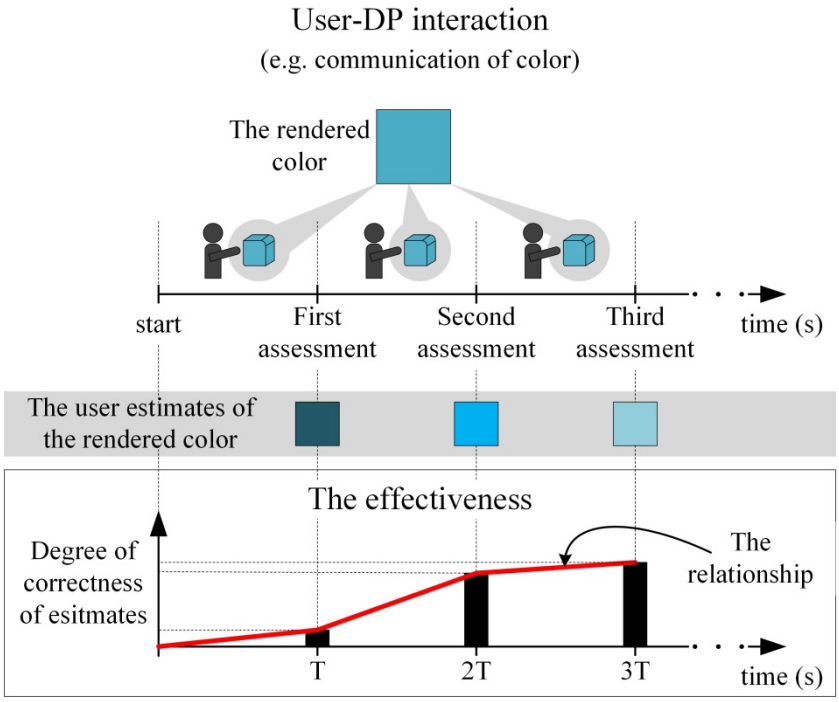

Figure 4.2 An example of evaluation of communication of color by the methodology

4.2 Assessment of communication of physical characteristics

To assess the communication, the Degree of Correctness of a user's Estimates at assessment Time *t* (DCET) is determined. At *t*, the assessment result is the expected DCET, i.e. the mean of DCET of all users.

4.2.1 Procedure of the assessment

A user's DCET at time *t* is a score (*s*) given to him/her based on the correctness (*D*) of his/her estimates of the values of the physical characteristics at *t*, i.e. DCET=$F(D,t)$. The score can be a real number in the interval (0,1], where ≈0 and 1 correspond to the lowest and highest scores respectively. Since defining F for the continuous interval is not easy, we consider a number (m) of scores for DCET of users; $s_1 \approx 0$, $s_i=(i-1)/(m-1)$, $i=2,3,\ldots,m$.

Measurement of D is a challenge because users' estimates are difficult to collect and interpret. In the methodology, a set of values (**V**) of the characteristics is realized and demonstrated to users. **V** also includes the values rendered in the communication.

Using **V**, users can illustrate their estimates to designers by attempting to find the rendered value. Figure 4.3-a shows an example of **V** comprising six values of color. As an advantage of using **V**, users may not have to explain their estimates, and also, designers may not have to interpret the users' explanations of the values.

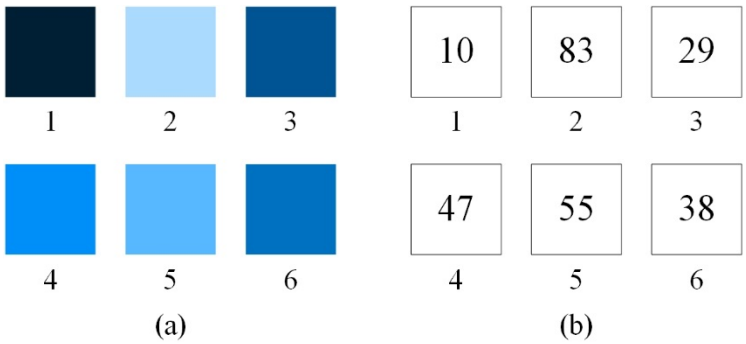

Figure 4.3 An example of **V** for color (a) the values and (b) their *d*

To measure *D* by using **V**, a numerical value (*d*) is assigned to each value of **V**. It is done in a way that the difference between *d* of two values reflects the degree of their similarity. *d* can be a scalar or a vector depending on the number of the physical characteristics or their parameters. For instance, the color can be defined by three parameters; hue, saturation, and intensity in HSI system [125]. *d* of the values of the color can be $(d_{\text{hue}},d_{\text{saturation}},d_{\text{intensity}})$. For the example in Figure 4.3-a, *d* is $(205,100,d_{\text{intensity}})$, and $d_{\text{intensity}}$ is given in Figure 4.3-b. *D* is measured as the geometric distance between *d* of the rendered value and the value chosen from **V**. By considering L^{∞}-norm [125] as the distance in the example of color (Figure 4.3), *D* of the first and sixth values is 28=max(|205-205|,|100-100|,|38-10|), where |·| denotes the absolute operator.

D is greater than or equal to zero. The degree of similarity of the values only depends on the distance between their *d*. *D* is not changed by exchanging the rendered and chosen values. In addition, two different values that have the same degree of similarity from a rendered value are given the same *D*. For example, in Figure 4.3, *D* of the third and fourth values from the sixth one is nine.

To specify *F*, Boolean expressions in terms of *D* and *t* for each score are considered. *F* gives a user a score corresponding to the expression that is true for his/her measured *D* and *t*. In other words, *F* is a look-up table that maps *D* and *t* into the

scores by using the expressions. F will be explained in detail in Sections 4.2.3 and 4.2.4.

F should satisfy the following conditions. A user's score will become higher if and only if his/her choice from **V** becomes more similar to the rendered value, or equivalently, D is decreased. As such, in the context of mathematics, F is strictly monotonically decreasing with respect to D, i.e. $\partial F(D,t)/\partial D<0$, where, ∂ is the partial differential symbol. This condition means that, at time t, the score is the most when $D=0$ and it decreases when $D\rightarrow\infty$ ('∞' is the largest distance that a value in **V** can have from the rendered one). Therefore, the Boolean expressions must be defined in order that F satisfies the condition, meaning that when D increases from 0 to ∞ at t, the expression that becomes true must correspond to a smaller score. Moreover, scores of users at t will be equal if and only if their Ds at t are equal. Thus, at t, F is one-to-one and the expressions must not have intersections, i.e. there must be only one true expression for each D.

A similar construct to F can be found in Kim and Lee's [61] work on developing a model for color. The model was used to elicit user preference for the color of digital hand-held devices. To investigate whether that model can help users correctly estimate the color, users participated in a study in which a user rated the degree-of-similarity between the digital and physical realizations of the color (i.e. rates→degree-of-similarity). We use similar construct to measure DCET (i.e. estimates→DCET). In contrast, our construct asks users to estimate the values, not to rate that degree-of-similarity. For example, we demonstrate a color to a user, and then, ask him/her to find it in **V**. We use the difference between the illustrated color and the users' choice to rate the degree-of-similarity (or to identify DCET). Our construct also takes time into account. This is to investigate whether certain intriguing relationships exist between the degree of correctness that users can estimate and how much time it would take.

4.2.2 Assessment dimensions

Measurement of D at each time is assessed on three dimensions, namely degree-of-correctness, time-to-estimate, and handling-of-variations. The dimensions reflect the degree of correctness of users' estimates as well as timing for achieving that degree.

Degree-of-correctness expresses the degree to which users can correctly estimate one value for each physical characteristic through interaction with the DP. This dimension

can be compared with the fidelity defined by [51, 126]. The fidelity shows the extent to which a DP can realistically render the characteristics (please see Section 2.1 for definition of fidelity), whereas, degree-of-correctness shows the extent to which users' estimates reflect the values of the characteristics. Degree-of-correctness compares user estimates of values of physical characteristics with the real values. When evaluating the values of physical characteristics of a design concept, it is important that user estimates correspond well with the values. The assessment on degree-of-correctness can provide how well the correspondence is.

Time-to-estimate expresses how quickly users can estimate one value for each physical characteristic through interaction with the DP. Time-to-estimate can be affected by interactivity defined by [53]. The interactivity shows the degree of similarity between the user-prototype interactions (e.g. manipulating DP in 3D space to explore the geometrical form of design concept) and their respective physical interactions (e.g. manipulating by using hand). The higher level of interactivity can generally reduce the estimation time [51]. The assessment on time-to-estimate provides the timing required for estimating the values of physical characteristics through interaction with a DP.

Handling-of-variations expresses the extent to which users can estimate a number of values of the physical characteristics after a period through interaction with the DP. DPs are typically flexible to change in order to render different values of a characteristic. This makes DPs quite helpful in eliciting user perceptions of the values [19]. However, when a user encounters several values of a physical characteristic, his/her estimates may not correspond well with the values, affecting their feedback. The assessment on handling-of-variations provides the number of the values that users can correctly estimate through interaction with the DP.

Figure 4.4 summarizes the explanations of the relationships between the existing assessment dimensions and our proposed dimensions. Fidelity, interactivity, and flexibility can be used to examine the ability of DPs to enhance their visualization and changeability. Such enhancement may not necessarily result in good user estimates of values of physical characteristics of design concepts [28, 53]. In comparison, the assessment of communication of physical characteristics on the proposed dimensions can be used to determine the extent to which users can estimate the values of physical characteristics correctly and quickly. Therefore, the proposed dimensions can better conform to evaluation of the effectiveness.

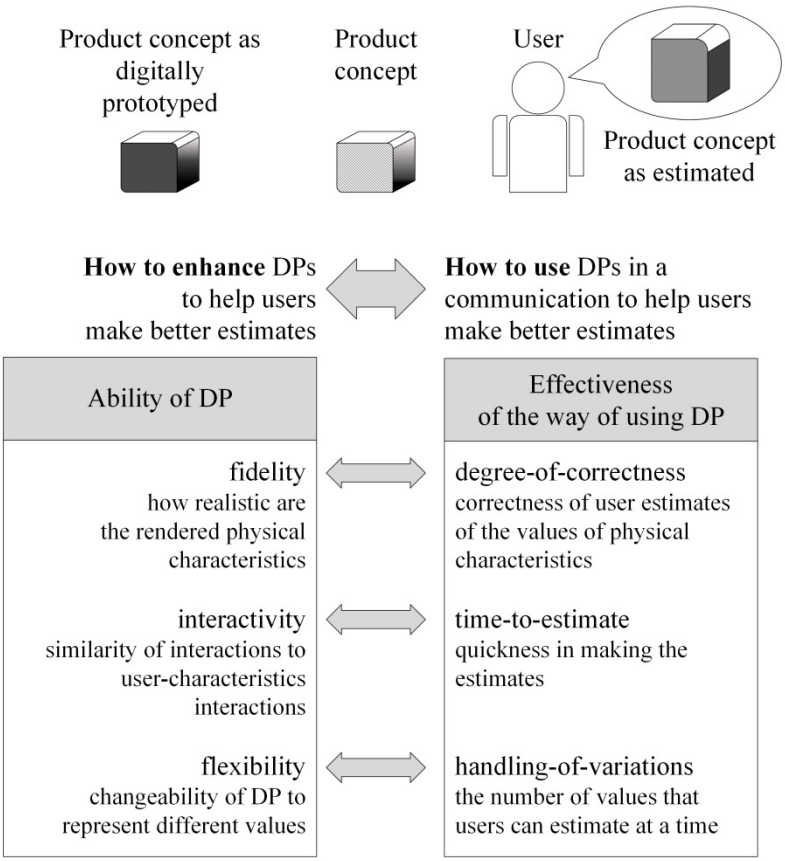

Figure 4.4 How to enhance DP vs. how to use DP

4.2.3 Assessment of communication on the dimensions

DCET of a user (or his/her score) on degree-of-correctness ($DCET_{DC}$) is determined by measuring D (Table 4.1). To obtain F_{DC} relating $DCET_{DC}$ to D and t, the range of D, i.e. $[0,\infty)$, is divided into j parts, and each part is corresponded to a score. In the example in Figure 4.3-a, D can be divided into 3 parts, [0,10), [10,30), and $[30,\infty)$, corresponding to the score of 1, 0.5, and ≈0 respectively. In this case, if D for a user is 17, then his/her $DCET_{DC}$ is 0.5 because $17 \in [10,30)$. $DCET_{TE}$ is determined by measuring time to reach a critical D (D_{crit}); D_{crit} is D that designers expect users to achieve. F_{TE} gives a user a score according to the time period that he/she reached D_{crit}. To define F_{TE}, the time $[0,\infty)$ is divided into j parts, and each part is corresponded to a score. To determine $DCET_{HV}^{N}$, $D/d_{rendered}$ (Dd) is computed at t; where N is the number of the different values of the characteristics. To define F_{HV}, the range of Dd, i.e. [0,1], is divided into j parts, and each part is corresponded to a score. The proposed F_{DC}, F_{TE}, and F_{HV} are strictly monotonically decreasing because

DCET is increased by decreasing D (Note that D is quantized to two levels for time-to-estimate and j levels for the other two dimensions).

Table 4.1 F and the outputs on the assessment dimensions

F			the output
F_{DC}	F_{TE} (D_{crit})	F_{HV} (t_{crit}[3] & N)	$DCET_{DC}$ $DCET_{TE}$ $DCET_{HV}$
$[0, D_1]$	$[0, t_1]$	$[0, Dd_1]$	s_j=1
$(D_1, D_2]$	$(t_1, t_2]$	$(Dd_1, Dd_2]$	s_{j-1}
⋮	⋮	⋮	⋮
$(D_{j-3}, D_{j-2}]$	$(t_{j-3}, t_{max}$[1]$]$	$(Dd_{j-3}, Dd_{max}$[2]$]$	s_2
(D_{j-2}, ∞)	(t_{max}, ∞)	$(Dd_{max}, 1]$	$s_1 \approx 0$

[1] t_{max} is the longest acceptable time for achieving D_{crit}.
[2] Dd_{max} is the largest acceptable Dd.
[3] t_{crit} is the duration that designers expect users to achieve Dd_{max}.

The expected $DCET_a$ at t ($M_{a,t}$) is the statistical mean of users' $DCET_a$ at t; where a represents an assessment dimension. $M_{a,t}$ is also represented qualitatively by a set of qualitative indicators QI_i, i=1,2,…,j, where QI_1 and QI_j are the lowest and best ones respectively as shown in (4.1).

$$\begin{aligned} &M = s_1 \approx 0 && \rightarrow \quad QI_1 \\ &M \in (s_1, s_2) && \rightarrow \quad QI_2 \\ &M \in [s_{i-1}, s_i),\ i=3,\ldots j-1 && \rightarrow \quad QI_i \\ &M \in [s_{j-1}, s_j=1] && \rightarrow \quad QI_j \end{aligned} \tag{4.1}$$

4.2.4 Aggregation of the assessments

DCET is obtained by aggregation of $DCET_{DC}$, $DCET_{TE}$, and $DCET_{HV}{}^N$ as shown in (4.2).

$$\mathrm{DCET}=\mathcal{F}(D,t)=\frac{w_{DC}\cdot w_{TE}\cdot \mathcal{F}_{DC}\cdot \mathcal{F}_{TE}+w_{TE}\cdot w_{HV}\cdot \mathcal{F}_{TE}\cdot \mathcal{F}_{HV}+w_{HV}\cdot w_{DC}\cdot \mathcal{F}_{HV}\cdot \mathcal{F}_{DC}}{w_{DC}\cdot w_{TE}+w_{TE}\cdot w_{HV}+w_{HV}\cdot w_{DC}} \quad (4.2)$$

Where, w is the weight reflecting the importance of a dimension, and belongs to [0,1]. In addition, at least one w is non-zero.

DCET is calculated for each user, and the mean of all the users' DCET at t is considered as the expected DCET at t (M_t). M_t is the result of the communication assessment at t. The qualitative indicators of M_t are given by (4.3). The range of DCET for each QI was obtained by (4.1) and (4.2), where each weight in (4.2) was equal to one.

$$\begin{aligned}
&\mathrm{M}=s_1^2\approx 0 && \rightarrow \quad \mathrm{QI}_1\\
&\mathrm{M}\in\left(s_1^2, s_2^2\right) && \rightarrow \quad \mathrm{QI}_2\\
&\mathrm{M}\in\left[s_{i-1}^2, s_i^2\right),\ \mathrm{i}=3,\ldots j\text{-}1 && \rightarrow \quad \mathrm{QI}_i\\
&\mathrm{M}\in\left[s_{j-1}^2, s_j^2=1\right] && \rightarrow \quad \mathrm{QI}_j
\end{aligned} \quad (4.3)$$

The expression in (4.2) indicates that the enhancement of user estimates at t can be larger if the user estimates are more correct at t-Δt (Δt>0). In Appendix A, we show that the expression gives this statement, and also satisfies the condition mentioned in Section 4.2.1. We will support the statement by using the results of our case study in Section 4.7 to justify $\mathcal{F}$.

4.3 Evaluation of communication of physical characteristics

4.3.1 Evaluation criteria

The methodology evaluates the assessments on two criteria, capability-of-communication (CAP) and significance-of-change (SIG). CAP_t shows how much of the best M_t can be fulfilled by the communication at t. CAP_t is given by:

$$\mathrm{CAP}_t=\frac{(\mathrm{M}_t\pm\mathrm{SD}_t)}{\mathrm{M}_{\mathrm{best}}}=\mathrm{M}_t\pm\mathrm{SD}_t \quad (4.4)$$

M_t is the best when DCET of all users at t are equal to one. As such, the best M_t 'M_{best}' is one. SD_t is the standard deviation of users' DCET at t. It shows how much we expect a user's DCET can be close to M_t. A small SD_t shows that the communication using DP can help users achieve DCET closer to M_t.

SIG shows whether M is improved over time by comparing the population of DCET at two successive assessment times. In practice, CAP_t is obtained by using DCET of a number of users. Therefore, the increase/decrease of its value may not show improvement/deterioration of DCET over t. SIG draws the inference about the changes in M_t by providing statistical evidence from the population of DCET at two successive assessment times.

SIG_t is the result of testing the hypothesis: 'M_t is greater than $M_{t-\Delta t}$'. H_0 stands for the difference in the other direction. To test the hypothesis, DCET of each user at t-Δt and t are paired, and paired two-sample student's t-test is used. SIG_t is given by (inference, P-value). If strong evidence is found against H_0, the inference is represented by ✓, meaning that the sample of DCET gives reasonable evidence to support the hypothesis with P-value<α; where α is the significance level. Otherwise, the inference is represented by ✗. P-value is the probability of obtaining the difference between the means at least as extreme as the one observed in the experiment, assuming the truth of H_0.

4.3.2 Effectiveness of communication

The effectiveness is the relationship between M and t. It gives the trend in improvement of DCET, and represented by **Tr**. **Tr** is a 3-by-r matrix, where r is the total number of the assessments. **Tr** at t is:

$$\mathbf{Tr}_t = \begin{bmatrix} CAP_t \\ SIG_t \\ QI \text{ of } M_t \end{bmatrix} \tag{4.5}$$

Tr can be depicted as shown in Figure 4.5. The white vertical bars show M_t and the black vertical lines show SD_t. SIG_t is illustrated on the line connecting M to show the significance-of-change. Such illustration can ease the use of effectiveness.

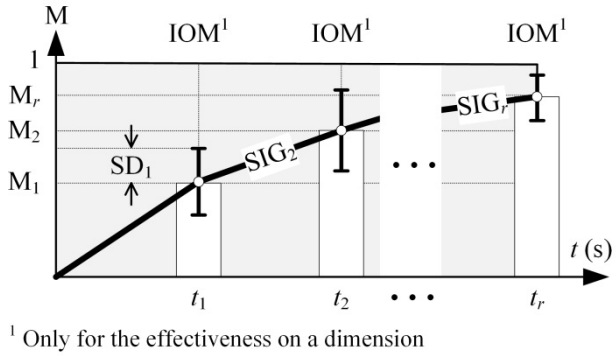

Figure 4.5 The graphical illustration of **Tr**

The effectiveness can also be considered on each assessment dimension:

$$\mathbf{Tr}_{a,t}=\begin{bmatrix} \mathrm{CAP}_{a,t} \\ \mathrm{SIG}_{a,t} \\ \text{QI of } \mathrm{M}_{a,t} \\ w_a w_b \mathrm{DCET}_{b,t}+w_a w_c \mathrm{DCET}_{c,t} \end{bmatrix} \tag{4.6}$$

Where, *a*, *b*, and *c* can correspond to any of DC, TE, and HV, and $a \neq b \neq c$.

The last row of $\mathbf{Tr}_{a,t}$ is the coefficient of the partial differentials in (A.1) of Appendix A, and it is called Impact on M (IOM). IOM of dimension *a* at $t\text{-}\Delta t$ shows the influence of improvement of M_a from $t\text{-}\Delta t$ to *t* on increasing M_t. The larger IOM can result in more increase in M. Besides, according to (A.1), a dimension on which the communication is weaker at $t\text{-}\Delta t$ (i.e. has lower $M_{a,t\text{-}\Delta t}$) has the larger IOM. This can encourage enhancing the communication on the weaker dimensions so that the communication becomes effective on all dimensions. Some of the applications of $\mathbf{Tr}_a$ are explained in Section 4.7.

4.4 Experiment design for conducting the evaluation

In designing the experiment, **V**, *d*, α, and the parameters in Table 4.1 need to be defined. The assessments are done at several stages during the communication (Figure 4.6). A stage comprises demonstration and representation processes. In the former, users interact with DP for a fixed period of time (DT). In the latter, they are given a time (RT) to which they should choose a value from **V** to represent their estimates. After each stage, the change in the measured *D* are analyzed (the analysis

boxes in Figure 4.6). The experiment is continued until there is no change in *D*, meaning that the user believes his/her estimates are correct. The period of the experiment for a user is $\leq r\cdot$(DT+RT), and the duration of communication of the physical characteristics is $r\cdot$DT. In the rest of this paper, the indices *t* is replaced by the stage number (e.g. CAP_{2DT} is represented by CAP_2).

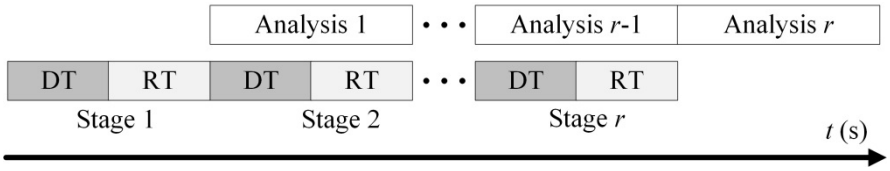

Figure 4.6 The timing of the experiment

4.5 Feedback on the experiment

The evaluation results are used as the feedback to enhance the experiment. The feedback (the dashed lines in Figure 4.1) may lead to the revision to the experiment design, the sample of users, or the evaluation results. For example, the evaluation results may show that DT is not well-set or the sample of users is not well-selected. The revision may update **Tr** and/or restart the process of the evaluation.

The revision to the experiment design can be the change of **V**, DT, or RT. For instance, small *D* for the majority of users may indicate that the rendered values are quite different from the other values in **V**. In this case, including the values more similar to the rendered ones can help to find out if the small *D* relates to **V** or it may be due to the high effectiveness of the communication. The revision can also result in the change of *d*, α, or the values in Table 4.1. In these cases, the revisions may just require updating **Tr** by using the new values.

The feedback on the sample of users may show that new users should be involved or some of the users should be excluded. For example, the correlated DCET of users may imply that the sample of users is not representative of the user population. In this case, increasing the sample size can help to find out whether the correlation relates to the samples or it may be due to the effectiveness of the communication. When users are excluded, **Tr** should be updated by removing the data of the excluded users.

Feedback on the experiment is an important part of the methodology. It helps to enhance the experiment to achieve **Tr** reflecting the effectiveness of communication.

4.6 Case study

This section demonstrates how the proposed methodology can be used in real scenarios through a case study. In the study, the effectiveness of two types of communication setups, namely virtual reality (COM-V) and mixed reality (COM-M), was evaluated. The setups were developed for rendering the size of electronic hand-held devices with the focus on smartphones. The same DP was used in both setups while both the background and input devices were different in the setups. The purpose of conducting experimental studies under such arrangements was to show that the evaluated effectiveness can demonstrate how successful a setup is, and also can help to select the better way of using DP, i.e. a better background or an input device or the combination of both.

4.6.1 Communication setups

In both COM-V and COM-M setups, the size of the smartphones was rendered by using a digitally-prototyped rectangular box. In COM-V, the prototype was projected with 'scale 1' on a 2D screen (i.e. the size could be measured by a ruler on the screen). The background was a solid white plane. The prototype could be rotated with 3 degree-of-freedom and moved in a 2D plane (parallel to the screen) by using a 2D mouse. Movement along the depth (i.e. towards the inside of the screen) was disabled since it might not be recognizable because of the 2D background. In COM-M, the setup used in EXP-D (Section 3.5.1) was used.

4.6.2 Experiment design

Seven subjects participated in the COM-V setup. Their age was between 25 to 31 years with the mean value ≈28 years. Eight subjects participated in the COM-M setup. Their age was between 26 and 31 years (mean value ≈28 years). Two subjects in each group were considered as control subjects. All the subjects were informed that the DP visualized the size of smartphones.

According to the experiment design (Figure 4.6), there are several interruptions to user-DP interactions during the communication of physical characteristics in order to measure *D*. An interruption at a time can affect user estimates of the values of physical characteristics for the rest of the communication period. It is important that the effects be negligible so that the evaluations can reflect the effectiveness of the

communication. Therefore, the control subjects were considered to determine the significance of the effects. For the control subjects, no interruption was incorporated into the communication.

The experiment comprised two tasks. The first task was the assessment of the setups on degree-of-correctness and time-to-estimate. In this task, the subjects interacted with the prototype with size of 60×130×8 mm^3 (width×height×depth). DT and RT was 30 s and 60 s respectively (Figure 4.6). In each stage, a blank millimeter paper was used for each subject. The second task was the assessment of the setups on handling-of-variations with N=3. Three smartphones with the sizes 60×130×8, 65×115×9, and 70×140×7 mm^3 were considered. The sizes were chosen based on the size of the existing smartphones in the market in the 2nd quarter of 2013. The subjects were given DT seconds to interact with the prototype. They could navigate between the sizes by using the left/right arrow keys on the computer keyboard. They had up to RT seconds to draw the sizes on a plain paper after each DT seconds. The three sizes must be drawn on the same paper because we wanted the subjects to express their estimates of the differences between the sizes. In each stage, a blank paper was used for each subject.

V was defined as the range 0<width,height,depth<300 mm, where 300 mm was the length of the longest line that could be drawn on the papers in the tasks. d was considered as the measurement of the length of the lines divided by the acceptable errors, which were 4, 6, and 2 mm for the width, height, and depth respectively. L^{∞}-norm was used to calculate D. The values of the parameters in Table 4.1 are illustrated in Table 4.2. Table 4.3 illustrates QI and their respective range for M_a and M. α was 0.05.

Table 4.2 The specification of the parameters of F

F			the output
F_{DC}	F_{TE} (0.75)	F_{HV} (180 & 3)	$DCET_{DC}$ $DCET_{TE}$ $DCET_{HV}$
[0,0.5]	[0, 60]	[0, 0.1]	1
(0.5,0.75]	(60, 150]	(0.1, 0.15]	0.67
(0.75,1]	(150, 240]	(0.15, 0.2]	0.33
(1,∞)	(t_{max}=240, ∞)	(Dd_{max}=0.2, 1]	≈0

Table 4.3 The quantitative indicators for the values of M_a and M

QI	M_a (4.1)	M (4.3)
high	[0.67, 1]	[0.45, 1]
medium	[0.33, 0.67)	[0.11, 0.45)
low	(0, 0.33)	(0, 0.11)
very low	≈0	≈0

4.6.3 Results

The experiments were conducted until Stage 4 because the subjects made no revision to their estimates from Stage 3 to 4 (for some subjects, from Stage 2 to 3). The results of the first three stages (90 s) are illustrated in this section. There were two interruptions during the communication period of 90 s. For the control subjects, the assessment was performed at t=90 s. The results of the non-control subjects are tabulated in Table 4.4.

Table 4.4 The results of the measurements[1]

parameter	stage	COM-V					COM-M					
		V1[2]	V2	V3	V4	V5	M1[3]	M2	M3	M4	M5	M6
D	1	1.50	2.00	1.50	1.00	1.75	1.00	0.75	0.75	0.83	1.00	1.00
	2	0.68	0.67	1.50	0.50	1.00	0.75	0.58	0.25	0.33	0.50	0.63
	3	0.68	0.50	0.75	0.50	0.75	0.50	0.38	0.25	0.50	0.38	0.25
t	1							86	37			
	2	125	112	×	119	×	97			104	132	121
	3	---	---	166	---	171	---	---	---	---	---	---
Dd	1	0.13	0.25	0.16	0.16	0.17	0.30	0.25	0.14	0.22	0.25	0.22
	2	0.11	0.17	0.17	0.09	0.12	0.23	0.26	0.11	0.26	0.21	0.18
	3	0.08	0.10	0.12	0.06	0.13	0.21	0.22	0.09	0.21	0.22	0.14

[1] the highlights show the values greater than the acceptable errors 1.00 for *D* and 0.2 for Dd.
[2] subjects in COM-V
[3] subjects in COM-M

The effectiveness of COM-V is shown in Figure 4.7. **Tr** in the black box is the effectiveness of communication of the size, and the rest are the effectiveness on a dimension. The highlights in the background of the plots represent the qualitative levels given by Table 3.

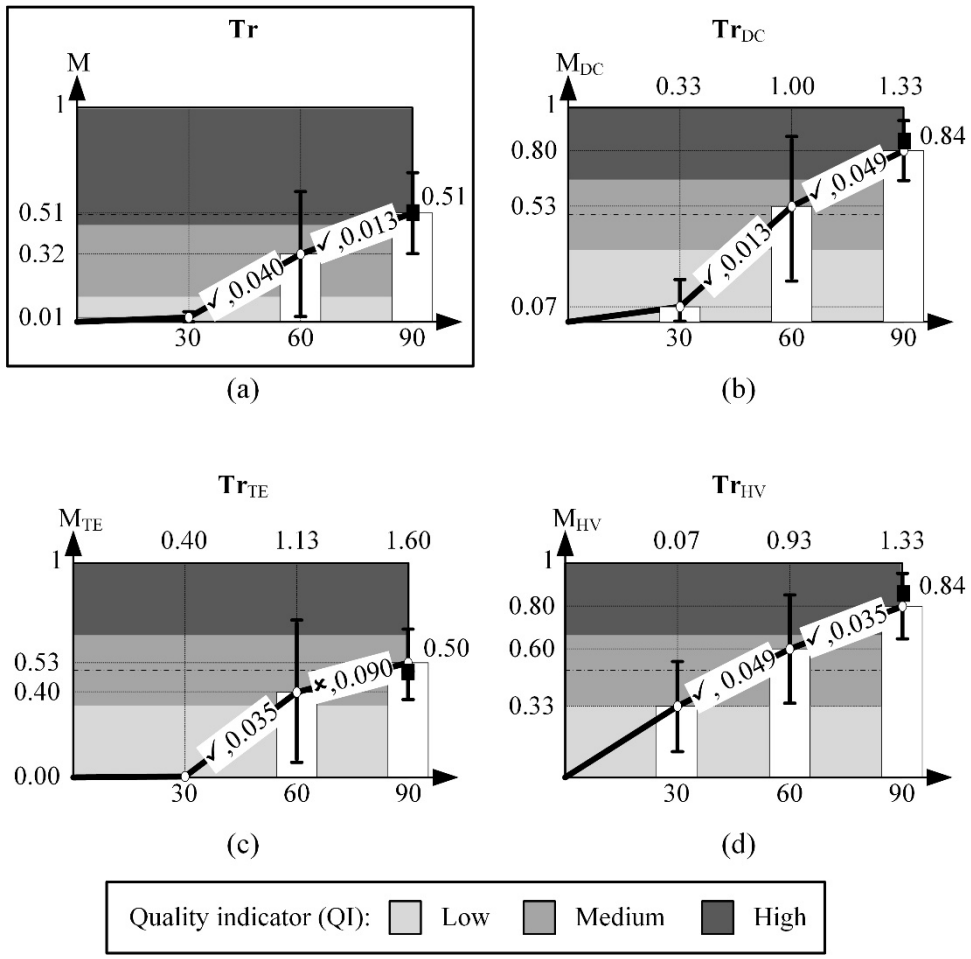

Figure 4.7 The effectiveness of COM-V

Referring to **Tr** (Figure 4.7-a), CAP_1 (0.01±0.02) may show that COM-V cannot help users to correctly estimate the sizes in less than 30 s. M_2 (0.32) is improved to the medium level of *q*, and SIG_2 shows that the improvement is significant, *P*-value<0.05. COM-V can reach the high M (0.51) after 3 stages. SIG_3 shows that M_3 can be greater than M_2, *P*-value<0.05. CAP_3 (0.51±0.19) may imply that a user's DCET can be medium to high after three stages. In $\mathbf{Tr}_{DC}$ (Figure 4.7-b), $CAP_{DC,1}$ (0.07±0.12) shows that $DCET_{DC}$ in Stage 1 is low. At stage 3, the high-level $DCET_{DC}$ is expected because $M_{DC,3}$ is 0.80 and $SD_{DC,3}$ is small. The large reduction (≈2 times) in SD_{DC} from Stage 2 to 3 can show that more users can correctly estimate the size

after 90 s. By using the COM-V setup, one can expect the high-level $DCET_{DC}$ after 90 s. Referring to $\mathbf{Tr}_{TE}$ (Figure 4.7-c), COM-V may not be useful for improving $DCET_{TE}$ in less than 30 s ($CAP_{TE,1}\approx 0$). M_{TE} rises to the medium-level after three stages. In $\mathbf{Tr}_{HV}$ (Figure 4.7-d), CAP_{HV} and SIG_{HV} show that M_{HV} has a steady improvement from Stage 1 to 3. $CAP_{HV,3}$ shows that the high-level $DCET_{HV}$ can be expected after 90 s. Therefore, COM-V is capable of helping users estimate the differences between three sizes of smartphones, i.e. how big/small the sizes are in relation to each other. However, it cannot help users estimate the width, height, and depth.

Referring to Figure 4.7-b-d, IOM is quite low (0.27±0.14) in Stage 1. To increase M by 0.31 from Stage 1 to 2, M_{DC}, M_{TE}, and M_{HV} are increased by 0.46, 0.40, and 0.27 respectively. In Stage 2, IOM is 1.02±0.08, almost four times larger than IOM in Stage 1. M could reach to 0.51 from 0.32 at Stage 3 by increasing M_{DC}, M_{TE}, and M_{HV} by 0.27, 0.13, and 0.2 respectively (almost half of the increases in Stage 1). Therefore, when IOM is larger, smaller increase in M_a is required to add a certain value to M. This supports the statement in Section 4.2.4, which implies that F is a good choice for the aggregation of the assessment on the proposed dimensions.

Figure 4.8 shows the effectiveness of COM-M. Referring to **Tr** (Figure 4.8-a), the subjects' estimates become more correct from Stage 1 to 3. CAP_3 (0.48±0.22) shows that a subjects' DCET can be low to high, meaning that the user-DP interaction time should be longer than 90 s to achieve high users' DCET. $\mathbf{Tr}_{DC}$ (Figure 4.8-b) demonstrates that COM-M can deliver the best performance after 90 s ($CAP_{DC,3}$=1.00±0.00). In $\mathbf{Tr}_{TE}$ (Figure 4.8-c), COM-M reaches the high-level $M_{TE,2}$ in 60 s. $\mathbf{Tr}_{HV}$ (Figure 4.8-d) shows that M_{HV} has a steady but not significant increase from Stage 1 to 3. Therefore, COM-M is capable of helping users estimate the width, height, and depth. However, it cannot help them estimate the differences between three sizes of smartphones.

The black squares at t=90 s in Figure 4.7 and Figure 4.8 illustrate the mean of the results of the control subjects. As can be seen, M of the control subjects are similar to M of the non-control subjects at 90 s. Pearson correlation coefficient was adopted to show the degree of the similarity. The correlation coefficient was 0.998±0.001, and this high correlation shows that the effects of RT were not significant on the users' estimates of the size. Therefore, the duration of the interruptions can be set so that the evaluations can reflect the effectiveness of a communication.

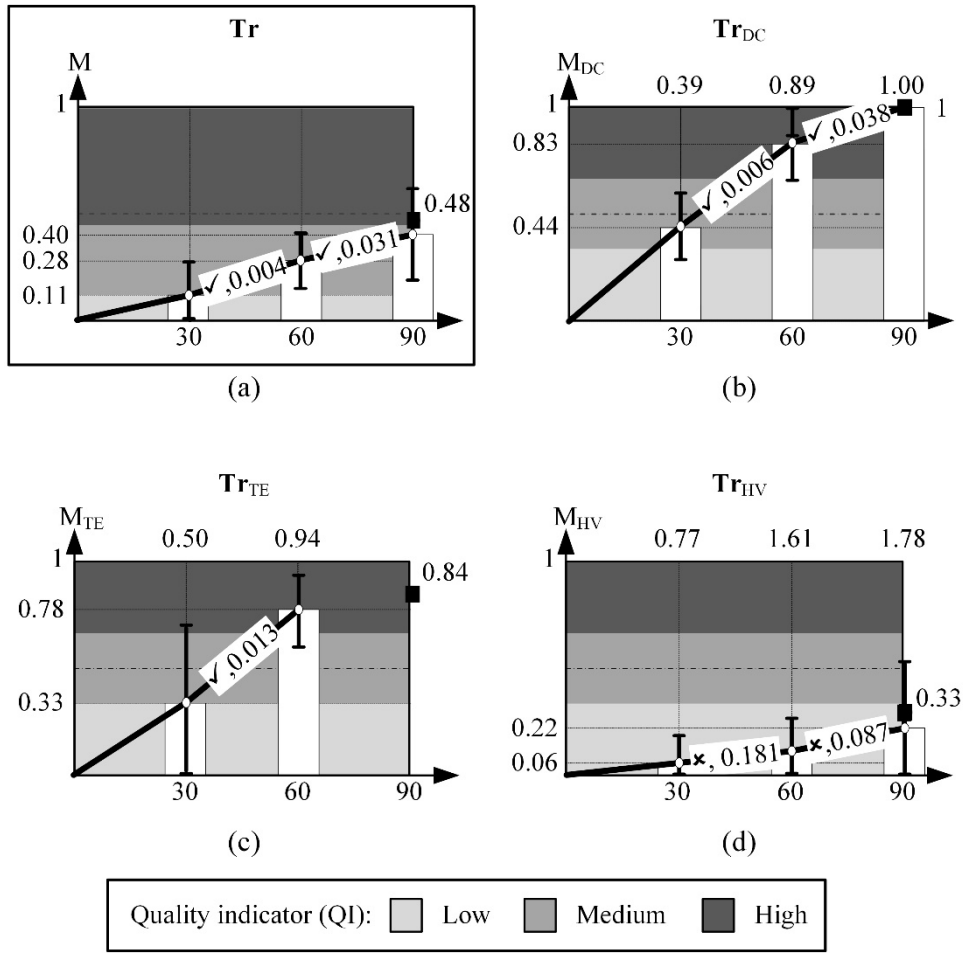

Figure 4.8 The effectiveness of COM-M

4.7 Discussion

We showed that how the methodology can be used in real scenarios in the case study. The effectiveness of two communication setups, COM-V and COM-M, was evaluated and compared.

Tr$_{DC}$, shown in Figs. Figure 4.7-b and Figure 4.8-b, demonstrate that the degrees of correctness for COM-M are greater than COM-V in all Stages. After 90[5] s, the former achieves the best performance, while the latter achieves 80% of the best performance. Therefore, COM-M outperforms COM-V in terms of users' correct estimate of the size. In COM-M, the DP and the user's hand are projected in the same perspective view and scale on the screen. The size of the hand of a user is generally well-known

[5] It should be noted that for all **Tr** in Figs. 8 and 9, M is not changed after 90 s.

to him/her. Thus, a user can easily estimate the size of the DP in relation to the size of his/her hand. In contrast, the DP in COM-V is projected in a fixed perspective view and with a fixed scale. In this case, the user needs to understand the perspective view before estimating the size, which may not be easy especially for the users with no experience with virtual environments. The level of the user's understanding of the perspective view can affect user estimates of the size. It would be helpful to add an object with a well-known size (e.g. a coin) in the environment and in the same perspective view of the DP when rendering the size of smartphones in COM-V. This can increase the degree of correctness of the estimates so as to enhance the effectiveness of COM-V.

Referring to $\mathbf{Tr}_{TE}$ (Figure 4.7-c and Figure 4.8-c), COM-M reaches the high M_{TE} (0.78) at 60 s, meaning that the users make the correct estimates (i.e. as correct as D_{crit}) at 60 s, whereas, COM-V cannot reach the high M_{TE} (Figure 4.7-c) at all. Therefore, the former is superior to the latter in terms of the timing for a user to make the correct estimates with the DP. In COM-V, the DP is projected on a 2D background, and the interactions are done by a 2D computer mouse. In the case study, the subjects sometimes lost their concentrations because they got confused about the orientation of the DP in COM-V. It was observed that the subjects used the 'reset view' button several times (2.6±1.9 times during the 3 stages), showing the distraction from estimation of the size in COM-V. Such distractions can lengthen the time required to achieve the estimates with a certain degree of correctness. In contrast, the virtual interactions in COM-M are similar to physical interactions with smartphone, helping the subjects to immerse in the environment and conveniently explore the DP.

$\mathbf{Tr}_{HV}$ (Figure 4.7-d and Figure 4.8-d) illustrate that COM-M is markedly inferior to COM-V in terms of users' estimates of the differences between three sizes of a smartphone. The effeteness of COM-V on handling-of-variations is high after the period of 90 s, and it is ≈3.56 times higher than COM-M. In both setups, the user can navigate between the sizes during interactions with the DP. When navigating, the size of the DP is changed, but its scale and perspective view are not changed so that the user can easily compare the sizes. However, in COM-M, the users are required to change their hand pose to grasp the DP of the smartphone possessing the current size. This affects the users' concentration on the values of the previous and current sizes in COM-M.

Overall, **Tr** (Figure 4.7-a and Figure 4.8-a) shows that COM-V is more successful than COM-M in communicating the size of smartphones. When using the DP in the same way as it is used in COM-V, users can estimate a single size and the differences between three sizes. Although COM-M is better than COM-M in the case of a single size, it is incapable of helping users estimate the differences between three sizes. According to **Tr** (Figure 4.7 and Figure 4.8), the best way of using the DP for communicating a single size of smartphone is the projection of the DP on the user's hand. Besides, the best way for communicating three sizes can be achieved when the users are kept focused on the sizes at the time of the navigation between the sizes.

Some other applications of the evaluated effectiveness are discussed in the following. An important question at design concept evaluation is: *when can designers start eliciting user feedback?* The feedback is helpful if it is collected after the time at which the users' estimates are good. The effectiveness of a communication on degree-of-correctness provides the information regarding the time to achieve a certain degree of correctness of user estimates in order to address the question. For example, $\mathbf{Tr}_{DC}$ (Figure 4.8-b) shows that 100% of M_{best} is achieved after the time period of 90 s. Moreover, at design concept evaluation, designers might require users to evaluate several values of a physical characteristic (e.g. different sizes of smartphones). For instance, Ren and Papalambros [18] parameterized the exterior form of a car with 20 parameters (each form can be considered as a set of values of the parameters), and in an evolutionary process, they asked users to choose one out of six forms at each iteration step. By evaluating the effectiveness of the communication of the six different forms on handling-of-variations, $\mathbf{Tr}_{HV}$ provides the information regarding the time for users to compare the forms at each iteration step. For example, $\mathbf{Tr}_{HV}$ in Figure 4.7-d shows that COM-V successfully helps users estimate the differences between three sizes (with the three parameters, i.e. width, height and depth) after 90 s. $\mathbf{Tr}_{HV}$ in Figure 4.8-d illustrates that COM-M is not helpful in the case of three different sizes.

One importance of the methodology is the use of **V** to assess how correctly users can estimate the values of the physical characteristics. Once **V** is defined, the methodology can be used to evaluate the effectiveness of the communication of the physical characteristics. In Sections 4.2.1 and 4.6.2, we showed that how **V** can be defined for the characteristics 'color' and 'size' respectively. Defining **V** is fairly challenging. The values in **V** should be selected to not guide the users to the rendered values, meaning that they should not be obviously dissimilar from the rendered

values. Besides, the users should be able to find the rendered values before their estimates of the rendered values are affected by seeing the other values in **V**.

Overall, the case study showed that the methodology can be capable of determining the best way of using the DP for communicating the size of smartphones so that users can estimate the sizes correctly and quickly. Different ways affect the degree of correctness of the users' estimates. And, the degree of correctness impacts the extent to which the users' feedback on the values of the physical characteristics is helpful in selecting the better values. Therefore, the ways of using a DP can be related to the helpfulness of the feedback.

This methodology is utilized to help using DPs of electronic consumer products in a better way in the communication of form and size in order to enhance the correctness of user estimates. In this Chapter, we evaluated the effectiveness of the tool developed for specification solicitation. We evaluate the effectiveness of the tool developed for concept selection in Section 9.5. The methodology developed in this chapter helped us to develop effective tools for the communications at specification solicitation and concept selection.

Chapter 5 Collection and analysis of user feedback

The number of involved users at conceptual design is limited. Assessing the quality of specification values and design solutions by using the feedback of a limited number of users can incorporate fixation into selection of specification values and design solutions (Section 2.4). The fixation can adapt the selected solutions (i.e. output of a mapping) to the needs of the involved users. In Section 2.4, it was discussed that the fixation can be incorporated if the mean of the users' quantitative feedback is considered as the quality of a represented specification value or a solution. To avoid the fixation, this chapter introduces a process for analyzing users' quantitative feedback collected by scoring. The process adopts statistical hypothesis test to infer whether unequal means can imply unequal qualities. Thus inferred, the process attempts to give a score to each solution or a group of them as their quality. Such process can prevent fixation when choosing the quality values or solutions because the decisions on the quality is made based on the population of the scores not the single mean values. To assess the performance of the process, a case study was done to determine the quality of values of two specifications, width and height of the front face of smartphones. We will show that the process is helpful even if the users or samples of the values are low in number. Besides, it can estimate the quality of the values that are not included in the samples.

5.1 Determining the quality by using user feedback

This section describes the scores and their relationship with the quality. Second, it introduces the process for analyzing the scores to determine the quality. In the rest of this chapter, we describe the process for the design solutions.

5.1.1 Measurement of the quality by using scores

The quality is quantitatively measured by scores defined on a cardinal scale of real numbers in the range of (0, 10]. The scale is cardinal because the differences and ratios between the scores are intended to reflect the degree to which the qualities of solutions are different, e.g. 5 means 2 times lower quality than 10. The scores ≈0 and 10 show that the quality of a solution is the lowest and highest respectively. The score

of 0 is excluded from the scale, as there is no '0 quality' solution in conceptual design, and the lowest quality solution receives the least score of ε>0.

The quality is represented by q and the cardinal scale is denoted by **Q**. Users are asked to assess the quality of solutions by assigning an integer number from **Q** to the solutions. The integer numbers are considered in order to simplify the scoring for users. A score given by user is represented by q_u and defined on the scale $\mathbf{Q}_u$.

5.1.2 A process for analyzing user feedback

A process (PROC) (Figure 5.1) is proposed to assign scores to solutions. To do this, it gathers statistical evidence from q_u of solutions to infer whether the solutions have the same quality or not. Statistical hypothesis test is adopted to draw the inference. The process is explained below for q_u of the solutions from $\mathbf{S}=\{s_1,s_2,\ldots,s_m\}$, and the mission is to assign each solution a score q by using q_u.

PROC comprises several loops (at most m loops). In a loop, in Step-1, all k-combinations (C^k) of **S** are created, where $k \leq m$. This is to test whether there are k solutions that have the same quality but have different means. If the test is positive, the same score is assigned to the solutions. An example of C^k for $k=3<m$ is $C^3=(s_2,s_5,s_6)$.

In Step-2, the mean of q_u, represented by $\overline{q}_u$**,** of all s of each C^k are compared by using statistical hypothesis test to infer whether they are equal or not. The hypothesis H_A states that $\overline{q}_u$ are unequal, and H_0 stands for equal $\overline{q}_u$. Repeated Measures ANOVA (analysis of variance) and paired two-sample student's t-test are utilized for $k>2$ and $k=2$ respectively. H_0 is rejected if at least one $\overline{q}_u$ is different to another one.

In Step-3, when H_0 of a C^k is supported, the entire populations of q_u of the solutions in that C^k are merged. Then, solutions in C^k are given the same score which is the mean of the merged population. After grouping and assigning the score, the merged solutions are removed from **S**, and PROC will not consider them in the subsequent loops after removal. For example, consider that s_2 and s_3 have the scores of {5,10,7,6,5} and {4,8,7,9,6} respectively. For $C^2=\{s_2,s_3\}$, the hypothesis is: the mean of the scores of these solutions are equal. Since k is 2, we use t-test to test the hypothesis. The results of the test are: t-stat=-0.23 and P-value=0.83. According to these results, we fail to reject the hypothesis. Therefore, we consider that s_2 and s_3 has the same quality that is the mean value of their merged scores, i.e. mean value of {5,10,7,6,5,4,8,7,9,6}. This example was based on the results of Section 5.2.3.

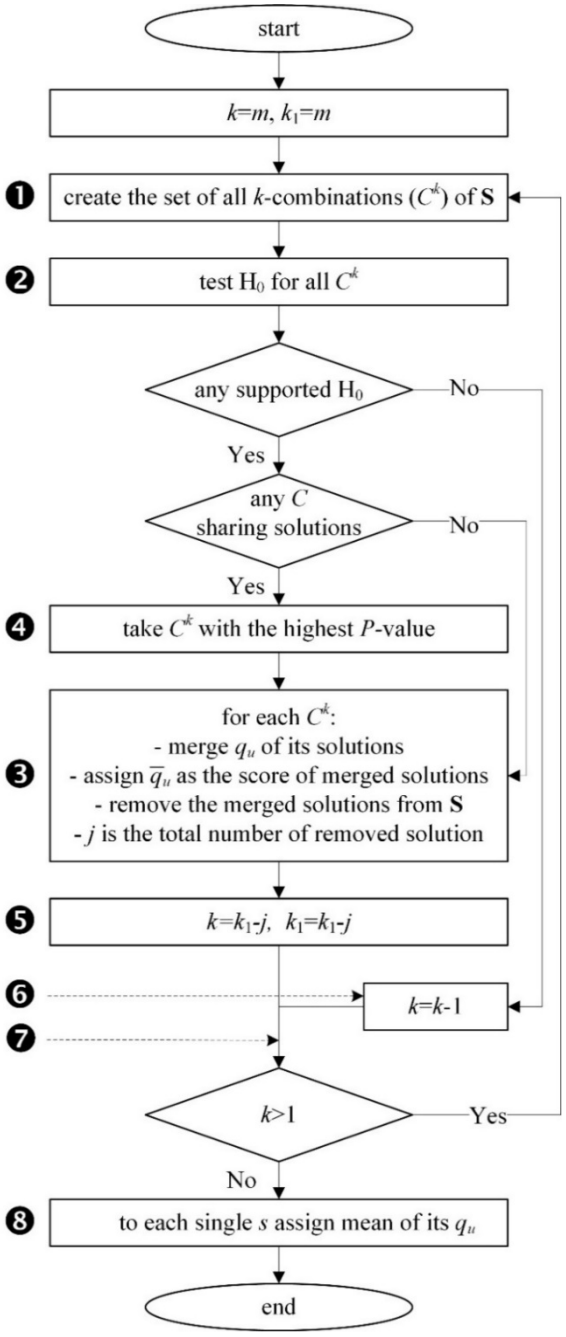

Figure 5.1 PROC for analyzing the scores given by users

In Step-4, when $k<m$, H_0 can be supported for some C^k sharing some common solutions. In this case, q_u of C^k having the highest *P*-value are merged. For example, we assume that H_0 is supported for ${C^3}_1=(s_2,s_3,s_4)$ with *P*-value=0.7 and for ${C^3}_2=(s_2,s_5,s_6)$ with *P*-value=0.6. ${C^3}_1$ and ${C^3}_2$ share s_2. In this case, either solutions in ${C^3}_1$ or ${C^3}_2$ are merged. Since ${C^3}_1$ has the higher *P*-value, first, q_u of s_2, s_3, and s_4 are merged, and then, these solutions are removed from **S**. As such, ${C^3}_2$ is not considered because s_2 is no longer in **S**.

PROC goes to Step-5, if H_0 is supported at least for one C^k. In this step, k that is representing the size of the largest C^k is updated; j is the total number of solutions removed from **S**. For the above example, 6 solutions (i.e. s_1,s_2,s_3,s_4,s_5,s_7) are removed from **S**, and thus, j is equal to 6. PROC goes to Step-6, if all H_0 are rejected. Then, the process continues with a smaller k. In Step-7, k is the size of the largest C^k for the next loop. The process continues in the loop until k>1. After breaking the loop, there may remain some single solutions not merged with the others. In Step-8, each single solution is given the mean of its q_u as its score. k_1 is a temporary variable.

PROC helps to find the solutions that have different $\overline{q}_u$, but may have the same quality. It gives them the same score that is the mean of their united q_u. This can help to avoid the fixation with selecting a particular solution when choosing solutions based on the mean of their scores.

5.2 Case study

This chapter demonstrates that whether the scores assigned by PROC (S-PRO) can reflect the quality of solutions better than the scores obtained by averaging (S-AVE). PROC is evaluated on its predictive validity, meaning that how well it estimates the quality of solutions that are not represented [127-130]. For this end, we considered a set of specification values, sampled them, and divided the samples into two parts called control and non-control parts. Then, we collected user feedback on all parts (S-USE), and adopted S-USE of the non-control part to estimate S-PRO and S-AVE of solutions of all parts. Next, we compared S-PRO and S-AVE of the control part with their corresponding S-USE to determine which one can reflect S-USE better. This case study used the size of the front face (width and height) of smartphones.

5.2.1 Study design

The width of [60,67.5] mm and height of [125,140] mm were considered as the size. Sixteen sizes were taken into account by sampling four values for each of width and height. The samples of width and height were {125,130,135,140} and {60,62.5,65,67.5} mm, respectively. Twenty subjects participated in the study. The subjects aged between 24 to 29 years with mean age of 27 years. The samples {125,130,140}×{60,65,67.5} were considered as the non-control part, and the rest made the control part. The feedback on the non-control part was utilized to estimate

the scores over the domain of sizes (i.e. [60,67.5]×[125,140]) for each subject. The estimation was performed by using the triangulation method [117]. Then, S-AVE was calculated. By using PROC, S-PRO was obtained. All scores are normalized to 10.

5.2.2 Method

S-USE of the solutions in the control part was used to determine their quality. To investigate which of S-PRO and S-AVE can be similar to S-USE, paired two-sample *t*-test was used. Root-mean-square-error (RMSE) was also employed to obtain the estimation error for S-PRO and S-AVE. To calculate RMSE, S-AVE, S-PRO, and S-USE were sampled by sampling step of 1 mm.

5.2.3 Results

S-USE, S-PRO, and S-AVE are illustrated in Figure 5.2. A visual comparison between the graphs can lead to the conclusion that S-PRO can reflect S-USE better, especially for the three sizes (62.5,130), (62.5,135), and (67.5,135) in the control part. These sizes are labelled by vertical black bars.

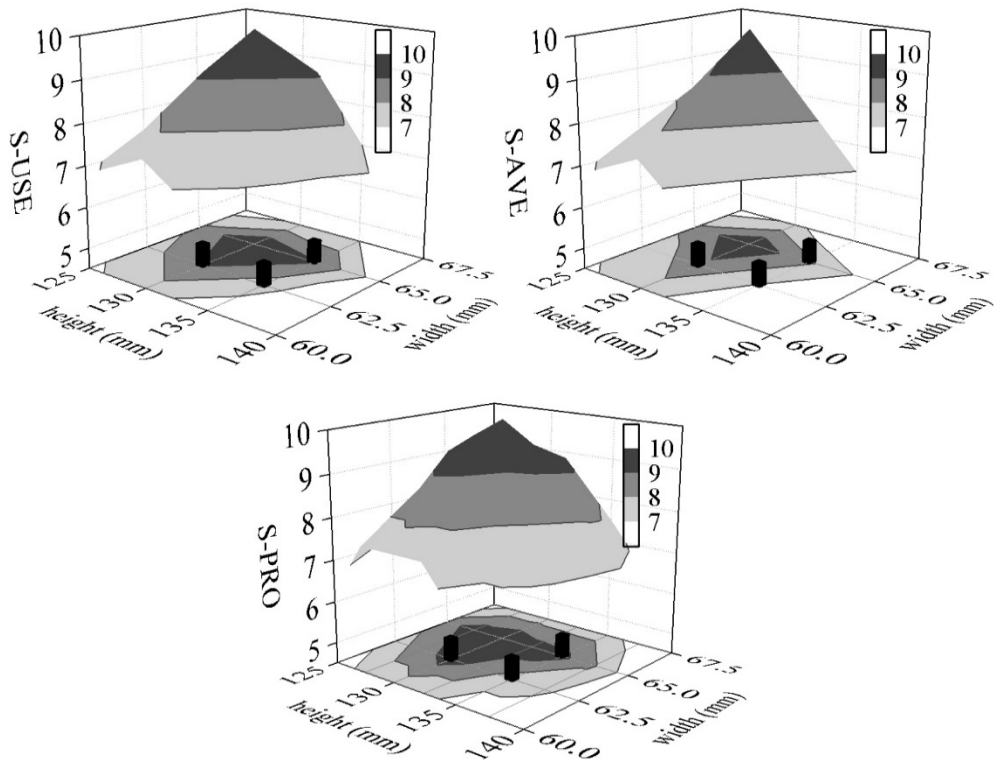

Figure 5.2 The quality of solutions in width×height with scores of greater than 7

The scores (mean±SD) of the sizes in the control part are demonstrated in Figure 5.3. Table 5.1 illustrates the results of the *t*-tests. According to the results, S-PRO can result in the scores similar to S-USE. In contrast, strong evidence could be found against equality of S-AVE and S-USE. Moreover, RMSE between S-PRO and S-USE was 0.30 and for S-AVE and S-USE was 0.48, showing that S-PRO can be more similar to S-USE. Overall, it can be concluded that PROC can outperform averaging.

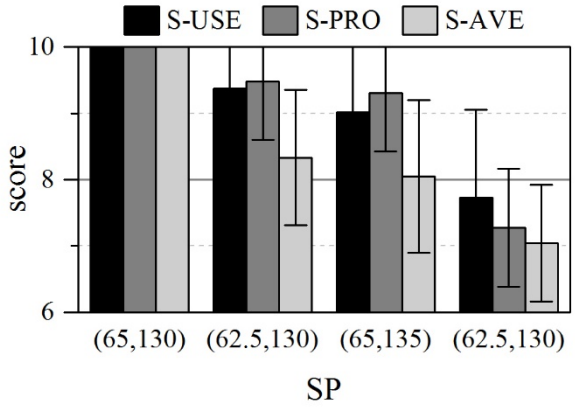

Figure 5.3 The scores of the size in the control part

Table 5.1 The results of the *t*-tests

solution	S-PRO		S-AVE	
	P-value	state	*P*-value	state
(62.5,130)	0.7144	failed to reject	0.0036	rejected
(65.0,135)	0.3629	failed to reject	0.0090	rejected
(62.5,135)	0.2777	failed to reject	0.0001	rejected

5.3 Discussion

S-USE can better estimate the quality of the sizes because more data points were used for the approximation of S-USE in comparison with S-PRO and S-AVE. The number of data points was almost two times greater for approximation of S-USE. S-USE (Figure 5.2-a) identifies the darkest shaded area as high quality sizes ($q > 9$). According to the results of the case study (Figure 5.2), S-AVE, by considering only the mean values of user feedback, incorporated fixation with choosing the sizes

narrowly around (65, 130) mm^2 as high quality sizes. In contrast, the small RMSE between S-USE and S-PRO shows that our proposed method could prevent fixation. Our method could successfully identify the area that contains the high quality sizes (darkest area in S-PRO in Figure 5.2-c) by considering the variance of user feedback on the non-control part. Moreover, the qualities of the sizes in the control part (S-USE) and their interpolated qualities (S-PRO and S-AVE) were also compared (Figure 5.3). Strong statistical evidence was found to support that S-PRO could result in the qualities equal to S-USE, whereas, for S-AVE, we could not find strong evidence. Thus, first, our method successfully interpolated the quality of non-represented design concepts. Second, our method outperformed a recently revealed method in terms of estimating the quality, where the number of samples (nine samples) and the number of user quantitative feedback (five scores) were small. Overall, the developed method effectively reduces the fixation and estimates the quality of design concepts in SDS by using small population of user feedback on a small number of design concepts.

Furthermore, Villa's et al. method is one of the low sensitive methods to the noise in user feedback. As such, to evaluate the sensitivity of our method to the noise, the sensitivity was measured and compared with Villa's et al. method. To do this, the noise of ±10 percentages was introduced to the mean value of three non-control data points that were highly influential to the three control data points marked by vertical black bars in Figure 5.2. The three non-control data points were (60, 130), (65, 130), and (65, 140) mm^2. These points were highly influential because they were the immediate neighbor of the three control points. The impacts of the noise on the estimates of the quality of the control points were measured. RMSEs between S-USE and noisy ones were 0.21 and 0.42 for S-PRO and S-AVE respectively. According to the RMSEs, our method was 2 times less sensitive to the noise than Villa's et al. method. This shows the low sensitivity of our method to the noise.

As a limitation, PROC becomes time-consuming and computationally expensive by increasing the number of samples. We argue that preventing the fixation in concept selection leads to identification of better design concepts and can be worth the imposed time and cost. To address the limitation, clustering the samples before going through PROC can be helpful. As a future work, we aim to incorporate the clustering into the method. In addition, we showed that the method worked well with quantitative feedback collected by scoring method. Further studies are required to

investigate how successfully the method works with other types of quantitative feedback and/or quantified qualitative feedback.

A process was proposed to perform statistical analysis on user feedback to estimate the quality of design solutions better. This process will be used in Chapter 6 to analyze user feedback on the specification values of hand-held electronic consumer products.

Chapter 6 Specification solicitation to identify the best specification values

This chapter introduces the methodology of specification solicitation (Task 1 of the framework). Specification solicitation aims to identify highest quality SPs (Task 1, Section 3.4) from PDS so that the product can evoke users' positive purchasing decisions in the market. By increasing the dimensionality of PDS (i.e. the number of specifications and the range of their values), identification of the highest quality SPs becomes difficult because of user fatigue [35, 36]. Users may be able to deal with one to two specifications, whereas, when encountering more than two specifications, taking account of the correlation between the values of the specifications can cause user fatigue [36]. Therefore, the methodology is devised to determine the quality of SPs with large number of specifications. The capability of the methodology is demonstrated through a case study attending to five specifications of smartphones.

6.1 The methodology of specification solicitation

The methodology identifies f to determine the quality of SPs, i.e. f:SP$\rightarrow q$ (PDS$\rightarrow$**Q**). The quality of a SP is because of its specification values and the correlations between the values (e.g. the ratio between width and height of smartphone) [8, 131, 132]. Collection of user feedback on the correlations requires users to take account of several values at the same time, which can cause user fatigue. To facilitate this, the methodology borrows the approach of WSM to assessment [86], and makes a modification to it to better determine the quality.

WSM comprises two phases, analysis and synthesis. In the analysis phase, WSM decomposes PDS into 1-dimensional intervals each of which representing the value range of a metric. Then, it collects user feedback on SPs against each metric, resulting in the scores of SPs in relation to each metric. This can reduce the likelihood of causing user fatigue because dealing with the values of a single metric at a time may not be difficult for users. Users also assign each metric a weight reflecting the relative importance of the metrics with respect to each other. In the synthesis phase, the scores are weighted and totaled to give the quality of SPs. The correlations between the values of metrics also affect the quality of SPs. However, WSM does not takes the correlation into account and assumes the values are independent, which is not always

true [87]. Therefore, we tailor the approach of WSM to consider the correlations so as to identify *f* reflecting the quality better.

The methodology (Figure 6.1) comprises 4 sequential stages. Stage 1 decomposes PDS for representation to users. Stages 2 and 3 collect user feedback and process the feedback to give scores to each SP. Stage 4 identifies *f* by aggregating the scores.

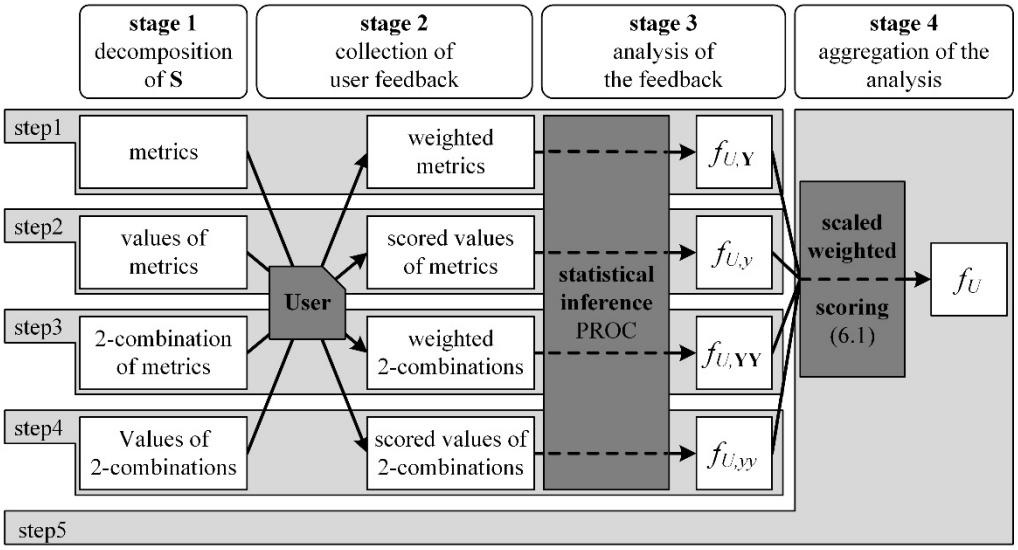

Figure 6.1 The methodology of specification solicitation

6.1.1 Decomposition of product design specification

Considering PDS comprising *m* specifications, the methodology, first, decomposes *m*-dimensional PDS into *m* 1-dimensional intervals of the metrics. The set of all metrics is shown by $\mathbf{Y}=\{y_1,y_2,\ldots,y_m\}$. Second, to take account of the correlations, the methodology considers 2-combinations of set **Y**, i.e. 2-dimensional $y_i \times y_j$, $i \neq j$, represented by *yy*. Each *yy* consists of feasible 2-tuple values. The combinations of two metrics are taken into account because *f* can be improved and taking account of the correlations between the values of two metrics may not be difficult for users [36]. The set of 2-combinations is denoted by **YY**.

By this decomposition, collection of user feedback can be facilitated. Users only require considering how the values of two metrics relate to each other, which is easier than considering values of *m* metrics at the same time. Besides, users can express their expectations about the correlations between two values easier.

6.1.2 Collection of user feedback and analysis

The methodology asks users to weight each metric and 2-combination and allocate scores to their values. Each user weights the metrics to specify their relative importance, and assigns a score to each value of a metric. The same is done for *yy* and their values. The weights and scores, which a user gives, are defined on $\mathbf{Q}_u$ and q_u refers to the collected feedback by weighting and scoring. Evaluating on cardinal scale is adopted so as to use cardinality in q_u for assigning cardinal scores to SPs. PROC (Chapter 5) is utilized to analyze the weights and scores. It is gone through for the weights of *y* and *yy* and the scores of values of each *y* and *yy*. The outcomes of PROC are represented by $f_{\mathbf{Y}}$, $f_{\mathbf{YY}}$, f_y, and f_{yy} (Figure 6.1).

6.1.3 Aggregation of the analysis

Aggregation gives a score from **Q** to each SP in PDS as the quality (6.1). According to WSM, the scores of SPs against each metric, i.e. $f_{y_i}(s)$, is multiplied by the weight of the respective metric, i.e. $f_{\mathbf{Y}}(y_i)$. The weighted scores of a SP against all metrics are totaled to obtain aggregate weighted score (AWS) for SP. The more important a metric is, the more impacts the scores against that metric have on AWS. We modify WSM to incorporate the correlations into the scoring. To do this, the i^{th} root of the scores against each 2-combination, i.e. $f_{yy_i}(s)$, is considered as a scale for AWS, where *i* is the weight of the corresponding 2-combination, i.e. $f_{\mathbf{YY}}(yy_i)$. Each scale is a nonlinear function defined over PDS, and depending on the values of metrics, it scales AWS of SPs. The result of multiplication of all the scales is called aggregate scale (AS). The greater weight of yy_i shows that the scores of SP against yy_i have larger impacts on AS. *f* gives the scaled weighted scores as the quality of SP, and thus, this extension to WSM is called Scaled-WSM. The divisions by 10 is to scale the codomain of the associated *f* to interval (0,1]. The division by *m* is incorporated because of *m* summations in AWS. *q* is in the interval **Q**=(0,10].

$$q=f(\mathrm{SP})=\frac{1}{m}\cdot\underbrace{\prod_{j=1}^{k}\sqrt[\frac{f_{\mathbf{YY}}(yy_j)}{10}]{\frac{f_{yy_j}(\mathrm{SP})}{10}}}_{\mathrm{AS}}\cdot\underbrace{\sum_{i=1}^{m}\left(\frac{f_{\mathbf{Y}}(y_i)}{10}\cdot f_{y_i}(\mathrm{SP})\right)}_{\mathrm{AWS}} \tag{6.1}$$

Where, $\sum$ and $\prod$ sings stand for summation and product respectively. k is the total number of considered correlations (i.e. the number of elements of **YY**).

The capabilities of Scaled-WSM to determine the quality of SPs are demonstrated in detail by using the results of our case study in Sections 6.3 and 6.4. Scaled-WSM is graphically illustrated in Figure 6.2. Scaled-WSM incorporates AS in the typical table of WSM. The table is filled by using PROC and (6.1).

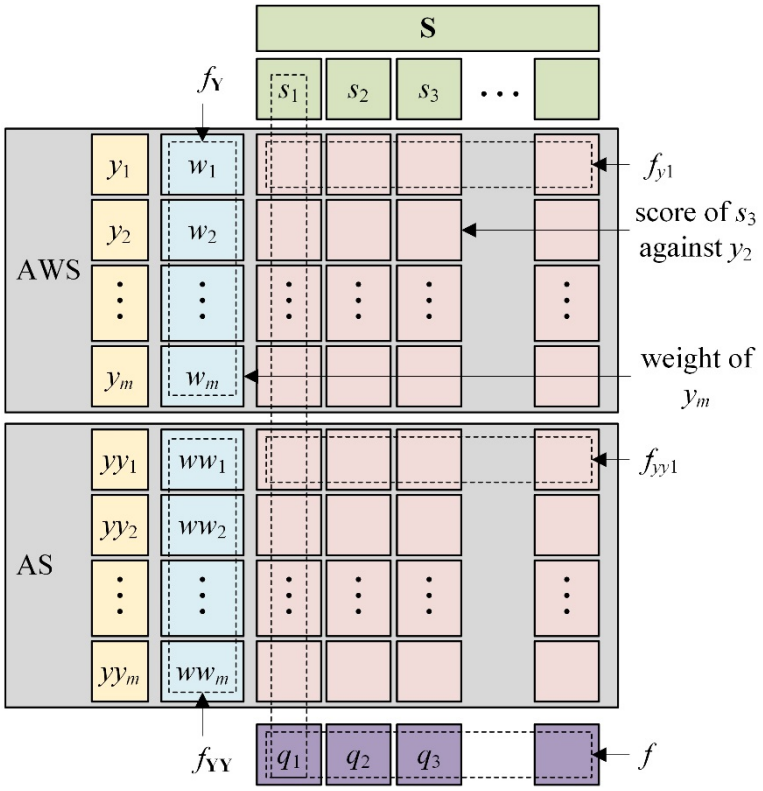

Figure 6.2 The table of Scaled-WSM (extended table of WSM)

6.2 Implementation of specification solicitation

This section explains how user feedback is collected, and $f_{\mathbf{Y}}$, $f_{\mathbf{YY}}$, f_{y}, and f_{yy} are formed and aggregated to obtain f. We describe the steps of the methodology (Figure 6.1). Each user follows all the steps.

Step 1: The weight of metrics. First, the user chooses the most and least important metrics, and then, he/she assigns them a weight from $\mathbf{Q}_u$. The most important metric must get the weight of 10. Second, the user weights the rest of metrics by comparing them with the most and least important ones. As such, the weights by the user can

give the relative importance of metrics. After collecting feedback of all users, PROC is utilized to allocate a weight from **Q** to each metric. The outcome is $f_{\mathbf{Y}}$:**Y**→**Q**.

Step 2: The scores of values of metrics. The methodology gets users' help to define f_{y_i}(SP) on the interval of values of y_i. Each user draws a function over the interval to give a score to each value. Thus drawn by all users, PROC is employed to assign a score to each value of y_i.

To draw the function, first, the user is asked to find the highest and lowest quality values and assign a score to them. The highest quality one must get score of 10. Second, the user gives a score to the boundaries of the interval (if not scored) in relation to the scores of the highest and lowest quality values. The set of these scored values of y_i is called $\mathbf{SV}_i=\{v_{i,1},v_{i,2},\ldots,v_{i,n_i}\}$, where n_i is the total number of the scored values. Third, the user draws f_y by using Table 6.1. Table 6.1 maps the user's explanations (statements) into scores of the values by using the graphs corresponding to the statements. The graphs interpolate scores of values between each two successive v. An example of scoring of height by a user is shown in Figure 6.3. The user gave the scores of 10 and 1 to v_2 and v_3 respectively, and assigned scores to the boundaries (i.e. v_1 and v_4).

Table 6.1 can obviate the need for the users' vague and subjective statements about the quality of the values. Additionally, it can remove the need for interpreting the statements to estimate the quality.

Table 6.1 The statements and their corresponding graphs

	statements	graphs
1	Quality of values, very close to the highest quality value, is very high	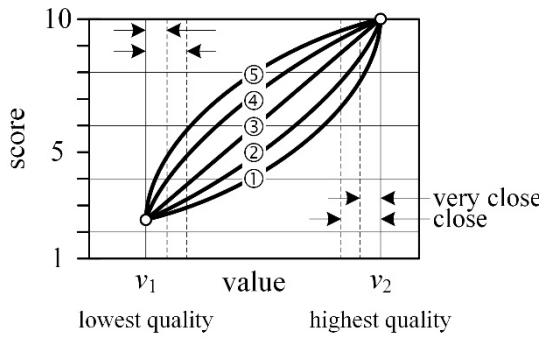
2	Quality of values, close to the highest quality value, is high	
3	Quality reduces gradually	
4	Quality of values, close to the lowest quality value, is low	
5	Quality of values, very close to the lowest quality value, is very low	

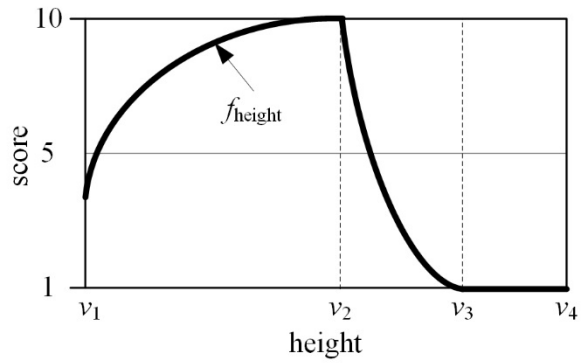

Figure 6.3 An example of drawn f_{height} by a user

The drawn functions by all users are aggregated to form f_{y_i}. If y_i has discrete values, the scores are assigned to each value similar to Step 1. For continuous y_i, its interval is sampled, and the samples are given scores similar to Step 1. Then, to have continuous f_{y_i} for a continuous y_i, the scores of values between two adjacent samples are interpolated by using straight lines connecting the scores. The output is f_{y_i}:$y_i \rightarrow \mathbf{Q}$.

Step 3: The weight of 2-combinations. This step is similar to step 1. The output is $f_{\mathbf{YY}}$:$\mathbf{YY} \rightarrow \mathbf{Q}$.

Step 4: The score of values of 2-combinations. f_{yy_i} draws a 3-dimensional surface over the values of a 2-combination. We take the approach of adaptive sampling to represent the values to users.

The methodology samples the domain of a 2-combination for each user and based on his/her drawn f_y of metrics of the 2-combination. The Cartesian product of **SV** of the metrics gives the samples. For instance, for y_1 and y_2, $\mathbf{VV}=\mathbf{SV}_1 \times \mathbf{SV}_2$ gives the samples. The total number of values in **VV** for combination of y_i and y_j is $n_i \cdot n_j$. **VV** contains combinations of the highest quality values, the lowest quality values, the highest and lowest quality values, the borders, and borders and highest/lowest quality values. These combinations can cover several relationships between the values of the metrics. Therefore, such sampling can be more effective than the typical sampling.

To identify f_{yy_i} of the user, scores of the other values are interpolated by using Shepard's method (6.2), which is an inverse distance weighting method [133]. Shepard's method gives a value a score that is the average of weighted scores of the samples (v). The weights are given according to the distance of the values from the samples. A weight decreases when the distance increases. The samples are given their original scores. Shepard's method was considered because it has no tunable

parameter. Besides, it deals well with the collinearity of samples, which occurs in our sampling method. Besides, in our case, the number of samples for the interpolation is small. Shepard's method works better than the other interpolation methods when the number of samples is small [133].

$$f_{yy_{ij}}\left(yy_{ij}\right)=\begin{cases}\dfrac{\sum_{l=1}^{n_i \cdot n_j} w_l \cdot q_l}{\sum_{l=1}^{n_i \cdot n_j} w_l}, w_l=\dfrac{1}{\left\|yy_{ij}-v_l\right\|^2} & \text{if } yy_{ij}\neq v_l \\ q_l & \text{if } yy_{ij}=v_l\end{cases} \tag{6.2}$$

Where, $\|\cdot\|$ denotes Euclidian distance, and q_l is the score of sample v_l.

f_{yy} of all users are aggregated similar to aggregation of f_y. But, the interpolation is done by triangulation method [117]. The output is f_{yy_i}:$yy_i \rightarrow \mathbf{Q}$.

Step 5: The score of SPs. It is estimated by using (6.1). To use this equation, the domain of f_{yy} and f_y must be extended to PDS. They are defined on 2- and 1-dimensional domains in steps 3 and 4, respectively. To extend the domains, each SP that has *yy* and *y* as entry inherits the scores of *yy* and *y*. For example, considering $SP_1=(y_1,y_2,y_3)=(0.2,150,35)$, $f_{y_1}(SP_1)$ is equal to $f_{y_1}(0.2)$ because the value of y_1 of SP_1 is 0.2. Thus extended, (6.1) aggregates the functions to obtain *f*.

6.3 Case study

To demonstrate the feasibility of the methodology and its capabilities to determine the quality of the specification values, an experimental study was conducted on identification of the highest quality SPs of smartphones. We considered y_{width}, y_{height}, y_{depth}, y_{weight}, and $y_{\text{talk-time}}$.

6.3.1 Experiment Setup

The PDS is a 5-dimensional space, comprising feasible values in $y_{\text{width}} \times y_{\text{height}} \times y_{\text{depth}} \times y_{\text{weight}} \times y_{\text{talk-time}}$. It was decomposed to five metrics and three highly correlating 2-combinations, $\mathbf{YY}=\{yy_{\text{width}\times\text{height}}, yy_{\text{talk-time}\times\text{depth}}, yy_{\text{talk-time}\times\text{weight}}\}$. The intervals of the metrics are illustrated in Table 6.2. They were specified based on specification values of several smartphone products available in the fourth quarter of 2013.

Table 6.2 The list of metrics and their intervals

y	interval	units
height	[100,150]	mm
width	[50,80]	mm
depth	{5,5.5,6,…,9.5}	mm
weight	{100,110,…,160}	g
talk-time	{8,9,…,15}	h

Twenty subjects participated in the study. Their ages were between 23 to 30 years with mean age of 26 years. All the subjects were users of smartphone and informed that they were assigning scores to the values of smartphone specifications. **Y** and **YY** were explained to the subjects. Each metric and its values were demonstrated by using a smartphone product as an example. The scores were also described.

Figure 6.4 shows a screenshot of the interface used to help the subjects draw f_y over the values of the metrics. To communicate **VV** of $yy_{\text{height×width}}$ to the subjects, the mixed reality system introduced in EXP-D (Section 3.5.1) and validated in COM-M (Section 4.6.1) was utilized.

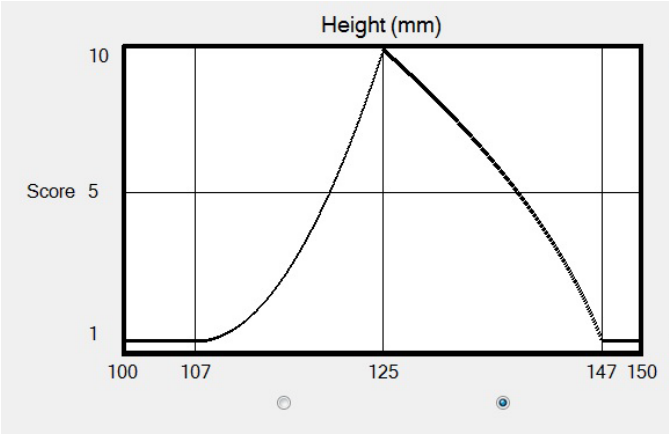

Figure 6.4 The interface for drawing f_y over the interval of the height

We interviewed each subject to determine the quality of the values of y_{weight}, $y_{\text{talk-time}}$, $yy_{\text{talk-time×depth}}$, and $yy_{\text{talk-time×weight}}$. Regarding the metrics, the values were scored by using the same interface used for the geometrical dimensions (Figure 6.4). Regarding yy, we used tables showing the values of the metrics against each other. The tables illustrated values of $y_{\text{depth/weight}}$ and $y_{\text{talk-time}}$ in the rows and columns respectively

(Figure 6.5). In the tables, the cells corresponding to infeasible values were crossed (the feasible values were specified based on the specifications of the smartphone products in the market). To score the correlations, the table were given to each subject to allocate a score to his/her associated values in **VV** (the cells corresponding to his/her **VV** were highlighted). They were also asked to find all values that could get the scores of 1 and 10 so as to collect more feedback.

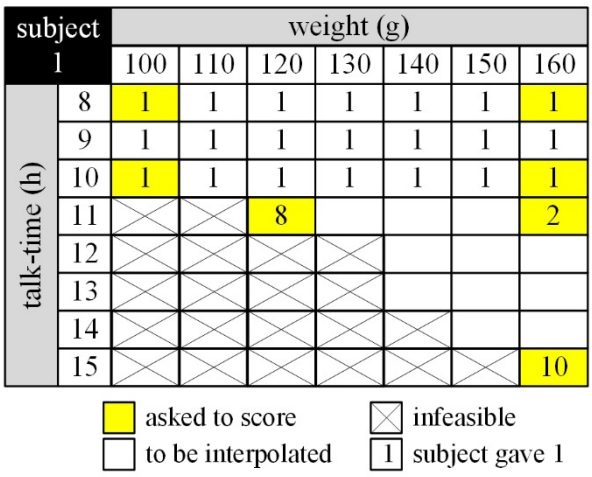

Figure 6.5 An example of the table of correlations of talk-time and weight, the table was filled by subject 1

The subjects were also asked to allocate scores to two groups of SPs (Table 6.3). Group 1 comprised six SPs based on specification values of Apple iPhone 5S, and Group 2 consisted of six SPs based on Samsung Galaxy S5. To allocate the scores, the highest quality SP in each group must be assigned the score of 10, and the others were given scores in relation to their respective highest quality ones. These scores were considered as the control scores to evaluate the validity of the results.

6.3.2 Results

Each subject allocated scores to 32 values (13 values for the metrics and 19 values for the 2-combinations), and weighted five metrics and three 2-combinations, in total. The results of the steps of the methodology are given in the following.

Step 1. Figure 6.6 illustrates $f_{\mathbf{Y}}$. PROC, in its third loop, found that the levels of importance of y_{width}, y_{height}, and y_{weight} can be similar, P-value<0.05. Thus, the mean of their merged weights was assigned to them. In the fourth loop, for $y_{\text{talk-time}}$ and y_{depth},

strong evidence was found to reject H_0 (Section 5.1.2), *P*-value<0.05. Therefore, $y_{\text{Talk-time}}$ and y_{depth} were given the mean of their own weights as their level of importance. These two metrics got the most and least weights respectively, suggesting that it is better to focus on the values of $y_{\text{talk-time}}$ 'more' than y_{depth}. The term 'more' can be described by using the difference between the weights of these metrics.

Table 6.3 The specification values defined based on the smartphone products

group	SP	height (mm)	width (mm)	depth (mm)	weight (g)	talk-time (h)
1 based on Apple iPhone 5S	1	125	60	7.5	110	10
	2	125	60	8	130	11
	3	130	60	7	120	10
	4	130	60	8	120	11
	5	130	65	7	110	10
	6	130	65	7.5	150	11
2 based on Samsung Galaxy S5	1	140	80	7.5	145	11
	2	140	75	8	145	11
	3	140	75	7	130	10
	4	135	80	7	130	10
	5	135	80	7	145	11
	6	135	75	7.5	140	11

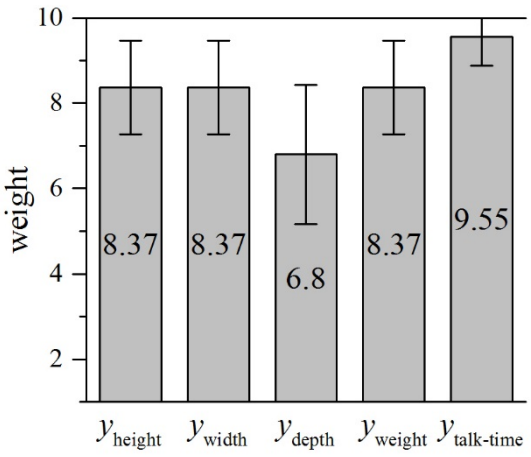

Figure 6.6 The weights of the metrics

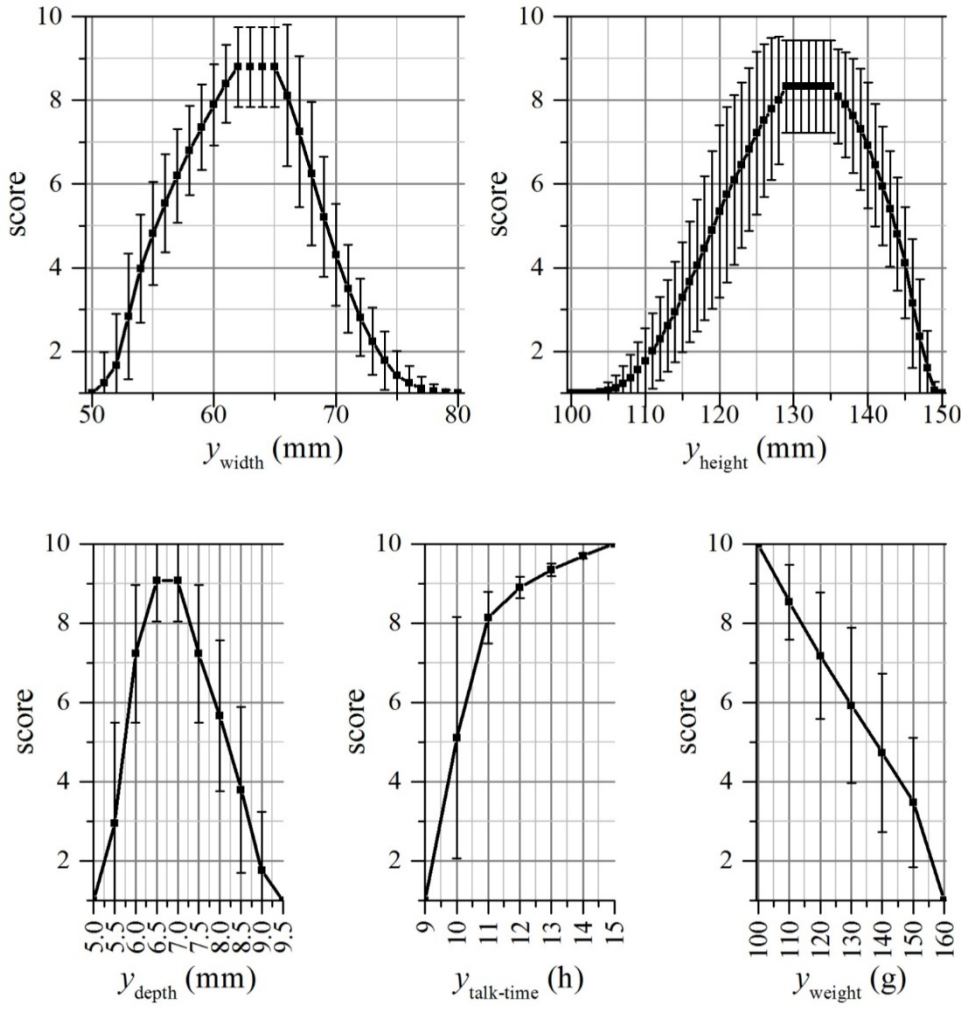

Figure 6.7 The scores of the values of the metrics

Step 2. f_y are illustrated in Figure 6.7. f_{height} shows that the interval [129,135] could get the highest score 8.33. f_{height} shows that the better values of y_{height} may be in [129-Δ,135+Δ]. f_{width} demonstrates that the better values of y_{width} may lie in the interval [62-Δ,65+Δ]. f_{depth} may suggest [6,8] as the target values for depth. $f_{talk-time}$ shows that the higher talk-time has higher quality. SD of talk-time of 10 h is wide, and may imply that its score can considerably vary for different subjects. $f_{talk-time}$ demonstrates that talk-time less than 10 h has low quality. f_{weight} shows that lighter smartphones have higher quality. The above f_y can help to set target specifications because they can give a rough idea about the higher quality values.

Steps 3 and 4. $f_{\mathbf{YY}}$ and f_{yy} are shown in Figure 6.8. It shows that the order of quality of *yy*, from highest to lowest, is $yy_{height\times width}$, $yy_{talk-time\times depth}$, $yy_{talk-time\times depth}$. $f_{height\times width}$ identifies an elliptical area (scores>6) whose values have higher quality than the other

values. The ellipses can provide design group with the correlations between y_{height} and y_{weight}. $f_{\text{talk-time×depth}}$ shows that the thinnest smartphone ($5 \le y_{\text{depth}} \le 6.75$ mm) has the lowest quality if their talk-time is less than 10 h. $f_{\text{talk-time×depth}}$ shows the highest quality correlations may be found inside and around the area of [7,8]×[10,11]. $f_{\text{talk-time×weight}}$ demonstrates that two regions with the highest quality. The region in the center shows that the lighter smartphones ($120 \le y_{\text{weight}} \le 130$ g) have higher quality than the heavier ones even though the talk-time is less. The other region implies that the heaviest phones (160 g) have high quality if the talk-time is considerably increased to about 15 h. $f_{\text{talk-time×weight}}$ also indicates that lower weight cannot compensate the low quality of talk-time less than 10 h.

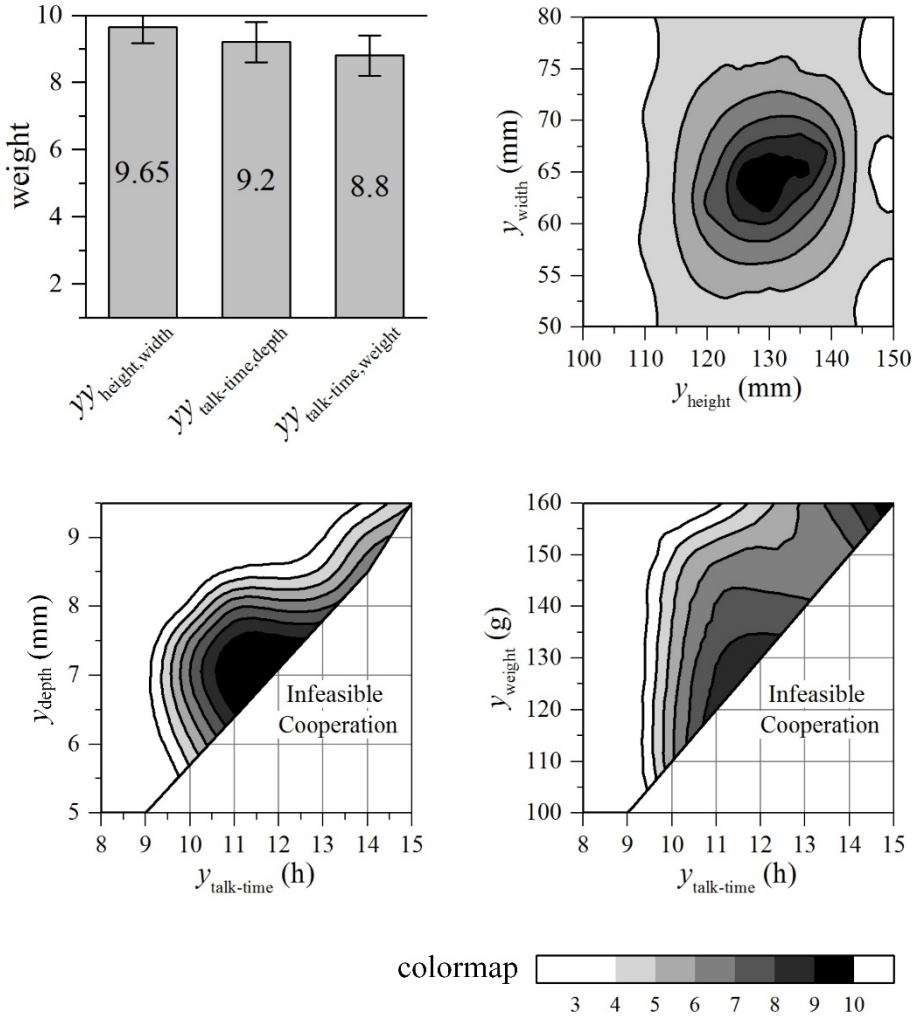

Figure 6.8 The weights and scores of 2-combinations

Step 5. f was obtained by using (6.1). To illustrate f, we plotted all the scores[6] assigned to the SPs with respect to the metrics (Figure 6.9). These plots can show the range of quality of a value by taking account of its correlations with values of the other metrics. For example, SPs with y_{depth} of 9 mm can get the scores of 1 to 4. Such plots can provide objective evidence for alteration of interval of metrics before starting concept generation. For another illustration of f, we focus on SPs with scores≥8 (Figure 6.10). Under this condition, the talk-time is around 11 h, and there are three combinations of y_{depth} and y_{weight}, (7,120), (7,130), and (7.5,120). As is clear, only (y_{depth},y_{weight})=(7,120) can get scores≥9.

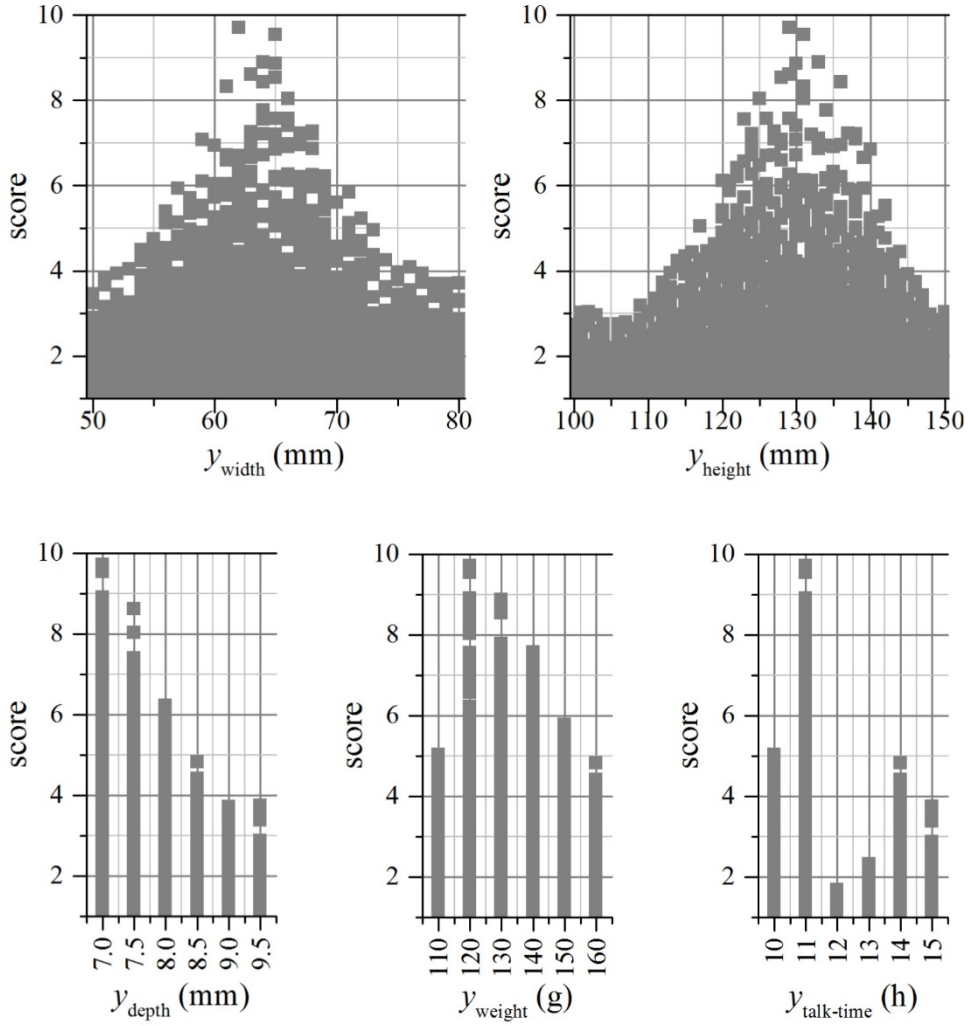

Figure 6.9 The scores that a value could achieve

[6] The scores are scaled so that the highest quality SPs gets score of 10

The pattern of scores in the height-width plane is almost similar for the three combinations. We also plotted the scores against each other; (7,120) and (7,130) against (7.5,120) (Figure 6.11). As can be seen, for each (y_{width},y_{height}), the scores of (7,120) and (7,130) are 1% and 11% greater than the scores of (7.5,120). To sum up, the methodology found that the domain in Figure 6.10-a has the highest quality values for the specifications. The alternatives can be the domains in Figure 6.10-b and Figure 6.10-c.

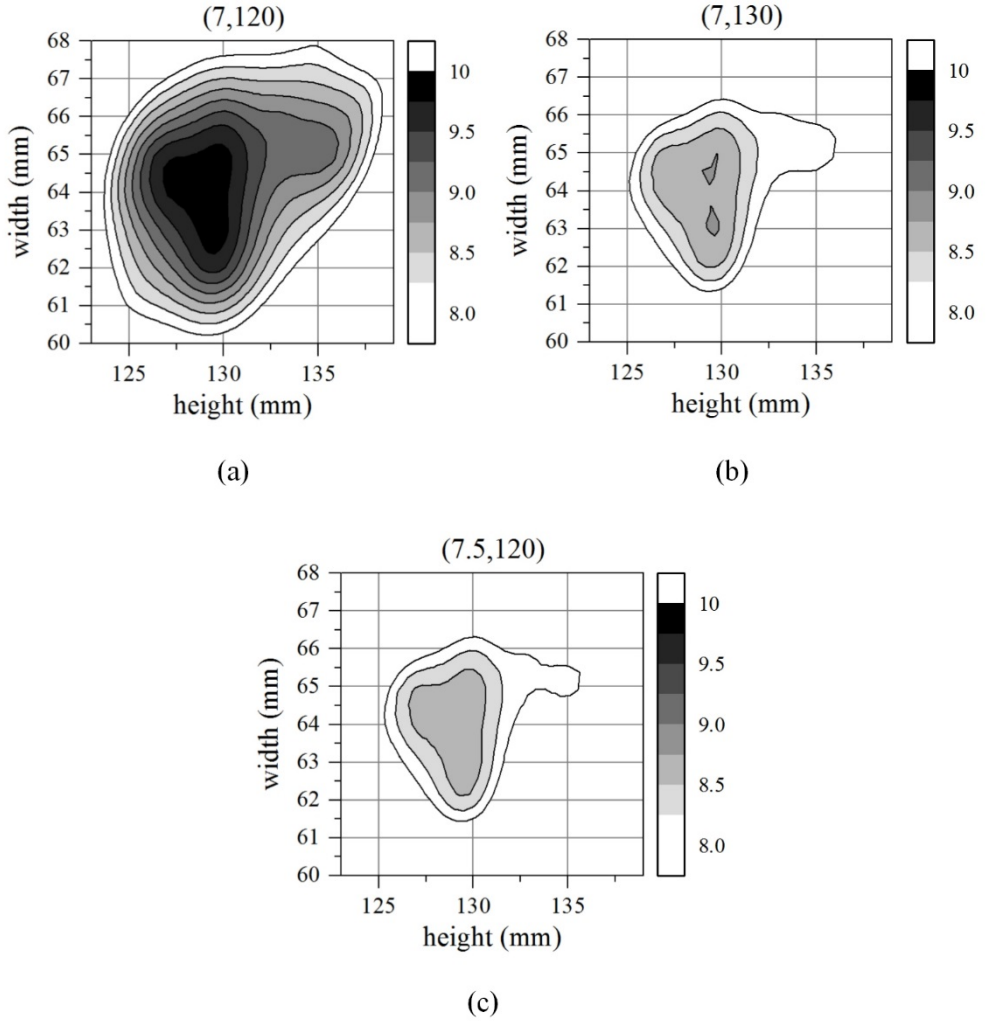

Figure 6.10 The SPs with the scores of more than 8

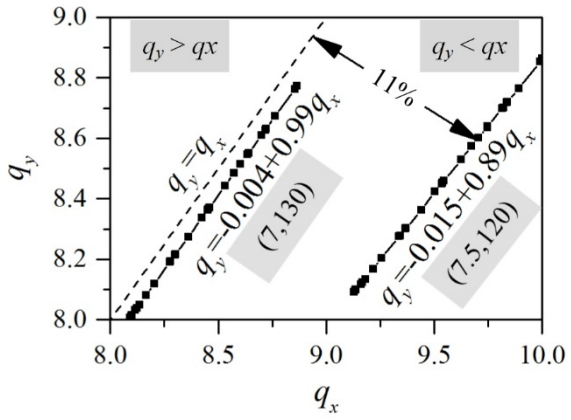

Figure 6.11 The difference between the scores

6.4 Discussion

A methodology was developed to determine the highest quality specification values from a large PDS. We used the methodology to tackle a complex problem with 5 metrics to show the capabilities of the methodology.

To evaluate the capability, we compare the control scores (Section 6.3.1) with the scores that the methodology gave to the SPs in groups 1 and 2 (Table 6.3). The mean±SD of the differences between the scores of the SPs is 0.21±0.40 (Figure 6.12). Such small mean and SD can show that our methodology can successfully give scores to the specification values by utilizing Scaled-WSM.

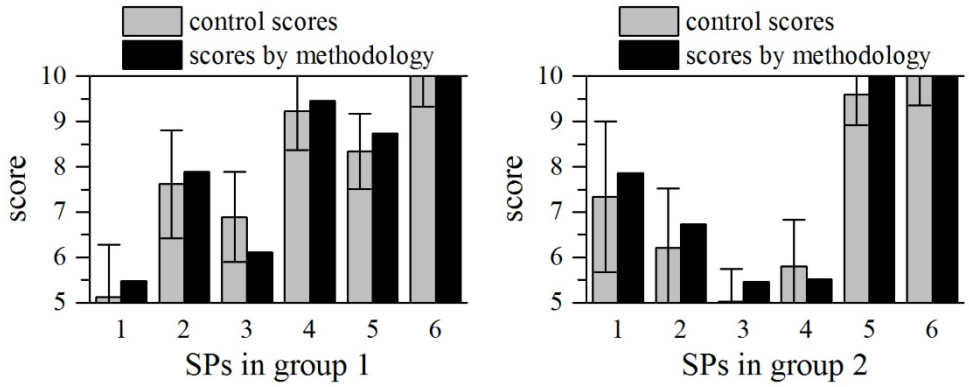

Figure 6.12 The control scores and the scores given by the methodology

The methodology identified a 6-dimensional *f* by using user assessments of only 13 1-dimensional values for the metrics and 19 2-dimensional values for the 2-

combinations. One of the main reasons for achieving this success was the cooperation between Scaled-WSM and our proposed sampling method, which effectively reduces the required number of samples for identification of *f*. Here, by using the results of the case study, we show the capability of this cooperation to identify the correlations between width and height by using user feedback on only nine samples. The correlation was initially obtained by WSM (Figure 6.13-a). Then, it is enhanced by the scale obtained by using feedback on only nine samples taken from the domain of width and height based on the results of WSM for each user (Figure 6.13-b). Figure 6.13-b illustrates that by using the feedback on the samples, the ellipses become smaller and rotate in the height-width plane with respect to their corresponding ellipses (i.e. with the same shading) in Figure 6.13-a. To investigate whether this situation means enhancement, we studied the ratio $y_{\text{height}}/y_{\text{width}}$ for the considered smartphone products. That ratio belongs to the interval of [1.95,2.10]. Two boundary lines of this interval are shown in the diagrams by the dashed lines. As is clear, the ellipses rotate to align better with these lines. Besides, they become smaller to not include the values furtherer from the region between the lines. This can indicate that the correlation shown in Figure 6.13-b can be valid. Therefore, the cooperation between Scaled-WSM and our proposed sampling method is effectively helpful in reducing the number of samples. Overall, our methodology successfully prevented user fatigue when identifying *f* with respect to five specifications, whereas, recent studies such as [35, 36] have not gone beyond two specifications.

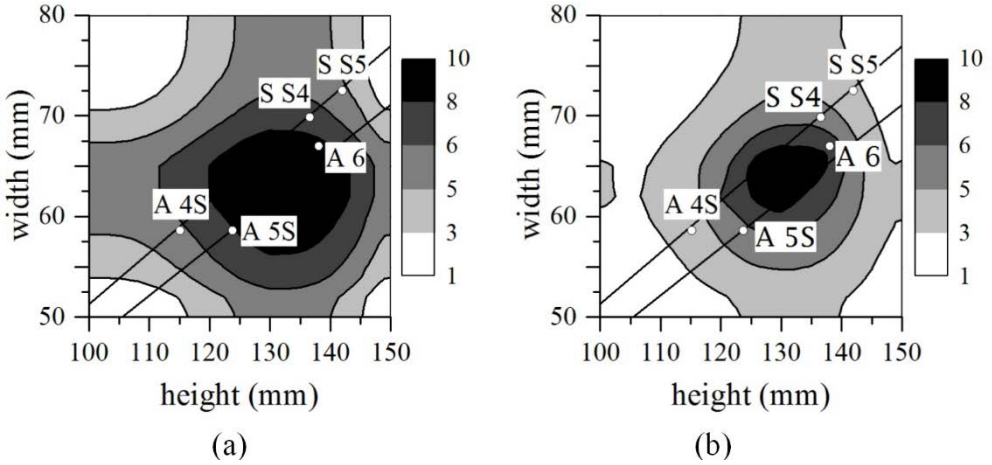

Figure 6.13 Scoring by WSM vs. Scaled-WSM in width-height plane (a) WSM and (b) Scaled-WSM

Furthermore, the methodology can effectively prevent intransitive and inconsistent feedback. This can be attributed to the strategy of the methodology when collecting user feedback. According to the methodology, the full ranges of the values of a metric or a 2-combination are represented to users. Thus, users can take all the values into account when giving feedback on a value. Besides, the interface (Figure 6.4) allows users supervise and revise their feedback. Therefore, the chance of collecting intransitive and inconsistent feedback is reduced.

In the next Chapter, f is used to set the intervals of parameters of design solutions in order to have higher quality solutions at concept selection. Besides, SDS in the next chapter is adaptively sampled by using f and according to users' settings. The application of f at concept selection will be explained in detail in the next chapter.

Chapter 7 Concept selection by using digital prototyping and quantitative feedback

Concept selection searches SDS to identify the highest quality design. A category of methods produces explicit mathematical functions for the quality. They estimate the unknown coefficients of the function by using statistical procedures and user feedback. Rating-based [134] and choice-based [135] conjoint analysis as well as preference mapping [136, 137] have been widely adopted. However, they are difficult to employ in practice for big SDS because users are required to give feedback on a large number of solutions [134]. Adaptive sampling can be used to overcome this difficulty so as to represent a big SDS to users [138]. Another category of methods is based on human-computer interactions. These methods gradually refine the propositions about user needs, based on user feedback on design samples. IEC, as an example, involves a user as an evaluator and goes through an evolutionary process [34]. It considers user feedback as an implicit function determining the fitness. However, such methods may cause user fatigue because giving feedback can be tiresome [139] and to converge, a user is required to give feedback on typically large number of solutions [140, 141]. Overall, there is a lack of a methodology to identify quality design solutions from big SDS.

Our approach to develop such methodology is to parameterize SDS and allow users to set the value of each parameter so that they can fulfill their needs of smartphone designs. It is based on the notion that users typically know what solutions do or do not fulfill their needs, but they are generally unable to justify their choices or formulate their needs in technical terms [15]. We utilized a system, based on digital prototyping, by which each user can produce a solution by setting the values of the parameters. During user-design interactions, the methodology utilizes the knowledge provided by f (from specification solicitation) so as to sample SDS and make suggestions to users. Users can continue the process by either taking or leaving the suggested solutions. If a user chooses his/her design, he/she continues with setting the values of his/her design. Otherwise, the user continues setting the values for the selected design. Setting the values is continued until the user converges to a satisfactory solution. Through the results of a case study based on smartphone design, we show that our methodology can be capable of identifying a quality solution while preventing user fatigue. For comparison, we also performed the study by using a recently revealed IGA method.

7.1 The methodology of concept selection

The key point of the methodology is that a user iteratively sets the values of the parameters and converges to a solution meeting his/her needs. Analysis of the solutions produced by all users can provide information relating to user needs of the product. The methodology (Figure 7.1) has the following stages:

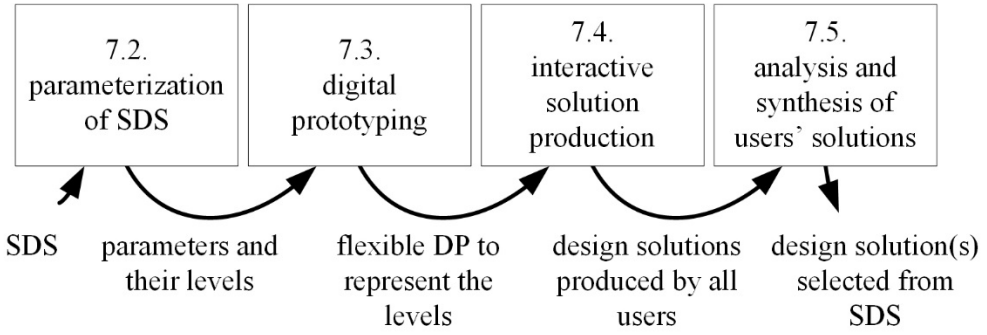

Figure 7.1 The methodology for concept selection

(1) Parameterization of SDS: The solutions, produced at concept generation, are decomposed to the space of parameters. For example, the form of front face of smartphone can come with a range of sharp to round corners, and the corners can be defined by the parameter 'radius'. The decomposition may result in several solution categories each of which sharing the same parameters. The set of parameters and their values are identified at this stage.

(2) Digital prototyping: A flexible DP, compliant with the variations of the parameters, is defined. By setting a value for all the parameters, a digital mock-up is automatically rendered.

(3) Interactive solution production: each user sets the values of the parameters iteratively. When value of a parameter is set, the methodology suggests values for the other parameters and represents the resulting solutions to the user. The suggestions are made based on f provided by specification solicitation. The user can choose either the solution he/she is working on and continue the process with it, or choose one of the suggested solutions and continue to modify the values of the chosen solution. The process continues until the user converges to a solution fulfilling his/her needs of the product.

(4) Analysis and synthesis of users' solutions: The final choices of all users are analyzed to categorize them according to the values of the parameters. This can give an idea about market segments. The solutions in each category are synthesized to propose a solution for each market segment.

7.2 Parameterization of the solutions

In this section, we explain the parameterization of smartphone designs by using f as well as the available smartphone products. Based on a careful investigation into form of smartphone products existing in the market by the 3rd quarter of 2014, we decomposed the designs into 10 parameters illustrated in Figure 7.2. By considering the results of specification solicitation as well, the parameterized SDS is characterized by (7.1). The specification values that could gain the score more than 5 (Figure 6.9), were chosen. p_1 to p_7 define the form of the smartphone. The least change to the values of the parameters except p_3 is set to ±1 mm, and for p_3, it is ±0.5 mm. p_8 corresponds to the morphological shape of the function button and has three options; circle, rounded rectangle, and 'no button'. p_9 and p_{10} give the talk-time and weight respectively. They are defined in terms of the geometrical parameters p_1 to p_4 (Appendix B), and their values are in the range that can achieve scores more than 5.

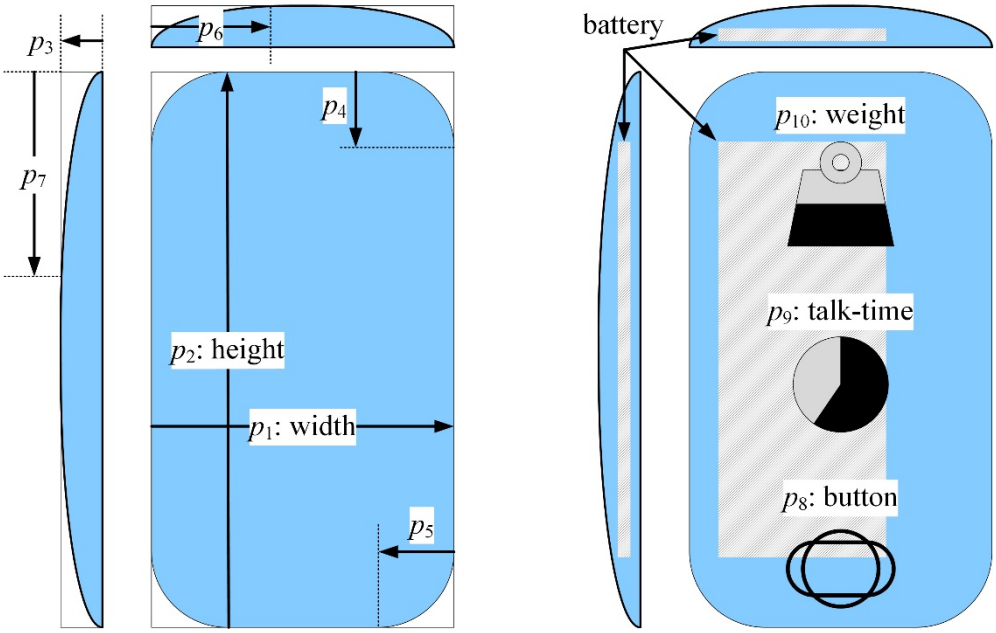

Figure 7.2 The parameters considered for the smartphone

$p_1 \in [58,73]$

$p_2 \in [116,143]$

$p_3 \in [7,8.5]$

$p_4 < 0.05 p_2$

$p_5 < 0.5 p_1$

$p_6 < 0.5 p_1$ (7.1)

$p_7 < 0.5 p_2$

p_8={CIR:circle, ROU: rounded rectangle, NO: no button}

$p_9 = 0.0023 p_1 p_2 - 6.3365, (\in [9,17])$

$p_{10} = 0.0013 p_1 p_2 p_3 + 42.701, (\in [104,158])$

7.3 Rendering the solutions by using digital prototyping

An interactive digital prototyping tool was developed for the Implementing the methodology. The tool was utilized to provide users with the 3D mock-up (DP) of the solution produced based on their inputs. The tool is a virtual working table on which users can produce the form of smartphone by using their hands (Figure 7.3). It comprises an A4 paper that is the working table, a single digital web-camera recording the environment, and a 2D digital screen displaying the environment and DP. The table comes with a simple drawing, and the drawing is a square with side length of 150 mm and a circle next to one of its corners. The drawing is to identify the position and orientation of the table. The tool augments DP on the table and at the center of the square. DP is projected with the same scale and perspective view as the table is being projected on the screen. DP moves with the table, and to explore the form in different views, users can translate and rotate the table.

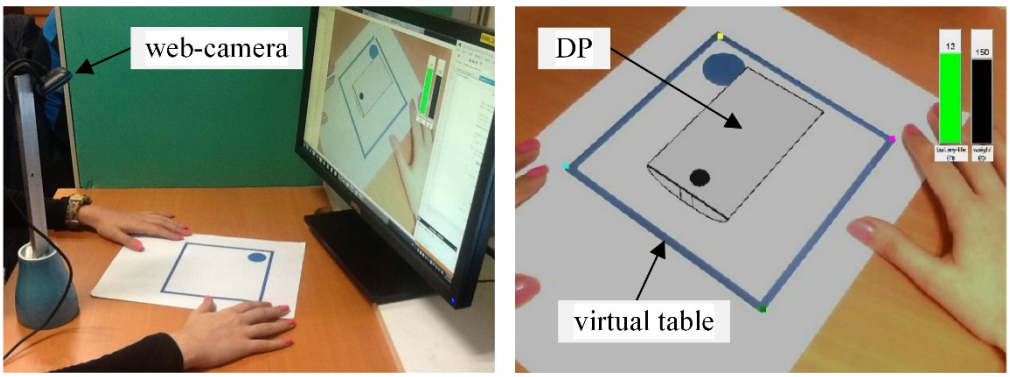

Figure 7.3 The tool and its components

Users can interact with the tool through a virtual menu augmented on the table (Figure 7.4). They can navigate between the items of the menu and change the parameter values by pointing with their fingers at them. In Figure 7.4-left, the user is selecting the item 'height'. In Figure 7.4-right, the user activated 'height' (yellow disc), and can change its value by pointing at the black line; the yellow and orange squares show the current and original values respectively. The menu is popped up by pointing at a corner of the square. The menu allows users to change the values of p_1 to p_8. Value of p_9 and p_{10} are automatically set by using (7.1). The tool is explained in detail in Chapter 9.

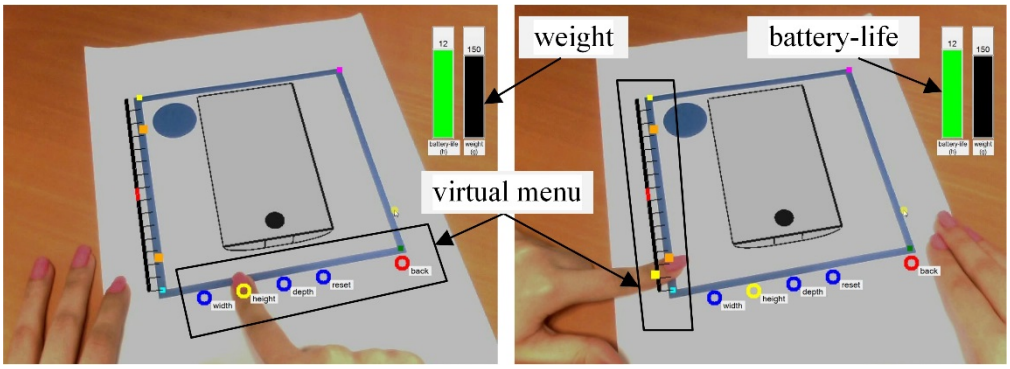

Figure 7.4 The virtual menu

7.4 Interactive solution production

User interaction with the tool is initiated by a raw material augmented on the table. That material is a rectangular box with the minimum value for all the parameters, i.e. (58,116,7,0,0,0,0,NO,10,102). Then, the user can start changing the values of any parameters, p_1 to p_8 (Figure 7.2). When a value is set, three solutions are sampled and simultaneously projected on the screen based on the following rules (it should be noted that when value of a parameter is changed, the value of the other parameters are updated by (7.1)):

(1) When p_1, p_2, or p_3 (p_i) is set, the solutions are suggested by using f. Solution 1 comes with p_j and p_k having the best correlation with p_i, where j,k=1,2,3 and $i \neq j \neq k$. Solutions 2 and 3 are the solutions with the best p_j and p_k for the current solution respectively. If height is changed, p_4 and p_7 are updated so that the ratio between them and height remains unchanged. The same is done

to p_5 and p_6 if width is changed. In any case, p_8 remains unchanged. p_9 and p_{10} are updated by using (7.1).

(2) When p_4, p_5, p_6, or p_7 (p_i) is set, the suggested solutions only come with different values for p_i. If value of p_i is set to 0, the solutions 1, 2, and 3 come with p_i of $Max_i/3$, $2Max_i/3$, and Max_i respectively; where Max_i is the maximum value of p_i. If it is Max_i, the solutions 1, 2, and 3 have 0, $Max_i/3$, and $2Max_i/3$ respectively. If it is between 0 and Max_i, solutions 1 and 3 have 0 and Max_i. Solution 2 comes with half of the new value of p_i if it is closer to 0 than Max_i. Otherwise, it comes with $(p_i+Max_i)/2$.

(3) When p_8 is set, only 1 solution (excluding the current and previous values of p_8) with the other value of p_8 is suggested.

Thus suggested, the user is required to choose one of the four solutions, including his/her solution and the suggested ones. Then, the user is supposed to continue working on his/her choice until producing a solution complying with his/her needs.

7.5 Analysis and synthesis of users' solutions

To provide a partition of users' solutions and to define groups of similar solutions, hierarchical agglomerative clustering (HAC) [142] is performed. HAC starts from singleton clusters (i.e. each cluster contains a single solution of a user), and keeps merging the closest cluster pairs until a desired number of clusters are achieved. After each merging, the merged ones are considered as a new cluster. The distance between the solutions is calculated by the Euclidian distance, and the clustering method is group averaging. The result is a hierarchical structure. After clustering, the centroid of each cluster is considered as the identified quality solution.

To measure the distance, the values of the parameters p_1 to p_7 are mapped to new values. (7.2) gives the mapping. p' can result in the distances reflecting the quality better. For example, we consider two users who set different height values (e.g. 140 and 130) and fully rounded side shape is their quality shape, i.e. $p_7=0.5p_1$. In this case, by using value of p_7, the distance is 0.5(140-130)=5, whereas, p'_7 gives the distance of 140/140-130/130=0. As can be seen, p'_7 can be better than p_7 because p'_7 shows that the fully rounded side shape is the high quality shape for both users, whereas, p_7 cannot reflect such similarity. For p_8, the distance between CIR and ROU is considered as 0.5. The distance of these options from NO is 1 because their

difference lies in putting or not putting the button, and is more major than the difference that can be between the shapes.

$$p'_i = \frac{p_i\text{-}\mathrm{Min}_i}{\mathrm{Max}_i\text{-}\mathrm{Min}_i},\ i=1,2,\ldots,7 \tag{7.2}$$

Where, Min_i is the minimum value of p_i.

7.6 Case study

A case study on the defined SDS for smartphones was done to show the capability of the methodology. We also employed interactive genetic algorithm (IGA) developed by Poirson et al. [20] to perform concept selection so as to compare the performance of our methodology with this high performance method [20, 143]. IGA is a particular case of IEC in which genetic operators such as crossover and mutation are used to modify design solutions. It has been used to capture the aesthetic intention of user, e.g. for car silhouettes [144], and for preference modeling [145]. The experiments conducted by using our methodology and IGA are called EXP-M and EXP-G respectively.

7.6.1 Study design

Twenty subjects participated in both experiments. Their ages were between 21 to 30 years with mean age of 24 years. All the subjects were users of smartphone. The interactions with the tool and virtual menu were explained to them. Each subject had 5 minutes hands-on training to get familiar with the interactions and virtual menu.

EXP-G was done first, and after period of 2 weeks, EXP-M was conducted. In both experiments, the subjects were given 15 minutes to produce their quality solution. After that, they were asked to allocate a score (from $\mathbf{Q}_u$) to the produced solution. For EXP-G, the parameters wheel rate (weight given to a selected solution), crossover rate, mutation rate, and selection rate were 16, 0.8, 0.15, and 0.05 respectively, according to Poirson at al. [20]. Poirson et al. [20] studied the convergence of their IGA method for different numbers of design parameters and levels. In our study, we had eight parameters with three to four levels and expected that the algorithm will be

converged before averagely 15 generations according to [20]. Different GA parameter values can lead to different results. We used the same GA parameter values as those of Poirson's to expect 15 generations for the convergence in order to reduce fatigue. In EXP-G, the population size was 4, which was equal to the number of solutions simultaneously represented to a user in EXP-M.

To compare our methodology with IGA method, the subjects were also asked to rate the methods against semantic dimensions. Four bipolar pairs of descriptive adjectives were considered, with the positive word on the right and its negative counterpart on the left; boring-fun, diverging-converging (whether the methodology/method could help the subject to approach his/her quality solution or not), leading-stimulating (whether the methodology/method could stimulate the subject's creativity when choosing the solutions after each iteration), and distracting-immersive. The rating was done on a scale of -5 to 5. On this evaluation scale, 5 points means that the subject has a very strong positive impression, whereas, -5 points means a very strong negative impression.

7.6.2 Results

In EXP-G (Figure 7.5), among the 20 subjects, 12 declined continuation of the experiment at time around 10±1 min and averagely assigned score of 6.08±1.04 to their solutions. Four finished the task at around 12±1 min and gave score of 10 to their solutions. The rest reached 15 min, and assigned score of 8.25±0.43 to their produced solutions. Those, finished the process, went through 73±11 iteration steps. Overall, 20% of the subjects produced solutions fully complying with their expectations; we call this the success rate. In addition, 60% stopped the process; we call this the fatigue rate because it is the ratio between the number of subjects declined to continue and the number of participants.

In EXP-M (Figure 7.5), 18 subjects completed the task and two stopped at 10 and 12 min. Fifteen out of those 18 subjects finished at around 10.6±1.4 min, and gave score of 10 to their produced solution, and three reached 15 min and gave 9, 9, and 8. The two subjects, who stopped the experiment, assigned 6 and 7 to their solutions. Those, finished the process, went through 20±5 iteration steps. Overall, the success rate was 75%, which is 3.75 times more than in EXP-G. Besides, the fatigue rate was 10%, which is considerably smaller (6 times) than that of EXP-G. Moreover, all the users gave higher scores (≈22±19%) to their solutions in EXP-M than those in EXP-G.

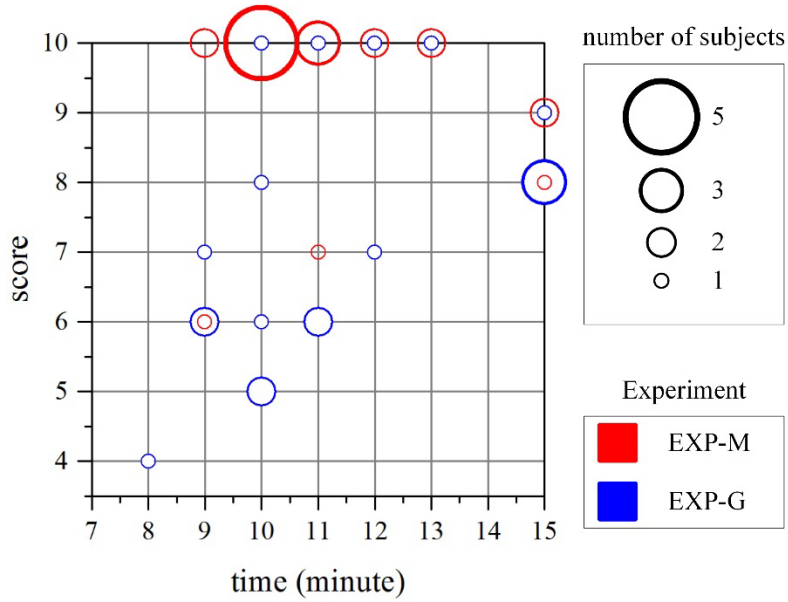

Figure 7.5 The results of the studies EXP-G and EXP-M

Both experiments came up with 4 clusters of solutions (Figure 7.6), labeled by CL-A, CL-B, CL-C, and CL-D. The clusters with the same label in EXP-M and -G are almost similar to each other. In EXP-M, as is clear in Figure 7.6 and Figure 7.7, the distance between solutions in a cluster is 42% shorter (more red, Figure 7.6) than EXP-G, and the distance between solutions of the clusters is 16% longer (more blue, Figure 7.6). This means that the methodology by using *f* could help to better distinct the market segments, and the solution for each segment could be identified easier because the produced solutions were more similar.

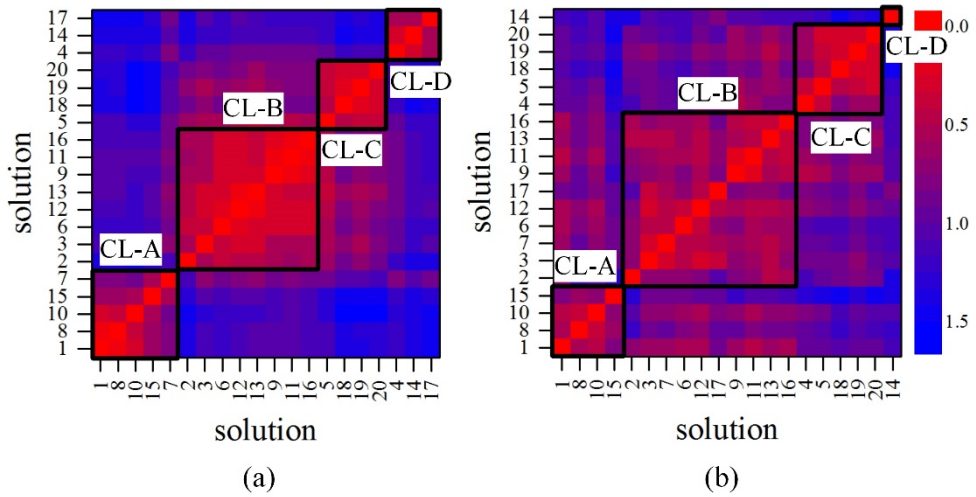

Figure 7.6 The clustering results (a) EXP-M and (b) EXP-G

The identified solutions for each cluster and their scores are shown in Figure 7.8 and Figure 7.9 respectively. The scores of the identified solutions in EXP-M are ≈17±10% greater than the solutions in the corresponding clusters in EXP-G. This can show that EXP-M can identify higher quality solutions than EXP-G. Overall, our methodology can result in more similar and higher quality solutions for each market segment than IGA method.

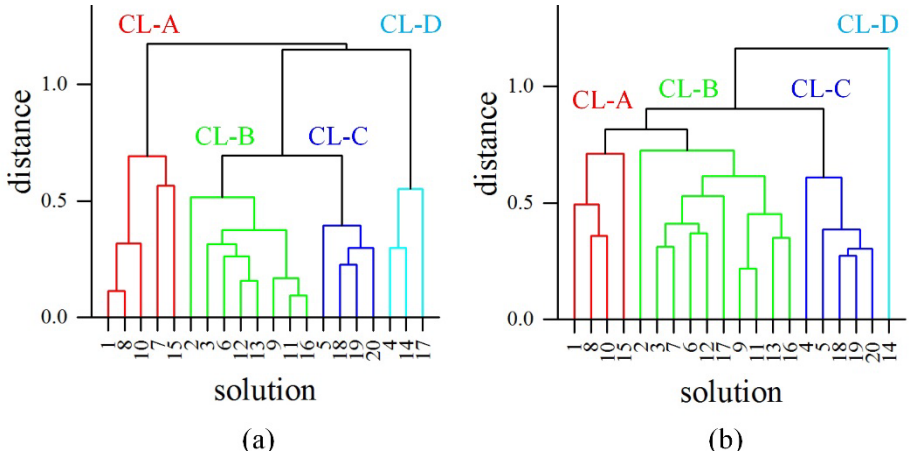

Figure 7.7 The dendrograms (a) EXP-M and (B) EXP-G

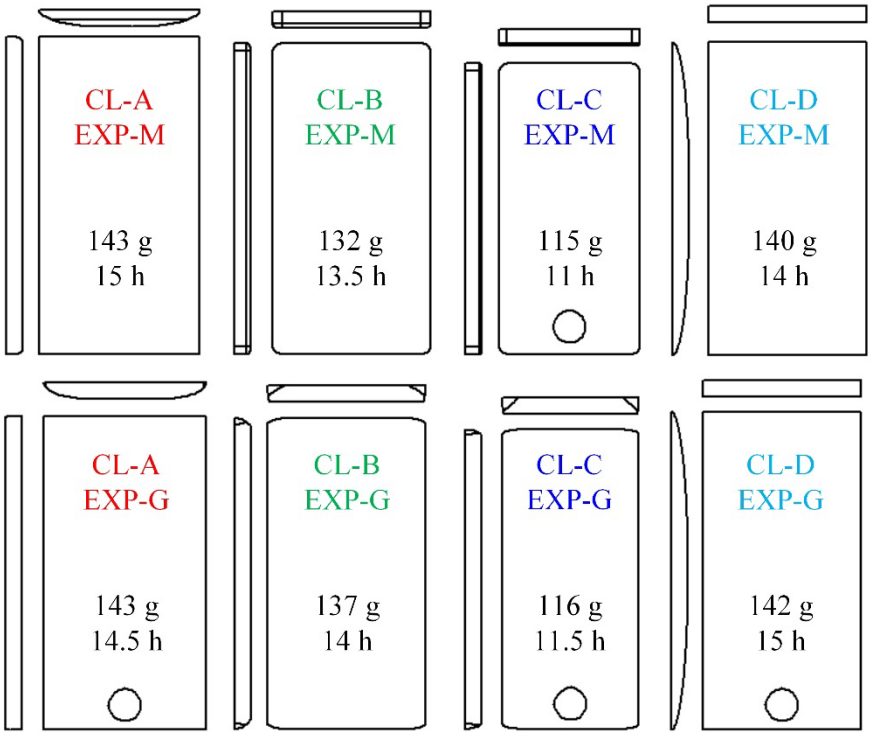

Figure 7.8 The identified solution for each cluster of EXP-M and EXP-G

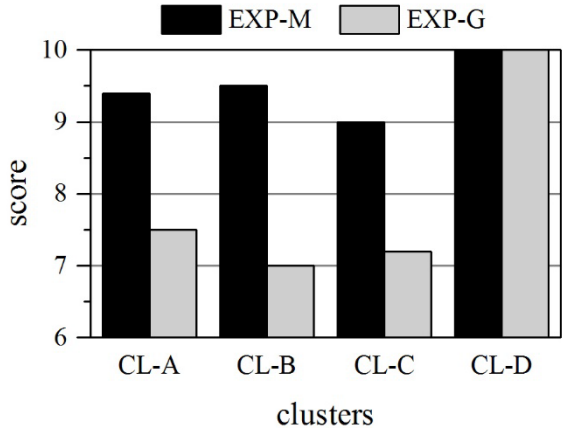

Figure 7.9 The scores of the identified solutions for the clusters

The results of rating (Figure 7.10) show that our methodology can outperform IGA method in terms of the sematic dimensions. Both methods are effective in converging to quality solutions. The ratings on the first and third dimensions can imply that our methodology can encourage users to continue the experiment. This is important because more knowledge of user needs can be acquired. Referring to the ratings on the last dimension, our methodology can immerse users in the process more effectively than IGA method. This can indicate that users can focus on their tasks better, and thus, may come up with higher quality solutions. To sum up, by considering the high success rate, the low fatigue rate, the high quality solutions, and the above evaluations, our methodology based on the proposed digital prototyping tool can be effective in concept selection.

7.7 Discussion

A methodology was proposed for concept selection by involving users. Its approach is to help users produce the solutions, which is different from the existing approaches getting users help to select the solutions. The methodology is based on an interactive digital prototyping tool helping users produce the solutions meeting their needs. A case study was done on a high dimension SDS comprising 10 variables. The study was performed by utilizing our methodology as well as IGA. The results show that the proposed methodology outperforms IGA in terms of less chance of user fatigue, more chance of success, and identification of higher quality solutions.

The main part of this thesis ends here. We have shown that our methodology successfully identified a good product concept at the end of conceptual design by

taking the PDS (Chapter 6) as the input. The next two Chapters explain the methods devised for the tools developed for communication of specification values and design solutions to users.

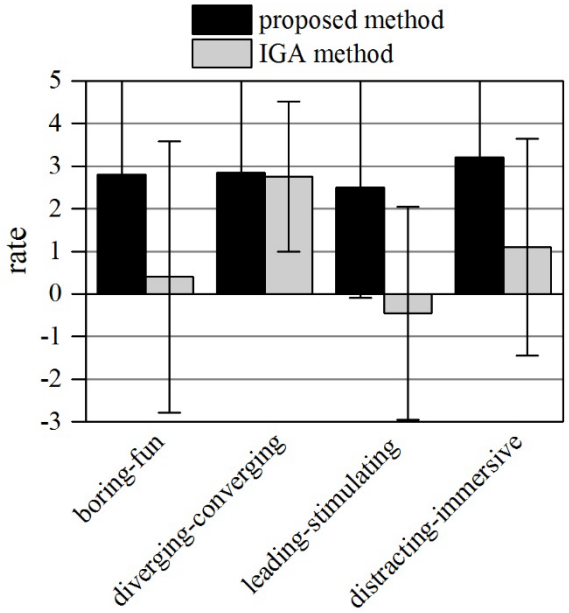

Figure 7.10 Ratings of the proposed methodology and IGA on 4 semantic dimensions

Chapter 8 A method to build hand-object natural interaction in the virtual environment

DP has been widely adopted to assist users in understanding design solutions. To speed up the understanding process, building user-DP interactions closer to natural user-objects (hand-held electronic consumer products) interactions can be of great help [2, 37]. Among these interactions, hand-object natural interaction is one of the important ones because to explore different aspects of the objects (e.g. form and size), users require to grasp and manipulate them in 3D space. As discussed in Section 2.5 and shown in Sections 4.6.3 and 4.7, the nonintrusive vision-based methods projecting DP on user hand with the hand's scale and perspective in real-time (likewise a smartphone in the hand) can speed up the understanding process and enhance the understanding. However, such methods were not developed before, to our knowledge. The available vision-based methods and technologies, offering hand-DP interactions, are limited to gesture-based communications in which users can manipulate DP by commanding through a few predefined gestures. In these cases, shaping the understanding can take longer time and the level of understanding may be lower because the scale and the perspective may not be easily recognized (see COM-V for the effects of the scale and perspective, Section 4.6). Besides, forgetting a gesture corresponding to a command can distract users, and accordingly, affect the understanding. To build hand-DP natural interactions, the hand pose and location (position and orientation) in 3D space should be estimated for grasping and manipulating DP. Therefore, this chapter proposes a method for bare[7] hand pose recognition and localization in 3D space by using a single web-camera[8]. The method relates the pose and location to the morphology of the hand silhouette in the frame plane (or image plane). It uses the information from only one frame to reduce the computation expense so as to build real-time interactions.

---

[7] Ergonomics is one of the major considerations for development of the method because it is used to build interactions with user. To make it easy to use, the method augments no object on the hand.

[8] The amount of computation is one of the major considerations for development of the real-time methods. It is worth mentioning that in digital image processing, a typically-large part of that amount relates to analysis of the inputs (images). Thus, when using several cameras, the analysis can be more computationally-expensive and time-consuming, affecting building real-time interactions. Therefore, we employ only one web-camera.

8.1 Introduction to hand-object natural interactions

Hand-object natural interactions have got particular attentions in augmented reality applications such as design review [38] and computer games [146, 147]. Building such natural interactions, especially for grasping and manipulating virtual objects in 3D space, has been widely addressed by wearable devices such as data glove [100, 101] and position sensors [148] or by vision-based methods [39]. Among the interfaces developed for this purpose, vision-based interfaces have come into interests because they are low cost, user-friendly, and nonintrusive [39-41]. Additionally, they obviate the need for wearing the devices that often inhibit the hand motions and distract users [41]. However, in vision-based interfaces, real-time estimation of the hand location and pose are highly challenging.

Vision-based bare-hand pose estimation has been addressed by two main approaches [104] finding the best match with 1) poses generated by articulated hand models (model-based methods/generative methods) [149, 150], and 2) learned appearances of hand (appearance-based methods/discriminative methods) [151-154]. In model-based methods, hand poses are acquired by capturing images of an articulated hand model generating the poses, whereas, in the appearance-based methods, the poses are taught to the system by taking images of a hand moving with different poses. Gorce et al. [41] developed a comprehensive model-based method to estimate hand pose from monocular video. Their hand model comprised 18 links and had 22-DOF in total. The method could estimate the pose in the presence of large self-occlusions. Bray et al. [155] integrated stochastic meta-descent optimization into particle filtering and proposed smart particle filtering for pose estimation. Smart particles played the role of bunch of particles, and this could reduce the computation expense. DOF considered for the hand was 5-DOF for each finger, 4-DOF for the thumb, and 6-DOF for the wrist. However, these methods may not satisfy the requirements for building the real-time interactions because they are quite computationally-expensive for such applications (e.g. in Gorce et al.'s work, identifying a pose took ≈40 seconds).

To achieve real-time tracking, several hand tracking and pose recognition methods have been developed by using Lucas Kanade algorithm [156], Markov model and particle filtering [150, 157], weighted elastic graph matching [158], Krawtchouk moment features [159], and cylindrical manifold embedding [39]. However, to reduce the computation expense, these studies considered some specific poses. Besides, they

localized the hand and tracked it in the image plane for identification of its 2D trajectory so as to recognize the command sent by it. Thus, these methods are well-suited for gesture-based interactions rather than 3D hand tracking. Some of these methods were extended to localize the hand in 3D space such as those developed by [148, 150] using the model-based approach, and by [146, 156] using the appearance-based approach. For instance, Lee et al. [39] developed a method for estimation of the orientation and pose of a hand in 3D space using cylindrical manifold embedding. However, the method could estimate the orientations for some pre-specified grasping poses. Besides, increasing the number of poses resulted in significant increase in the computing cycles. Alternatively, the hand localization has been performed by attaching 3D position sensors to the hands [148]. Although the hand position and orientation can be estimated in real-time by using the sensors, they are generally expensive and not user-friendly [103]. Overall, a vision-based method for building real-time natural hand-object interactions is considerably lacking.

8.2 An articulated model for the hand-object natural interactions

Grasping and manipulation are performed with the following conditions, in the context of this thesis. The hand grasps the hand-held electronic consumer products 1) between its palm and fingertips, 2) with adjacent fingers attached to each other, and 3) with upright thumb. The hand manipulates the objects with 6-DOF (3 for translation and 3 for rotation) in 3D space. To define these interactions, an articulated model of the hand is created. It comprises two independent articulated mechanisms; hand and manipulator mechanisms. The former grasps DP and the latter manipulates the hand. The mechanisms and their workspace are described below.

The hand mechanism (Figure 8.1-a) has four rigid links and three 1-DOF rotary joints. The joints are at the nodes of the fingers and represented by Z_1, Z_2, and Z_3. These axes are parallel. The coordinate system of the mechanism is represented by XYZ. Its origin is attached to the center (W) of rotations of the hand with respect to the wrist. The coordinate systems are defined according to Denavit-Hartenberg convention. The hand pose is characterized by the angle of the joints, i.e. θ_1, θ_2, and θ_3 (Figure 8.1-b). The joints provide a distance (L_{PF}) between palm (P) and fingertips (F) for grasping an object. F is at the endpoint of the last link, and P is on the line connecting W to F.

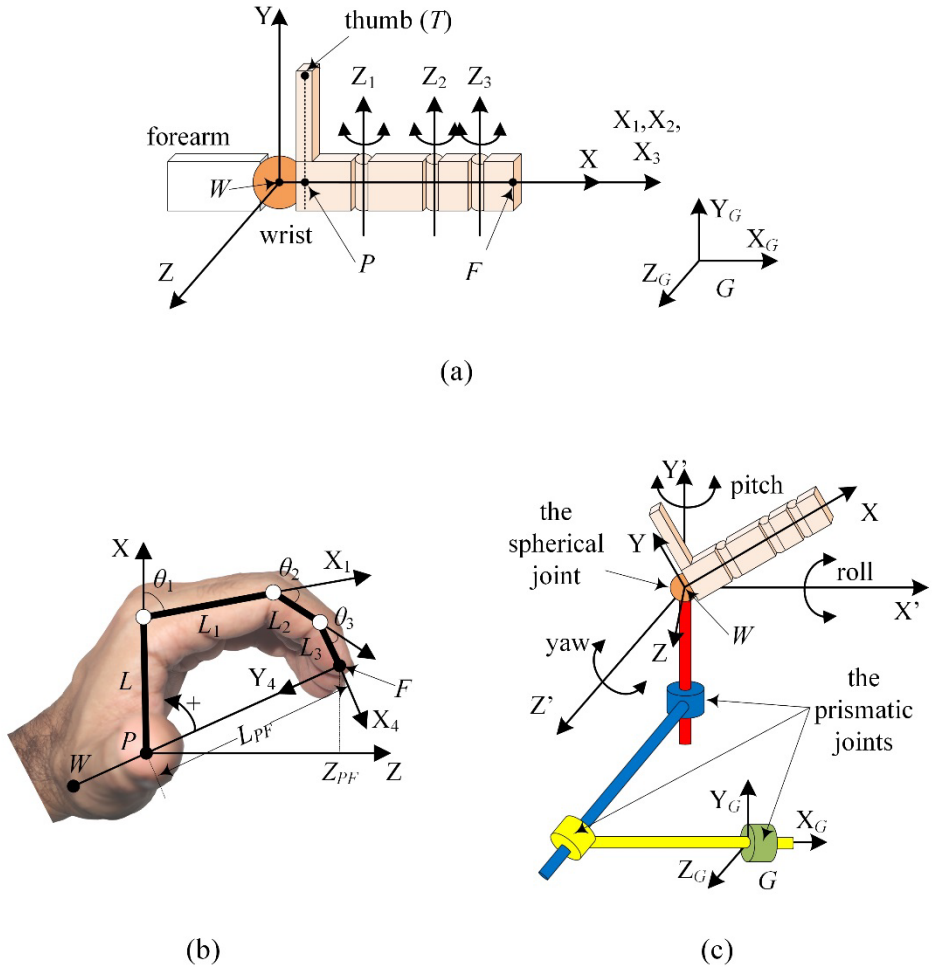

Figure 8.1 (a) the articulated mechanism of the hand, (b) the joint variables of the hand mechanism, and (c) the manipulator mechanism

The joint angles have relationships when the hand grasps an object, $\theta_2 \approx 0.6\theta_1$ and $\theta_3 \approx 0.5\theta_1$. These relationships were derived in a study on grasping objects (Appendix C). Thus, a pose can be characterized if one of the joint angles is known. θ_1 is considered, and it is in the range of [0,80]°. L_{PF} is given in terms of θ_1 (8.1). The relationship between L_{PF} and θ_1 is one-to-one. Appendix D derives the expression in (8.1) and proves its one-to-one property. Therefore, the hand pose can also be characterized by knowing L_{PF}. The abovementioned relationships are used to recognize the hand pose by measuring L_{PF}.

The manipulator mechanism comprises 3 1-DOF prismatic joints and a 3-DOF spherical joint to translate and rotate the hand mechanism respectively (Figure 8.1-c). The intermediate coordinate system X'Y'Z' is attached to the endpoint of the last prismatic joint to make the translations. The spherical joint plays the role of the wrist and its rotation center W is placed at the origin of X'Y'Z'.

$$
\begin{aligned}
&L_{PF}=\sqrt{X_{PF}{}^2+Z_{PF}{}^2}\\
&X_{PF}=L+L_1\cos(\theta_1)+L_2\cos(1.6\theta_1)+L_3\cos(2.1\theta_1)\\
&Z_{PF}=L_1\sin(\theta_1)+L_2\sin(1.6\theta_1)+L_3\sin(2.1\theta_1)
\end{aligned}
\tag{8.1}
$$

Where, L and L_i are the length of the links (Figure 8.1-b).

The hand location refers to estimation of the position of W and orientation of XYZ with respect to the global coordinate system G. The orientation is given by roll, pitch, and yaw in G, or equivalently in X'Y'Z'. These angles are limited to (-70,80)º, (-60,60)º, and (-60,20)º respectively, so that the hand cannot block DP and user can see DP in his/her hand (Figure 8.2).

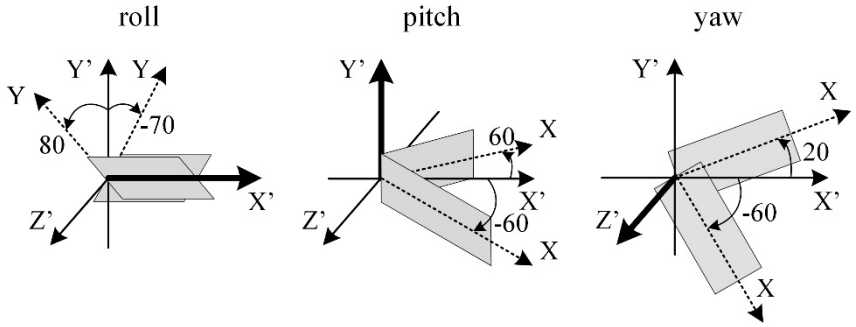

Figure 8.2 The orientations of the hand and the constraints to them

8.3 Idea generation

To develop the method, we aim to identify relationships between parameters that can be measured on a silhouette of the hand and each of L_{FP}, W, roll, pitch, and yaw. Hand pose recognition and localization are considered as two successive processes. Thus, an idea was generated for localization of the hand with known pose and the other for pose recognition.

8.3.1 Localization of the hand with known pose

A hand can be localized by using a single silhouette if three points on the hand with known distances from each other can be identified on the silhouette (Figure 8.3). In addition, the points on the hand must not lie on a straight line on the silhouette.

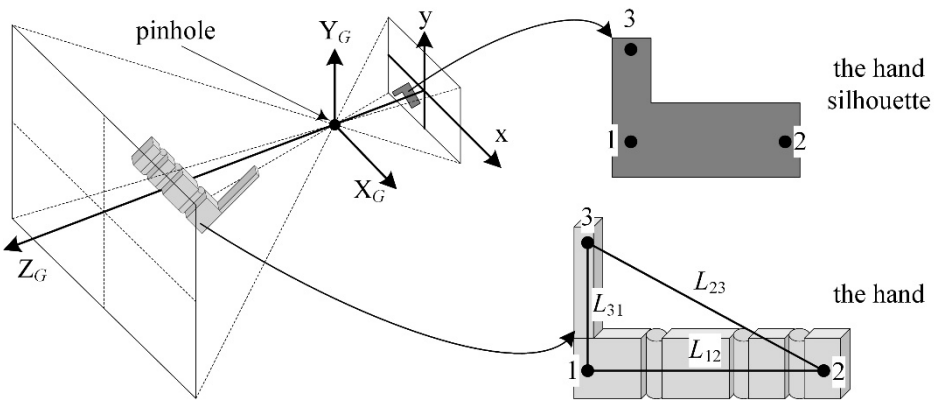

Figure 8.3 The hand in 3D space and its silhouette in the image plane

Proof: the relations between the points in 3D space and their corresponding points in the image plane are given by (8.2). According to (8.2), the three points can be localized in 3D space if Z_1, Z_2, and Z_3 can be obtained. The distances between the points are given by (8.3). By incorporation of (8.2) into (8.3), three quadratic equations are obtained (8.4). According to the parameters in (8.4), the quadratic equations correspond to three non-degenerate real ellipses that are rotated by γ (8.5) and centered at the origin of their respective 2D Cartesian coordinate Z_iZ_j, i,j=1,2,3 and $i \neq j$. (8.6) gives the radiuses of the ellipses.

A 3D Cartesian coordinate system is made by Z_1, Z_2, and Z_3. Thus, each quadratic equation draws an ellipse in its corresponding plane, and an elliptical cylinder by parallel spanning the ellipse along the other Z-axis. The world coordinate system, shown in Figure 8.3, illustrates that the depth of the points is a positive value. As such, the part of the ellipses that is in the first quarter of their coordinate systems is acceptable as the possible points for the depth of the points.

Assuming that the points make a triangle, the intersections of the elliptical cylinders give all the triangles mapped into the same triangle on the silhouette. The intersections of the three cylinders can either draw a curve in $Z_1Z_2Z_3$ or be two points, one point, or null; an example of the intersection at two points is shown in Figure 8.4.

$$x_i=\frac{\lambda\cdot X_i}{Z_i},y_i=\frac{\lambda\cdot Y_i}{Z_i},\ i=1,2,3 \tag{8.2}$$

$$\left(X_i^2-X_j^2\right)+\left(Y_i^2-Y_j^2\right)+\left(Z_i^2-Z_j^2\right)=L_{ij}^2,\ i\neq j \tag{8.3}$$

$$\begin{cases} A_{ii}Z_i^2+2A_{ij}Z_iZ_j+A_{jj}Z_i^2+C=0 \\ \left(x_i^2+y_i^2+\lambda^2\right)Z_i^2-2\left(x_iy_j+x_jy_i+\lambda^2\right)Z_iZ_j+\left(x_j^2+y_j^2+\lambda^2\right)Z_i^2-\left(\lambda\cdot L_{ij}\right)^2=0 \\ \Delta_{ij}=\begin{vmatrix} A_{ii} & A_{ij} \\ A_{ij} & A_{jj} \end{vmatrix}<0,\begin{vmatrix} A_{ii} & A_{ij} & 0 \\ A_{ij} & A_{jj} & 0 \\ 0 & 0 & C \end{vmatrix}=-\left(\rho\cdot L_{ij}\right)^2\Delta_{ij}\neq 0,\ i\neq j \end{cases} \tag{8.4}$$

$$\gamma=0.5\tan^{-1}\frac{2A_{ij}}{A_{ii}-A_{jj}} \tag{8.5}$$

$$\begin{aligned} a&=\sqrt{\frac{-C}{A_{ii}\cos^2\gamma+A_{jj}\sin^2\gamma+2A_{ij}\cos\gamma\sin\gamma}} \\ b&=\sqrt{\frac{-C}{A_{ii}\sin^2\gamma+A_{jj}\cos^2\gamma-2A_{ij}\cos\gamma\sin\gamma}} \end{aligned} \tag{8.6}$$

Where, λ is the focal length of camera. xy is the coordinate system of the image plane. L_{ij} is the length of the line connecting points i and j (Figure 8.3).

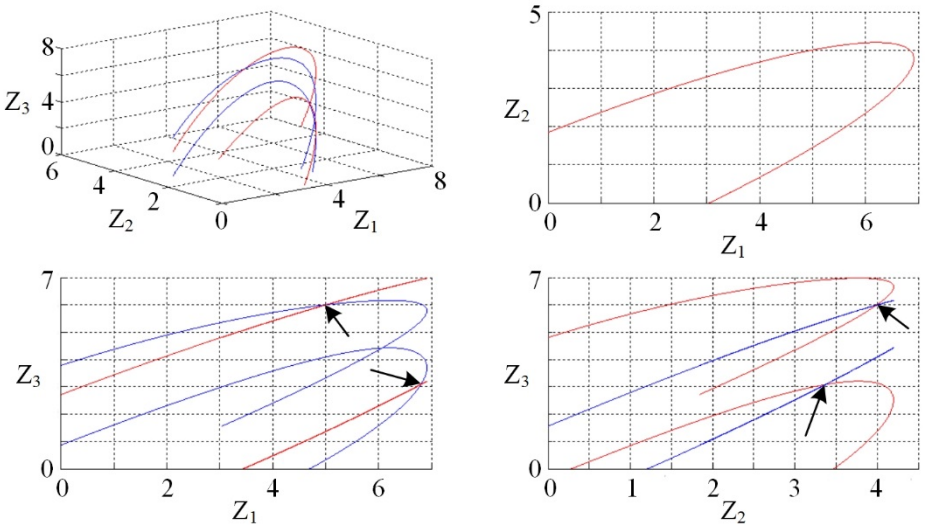

Figure 8.4 An example of two possible sets of depths for the points (the arrows show the two intersections in different planes)

The intersections cannot be null since the silhouette is resulted from a hand, and thus, there is at list one point at which these cylinders intersect. Moreover, the space of the

intersections can be a cure providing that the corners of the triangle in the image plane is collinear, which must not occur. Therefore, the problem is reduced to finding the single intersection and/or selecting one out of two intersections in $Z_1Z_2Z_3$. In the former case, thus found, the problem is solved. In the latter case, the intersection corresponding to the depths of the points can be chosen by knowing the concave direction of the hand silhouette. If we assume that the triangle, drawn by the points on the hand, has an orthogonal vector goes out of the hand palm, one of the intersections can be corresponded to the downward direction of the vector (roll<0) and the other to the upward direction (roll>0). The vector is downward (upward) if and only if the silhouette is a concave downward (concave upward). Therefore, the correct intersection (depths) can be chosen by determining the direction of the concave. After finding the depths, the points on the hand are obtained by (8.2), and the hand model is placed in a 3D virtual environment so that the points on it fit the obtained points. Thus fitted, the location of the hand is that of the hand model, and the hand is localized.■ **end of proof**

According to this proof, the idea can be valid when the points are exactly localized. However, in practice, the points may not be exactly localized because of the quantization of x and y in digital images and the estimation errors. Thus, to test the validity of the method, we investigate whether limited errors in the image plane ($0<E_{2D}<\delta$) cause limited errors in 3D space ($0<E_{3D}<\varepsilon$), i.e. limited errors of the orientations and radiuses of the ellipses ($0<E_{\gamma}<\varepsilon_{\gamma}$, $0<E_{a}<\varepsilon_{a}$, and $0<E_{b}<\varepsilon_{b}$). To do this, a simple case of paired points (a line) was considered and a population of 1,090,796 lines was produced. The line length was from 160 to 320 pixels in the image plane of 640-by-480 pixels. Each endpoint of a line was fluctuated inside a square that was centered at the points and had 11 pixels on each side, i.e. estimation error of δ=5 pixels. The error in 3D space was computed as the error in the estimation of the orientation (8.5) and radiuses (8.6) of the ellipses giving the possible depths of the endpoints (Figure 8.5). The results showed that δ of 5 pixels had negligible effects on the orientation of the ellipses (estimation error of 2.1e-4±0.11º). According to the results, the estimation error of the radiuses was 0.017±3.575 mm. Therefore, it can be concluded that $0<E_{2D}<\delta$ results in $0<E_{3D}<\varepsilon$, showing that the lines with close endpoints in the image plane draw ellipses similar in terms of orientation and radiuses. Consequently, in the case of triangles, the estimation of the intersections in $Z_1Z_2Z_3$ can be inside a sphere and/or two spheres with limited radiuses.

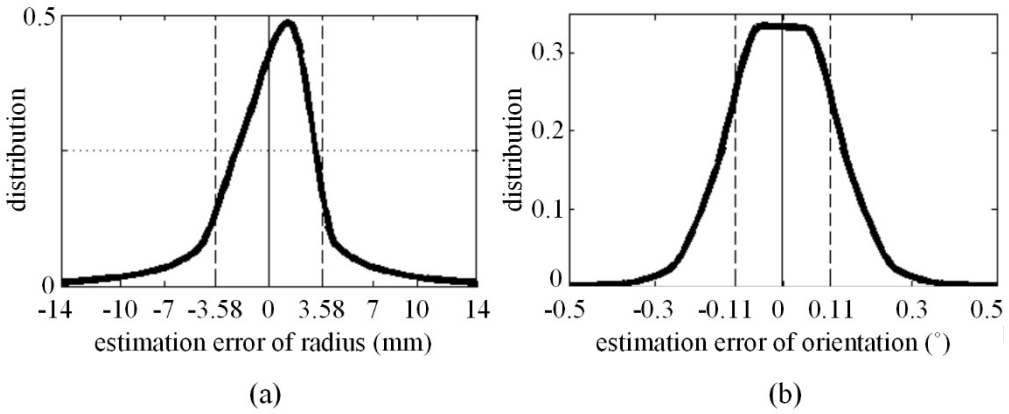

Figure 8.5 The distribution of the estimation error of (a) the orientation and (b) the radiuses of the ellipses

To reaffirm the validity, an experiment was done by generating triangles in 3D space and their silhouettes. In this experiment, a right-angled triangle with side lengths of 150, 170, and ≈227 mm was arbitrarily placed in 1000 locations in 3D space (Figure 8.6-a). It was placed by positioning the right-angled corner inside the area of -300≤X≤300, -225≤Y≤ 225, and 350≤Z≤ 650 mm, and rotating it around that corner by the angles within the defined range of roll, pitch, and yaw. Then, the triangles were mapped onto the image plane (Figure 8.6-b). Next, E_{2D}≤2 pixels (EXP-2) were made to the position of each corner, and this was also done for E_{2D}≤5 pixels (EXP-5). After that, the triangles in 3D space were recovered by using the noisy positions of the corners. In EXP-2, E_{3D} of the depths was 0.03±1.67 mm (Figure 8.7-a). E_{3D} of the intersections was 0.74±2.45 mm, and in 90% of the cases the intersections was inside a sphere with radius of 2.5 mm (Figure 8.7-b). In EXP-5, E_{2D} was 5 pixels for at least one of the corners in 23% of the cases, and in the presence of such major error, E_{3D} of the depths and the intersections were small, 0.42±5.07 mm and 1.08±7.12 mm respectively (Figure 8.7-c and -d). Consequently, $0<E_{2D}<\delta$ causes $0<E_{3D}<\varepsilon$, meaning that the estimation remains close to the real points in 3D space. To sum up, the idea can be valid in the presence of estimation error.

The triangle on the hand can be drawn by *P*, *F*, and *T* (Figure 8.8). The side *TP* has the constant length of L_{TP} because of the considered configuration of the hand. L_{PF} is also known because the pose is known. As such, L_{FT} is calculated by Pythagorean Theorem. Thus calculated, all the side lengths are known. As such, after estimating the positions of *P*, *F*, and *T* in the image plane, the points can be obtained by solving

the quadratic equations and (8.2). Section 8.4 proposes estimation of the positions of the corners in the image plane.

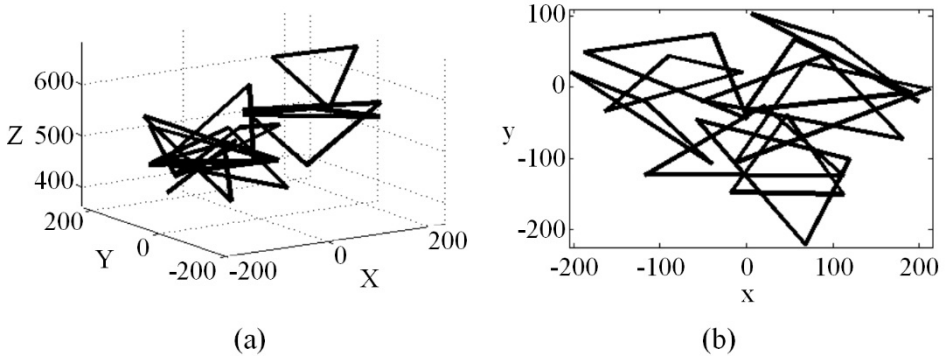

Figure 8.6 An example of (a) 10 triangles in 3D space and (b) their respective 2D images

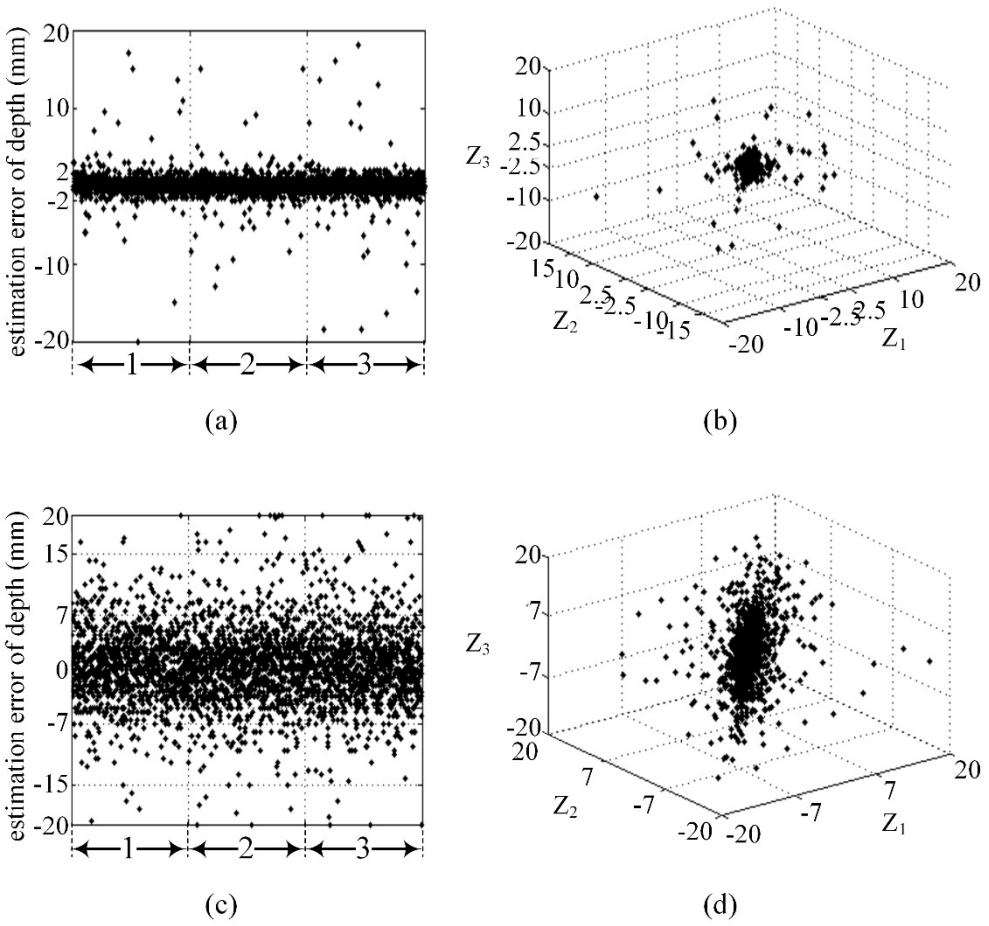

Figure 8.7 The estimation error of (a) depth of each corner in EXP-2, (b) intersections in EXP-2, (c) depth of each corner in EXP-5, and (d) intersections in EXP-5

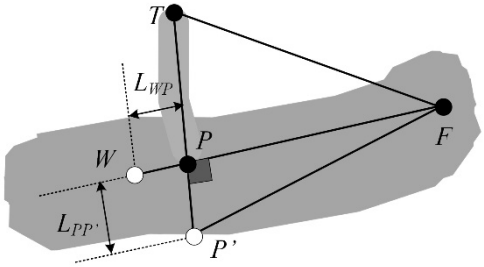

Figure 8.8 The triangle on the hand

8.3.2 Hand pose recognition

The hand pose can be identified by obtaining the orientation of the orthogonal vector (***V***) to the triangle plane in 3D space. In other words, if the right-angled triangles with the same L_{TP} and different L_{PF} are mapped on a unique triangle in the image plane, they can be distinguished by their ***V***. To illustrate, the triangles generated in the previous section were used. For each triangle in the image plane, in addition to its corresponding triangle (TRI) in 3D space, 5 more triangles were recovered. The recovered triangles had the same L_{TP} as TRI, while their L_{PF} was 1.1, 1.2, 1.3, 1.4, and 1.5 times greater than L_{PF} of TRI. There were 6000 3D triangles recovered from 1000 2D triangles (Figure 8.9). The minimum difference between the orientations of the triangles about Z_G was 1.78º (the differences were 17.24±6.78º), showing that each scale can result in different orientations. Thus, it can be concluded that, for a 2D triangle, each pose relates it to a 3D triangle with a unique orientation about Z_G. Therefore, the pose can be estimated by measuring the orientation (Section 8.5).

8.4 Estimation of the hand location

To find *P*, *F*, and *T* on the silhouette, first, its skeleton is obtained through thinning by means of hit-and-miss transformation. Hit-and-miss is a basic transformation for obtaining the skeleton of an object in the image. It was chosen because it does not change the hand's topology that is important for identification of the hand pose. Then, the skeletons are trimmed to remove short stems. Next, those pruned pixels connecting the current open endings of the stems to their previous furthermost open endings, are recovered. The structuring elements used for thinning and trimming are shown in Figure 8.10-a and Figure 8.10-b respectively.

In the skeletons, there are two main nodes (palm and fingertips nodes) and four stems (Figure 8.11-a). The fingers stems are those branching from the fingertips node and making the largest angle among the 2-combinations of the stems; it should be noted that this node can branch into more than two stems. The triangle on the hand is specified using this information as follows (Figure 8.11-b). *T* is estimated by the pixel at the open ending of the thumb stem. To estimate *P*, *P'* (Figure 8.8) is localized first. It is localized by the intersection of the line, fitted to the thumb stem, and the border of the hand silhouette. Then, since *P* is on this line and its distance from *P'* is constant and can be measured on the hand ($L_{PP'}$, Figure 8.8), *P* can be estimated on the line. *F* is estimated by the intersection of the line connecting the open endings of the fingers stems and a line drawn from the palm node. The latter line is obtained as follows. The palm node as a vertex makes two adjacent angles with the fingertips node and two open endings of the fingers stems. The line is obtained by rotating the side making the larger angle by the amount of the smaller angle towards the fingertips node.

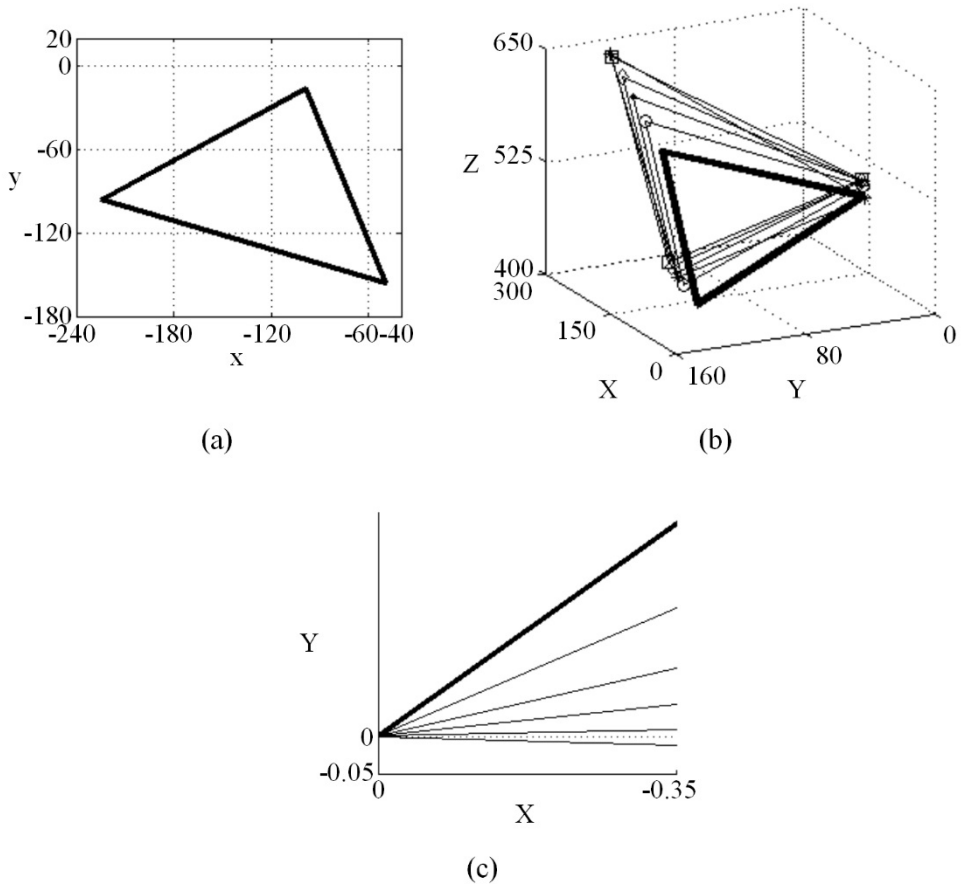

Figure 8.9 An example of a 3D triangle and its scaled L_{PF} (a) in the image plane, (b) in 3D space, and (c) their orientations about Z_G

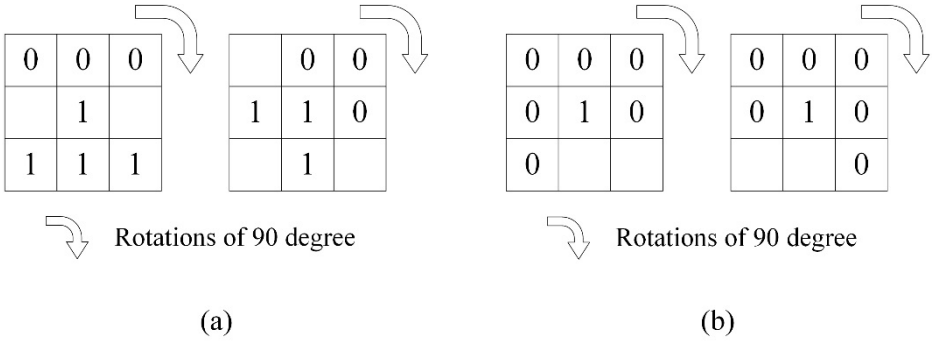

Figure 8.10 The structuring elements for (a) hit-and-miss and (b) pruning

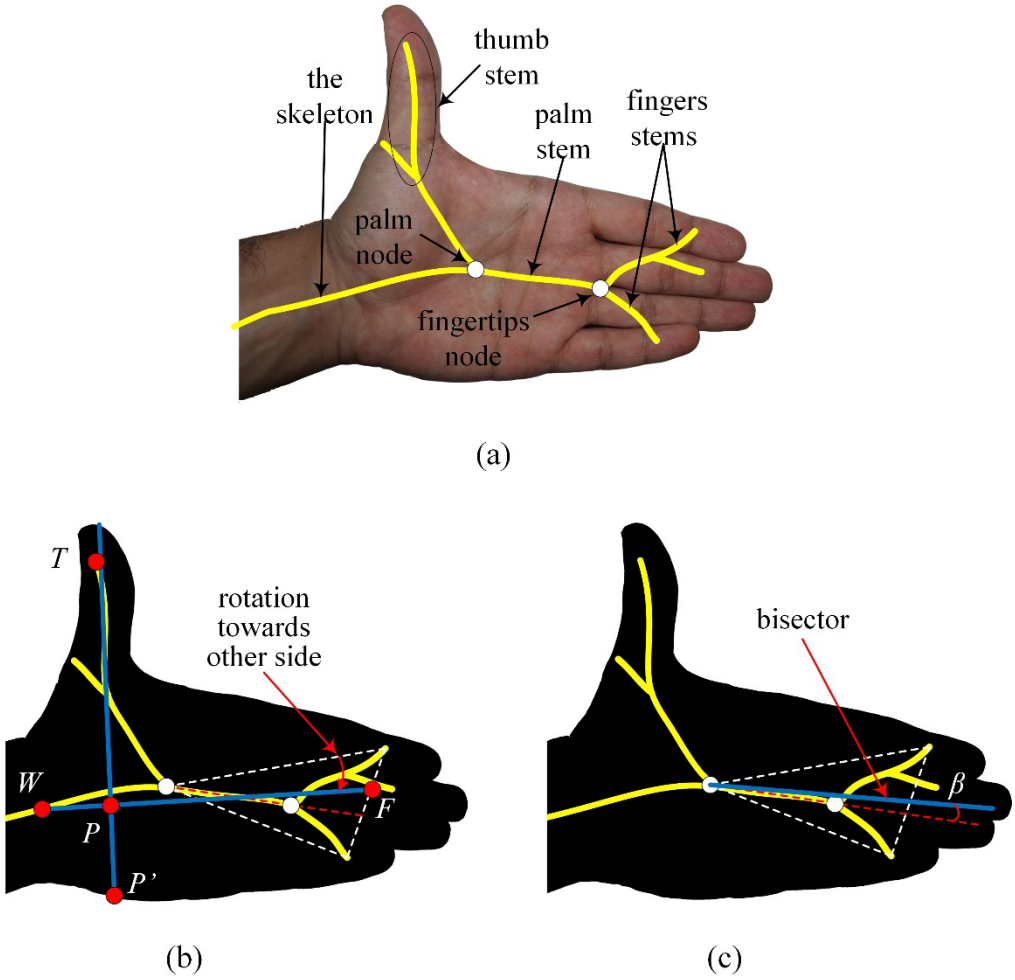

Figure 8.11 (a) the skeleton, (b) the parameters, and (c) the bisector and the angle β

As discussed in Section 8.3.1, to select one out of two possible sets of depths obtained by the quadratic equations, the direction (upward/downward) of the concave side of the hand should be recognized. A test, called bisector test, is designed to

decide on the concave side. The test specifies the direction by the sign of the angle β (Figure 8.11-c) measured with respect to the line connecting the palm node to the fingertips node in the counterclockwise direction. β is the orientation of the bisector of the angle made by the palm node and the open endings of the fingers stems. The test selects the downward direction if β is negative; otherwise, the concave is upward. After localizing the points on the silhouette, by knowing the lengths of the triangle sides on the real hand, the quadratic equations (8.4) are solved to obtain the possible depths of the points. Then, by performing the bisector test the correct set of depths are determined. The position of the points in 3D space is obtained by solving (8.2) for X_i and Y_i.

To perform experiments for verification of the method, an articulated model of the hand, a 3D virtual environment, and a virtual camera[9] mapping the environment onto a 2D virtual image were created in OpenGL (Open Graphics Library) by using Visual C#. A set of virtual hand images (Space-V) was generated. To do this, the hand model was put in 520 different positions in the virtual environment (Figure 8.12). In each position, 100 poses and orientations were arbitrarily selected. In total, there were 52,000 images in Space-V. Maximum L_{PF} was 172 mm.

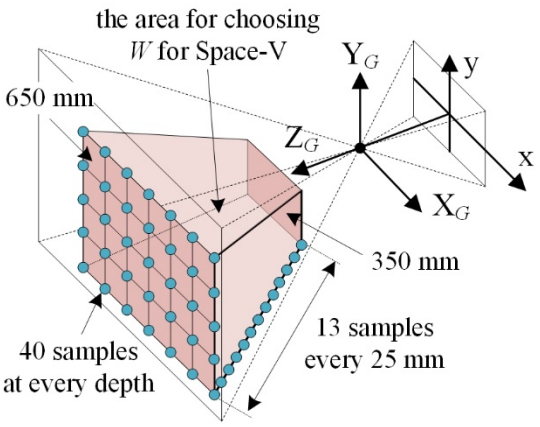

Figure 8.12 The area for positions of the hand model for generating Space-V

The estimation errors of *P*, *T*, and *F* were calculated as the Euclidian distance between the real and estimated positions of the points, and they were 0.85±1.05 mm,

[9] The virtual camera projects the virtual environment on a 640-by-480 pixel plane with Fovy (field-of-view in vertical axis) equal to 25º. The projection represents an image that can be captured by using a digital web-camera.

1.12±1.74 mm, and 2.04±2.42 mm respectively. The errors increased by increasing the depth of the hand. This can be attributed to the reduction in the total number of pixels on each triangle side when the hand goes farer from the pinhole. To test the effectiveness of the bisector test, the estimations were also done without this test. In this case, there were 24,672 (≈48%) wrong estimations, while by using the bisector test the total number of the wrong estimations was reduced to 378 (≈0.73%) cases. The majority (≈86%) of these 378 cases occurred at the deeper positions of the hand from the depth 600 mm to 650 mm. These results show that the bisector test is able to select the correct depth of the points. Overall, the proposed method can obtain the position of the three points, and thus, can be utilized for localization of the hand with known pose.

8.5 Estimation of the hand pose

A look-up table is provided for finding the pose. The look-up table, in each row, contains the angle of the corners of the triangle in the image plane, the angle β, and the percent of change in L_{PF} (the percentage is considered to make the table independent of users' hand size). L_{PF} can be obtained by estimation of the angles, finding the row whose angles are the closest to the estimated ones in terms of Euclidian distance, and scaling the longest L_{PF} (θ_1=0) by the percentage corresponding to the found row. The pose is estimated by solving (8.1) for θ_1 by using the obtained L_{PF}.

To fill in each row of the table, we produced totally 428,891 different cases for the hand pose, position, and orientation. To produce these cases, the hand model was translated and rotated in the virtual environment with different poses in front of a virtual camera. The hand location was kept at the depth of 350 mm, which was the smallest depth considered in our study. Thus, at this depth, the hand images contained the maximum number of pixels for each location and pose, leading to the highest accuracy of the elements of the look-up table in our study. At this depth, 240 positions were considered for the hand location. Table 8.1 illustrates the range of the joint variables and their minimum displacements. In total, 1800 cases for the orientations and poses were considered. Thus, we had 432000=240×1800 images. It should be noted that the images were filtered to remove those in which T was not identifiable in the silhouette, i.e. the machine could not identify the thumb stem because it was short.

Table 8.1 The range of the orientations and their displacements for Space-V

joint angle	range (˚)	displacement (˚)
roll	[-70,80]	30
pitch	[-60,60]	24
yaw	[-62,20]	20
θ_1,θ_2,θ_3	Section 8.2	10

Space-V was used to verify the method for the hand pose recognition. In this space, the angles on the silhouettes and L_{PF} on the virtual hand were recorded for each case. The recorded and estimated L_{PF} were compared to evaluate the method. The mean of the errors was small (≈0.56 mm) and SD depended on the position of the hand (Figure 8.13). As can be seen, the pose recognition can become critical when the hand gets closer to x=0 or y=0, especially to (x,y)=(0,0). The estimation accuracy increases by placing the hand closer to the pinhole and farer from x=0 or y=0. The estimation error of L_{PF} was 1.03±2.52 mm when θ_1<30º (24381 cases), and it was 0.15±1.78 mm when θ_1>30º (27319 cases). This shows that the method can work better when L_{PF} is smaller. These small errors demonstrate that the look-up table can relate L_{PF} to the angles measured on a silhouette. This may imply that our method for pose recognition can be considered as verified. The estimation error depends on the distance of the hand from the pinhole. The closer the hand is to the pinhole, the more pixels its silhouette has and the smaller the angle errors are, and accordingly, the smaller the pose estimation errors can be.

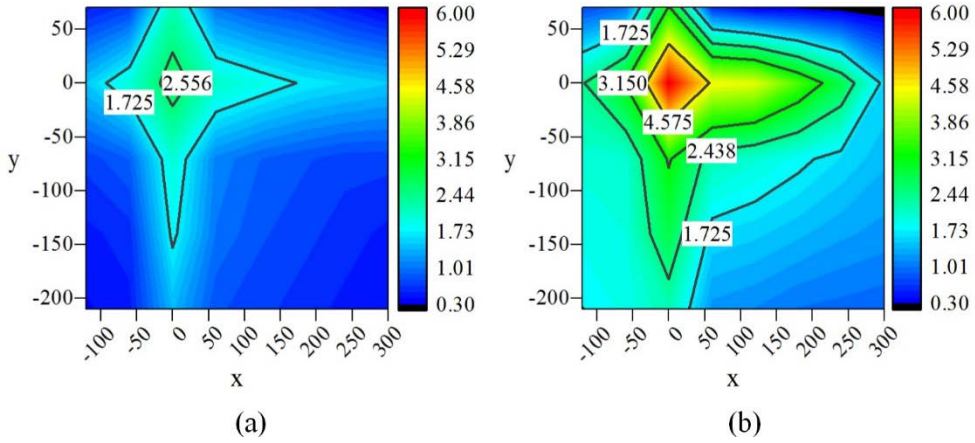

Figure 8.13 SD of the pose estimation error (mm) (a) *W* at Z=350 mm and (b) *W* at Z=650 mm

8.6 The method for hand localization and pose recognition

The method, first, measures β on the silhouette of the hand and estimates L_{PF}, and then, estimates the pose. Second, it estimates *P*, *T*, and *F* on the hand silhouette. Third, by solving (8.4) and the bisector test, it retrieves the depths of the points in 3D space. Then, it obtains the position of the points by using (8.2). The position of the points is utilized to calculate the position of *W* and roll, pitch, and yaw so as to localize the hand. They are obtained by solving the inverse kinematic equations for the hand mechanism. First, the position of *W* is obtained (8.7); it is on the line *PF*, and its distance from *P* is constant and known (L_{WP}, Figure 8.8). Second, roll, pitch, and yaw are calculated by (8.8). To derive (8.8), *PF* and *PT* was assigned as X and Y axes. According to the defined range of the orientations, the sinus and tangent functions are one-by-one. As such, (8.8) results in only one value for each orientation.

$$W=\begin{pmatrix}X_P\\Y_P\\Z_P\end{pmatrix}-\frac{L_{WP}}{L_{PF}}\begin{pmatrix}X_F-X_P\\Y_F-Y_P\\Z_F-Z_P\end{pmatrix} \tag{8.7}$$

$$\text{Pitch}=-\sin^{-1}\left(\frac{Z_F-Z_W}{L_{PF}}\right)$$

$$\text{Roll}=\sin^{-1}\left(\frac{1}{2\cos(\text{Pitch})}\cdot\left(\frac{Z_T-Z_W}{L_{PT}}+\frac{Z_P-Z_W}{L_{PP'}}\right)\right)$$

$$\begin{aligned}
&\text{Yaw}=\tan^{-1}\left(\frac{A\cdot M+C\cdot N}{C\cdot M+B\cdot N}\right)\\
&A=\bar{L}_{PP'}{}^2+\bar{L}_{PP'}{}^2+(Y_F-Y_W)^2\\
&B=\bar{L}_{PP'}{}^2+\bar{L}_{PP'}{}^2+(X_F-X_W)^2\\
&C=(X_F-X_W)(Y_F-Y_W)\\
&M=\sin(\text{Pitch})\sin(\text{Roll})\left(L_{PP'}(Y_P-Y_W)+L_{PT}(Y_T-Y_W)\right)\\
&\quad-\cos(\text{Roll})\left(L_{PP'}(X_P-X_W)+L_{PT}(X_T-X_W)\right)\\
&N=\sin(\text{Pitch})\sin(\text{Roll})\left(L_{PP'}(X_P-X_W)+L_{PT}(X_T-X_W)\right)\\
&\quad+\cos(\text{Roll})\left(L_{PP'}(Y_P-Y_W)+L_{PT}(Y_T-Y_W)\right)
\end{aligned} \tag{8.8}$$

For the verification of the method, the estimated poses for Space-V (Section 8.5) were utilized to localize the hand. The estimation error for *P*, *T*, and *F* were 1.33±1.28 mm, 1.79±1.93 mm, and 2.54±2.27 mm respectively. The estimation error

of *W*, roll, pitch, and yaw was 1.57±1.86 mm, 0.05±4.27º, 0.34±5.02º, and -0.22±1.87º respectively. These small errors can show that the method can be able to recognize the hand pose and localize the hand in 3D space using information extracted from a single silhouette of the hand.

8.7 Experimental study to evaluate the method

An experiment was performed to evaluate the method. An almost 2-minute video (1708 frames) of hand movements was recorded by using a web-camera. When recording, it was tried to move the hand in different positions and orientations with different poses, within the limitations and constraints defined in Section 8.2. The distance between the hand and the pinhole of the web-camera was kept between 350 mm to 650 mm. The web-camera was set to record 15 frames per second with resolution of 640-by-480 pixels. Its diagonal field of view was 55 degrees.

8.7.1 Parameters measured for the evaluation

For each frame, the estimated pose and location were used to configure the pose of the virtual hand and place it in virtual environment, respectively. Then, the virtual image was captured. To evaluate the method, the similarity between the silhouettes in the virtual image and the frame was measured. The similarity was calculated as the distance between the positions of three points (P_V) on the silhouette in the virtual image (S_V) and their corresponding points (P_R) on the silhouette in the real frame (S_R). To localize P_R, markers were attached at palm (PAL), fingertips (FIN), and thumb (THU) of the hand, and for P_V, their corresponding points on the virtual hand were highlighted by virtual markers. The centroid of the markers in the silhouettes was considered as the position of the points. Two circular markers with radius of 2.5 mm were attached on the hand at palm and thumb and a 7-by-20 mm rectangular marker was wrapped around the fingertip of the middle finger. The similarity was determined by the longest distance in each frame, and thus, the distance was the chessboard distance (L^∞-norm). The distance between P_V and P_R can show how correctly the virtual hand follows the real hand, and thus, the extent to which *W*, roll, pitch, and yaw are accurately estimated. Regarding the bisector test, since its two possible outputs have quite different silhouettes, the correctness of the choice can be determined by visual comparison. Therefore, to evaluate the bisector test, the frames were reviewed to check whether S_V corresponded with S_R.

8.7.2 Results and discussion

Several screenshots of the experiment and its results are shown in Figure 8.14. The method estimated the hand pose and location in real-time. Its computation expense sufficed real-time interactions when recording and displaying 15 frames per second.

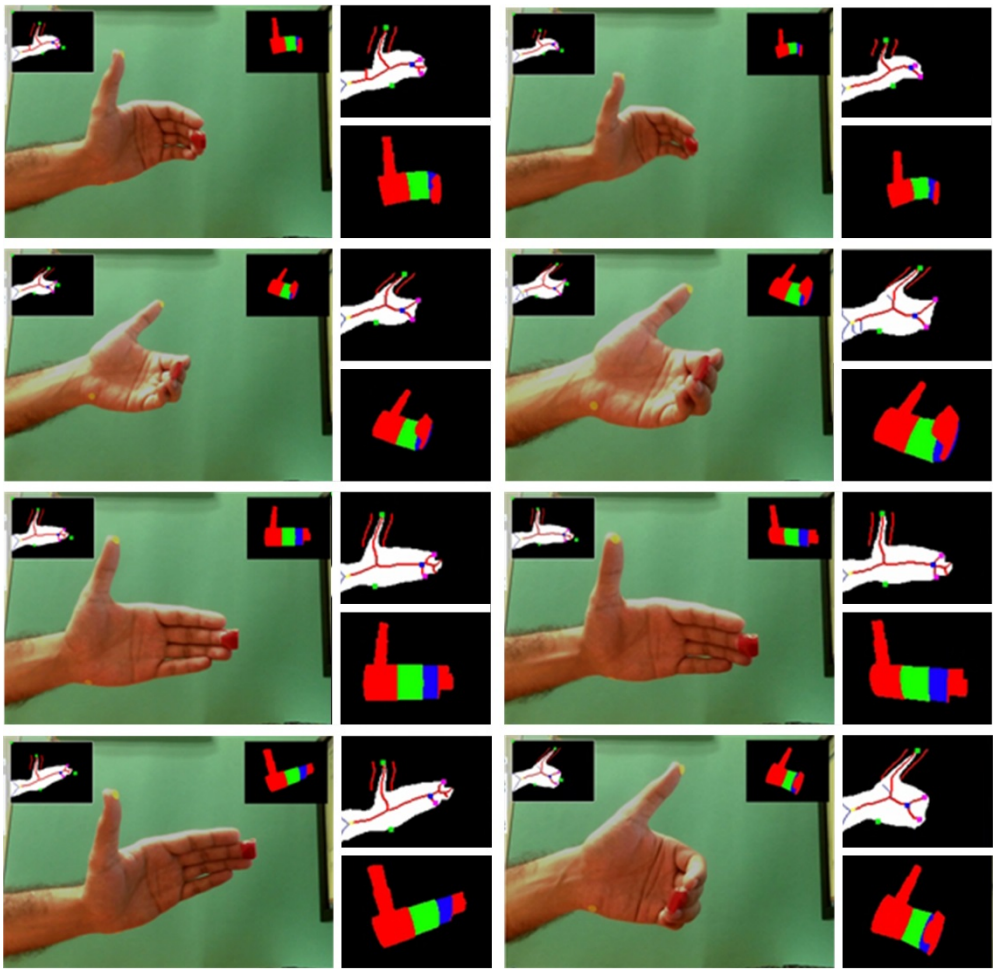

Figure 8.14 Several screenshots of the experiment (the hand silhouette and model are also illustrated)

The positions of PAL, FIN, and THU were calculated as the mean of the position of the points found for their corresponding marker. The matrices shown in Figure 8.15 depict the distance between P_V and P_R. The numbers show the frequency of the distances normalized to 10 (divided by 14). For example, for THU, the error -1 along both x and y was occurred in 56 (3.29%) out of 1708 frames. The maximum difference between P_V and P_R was less than or equal to 5 and 3 pixels along x and y respectively. Considering the estimation errors 2 and 5 as acceptable and marginal

errors according to the results of EXP-2 and EXP-5 (Section 8.3.1), 86% and 14% of the estimations had acceptable and marginal errors respectively. These small errors can show that the method were successful in the localization and pose recognition. Overall, through the proofs given in Section 8.3, the experiment results by using the virtual hand in Sections 8.4 and 8.5, and the experiment results in this section, it can be concluded that the method is capable of performing bare hand pose recognition and localization in real-time.

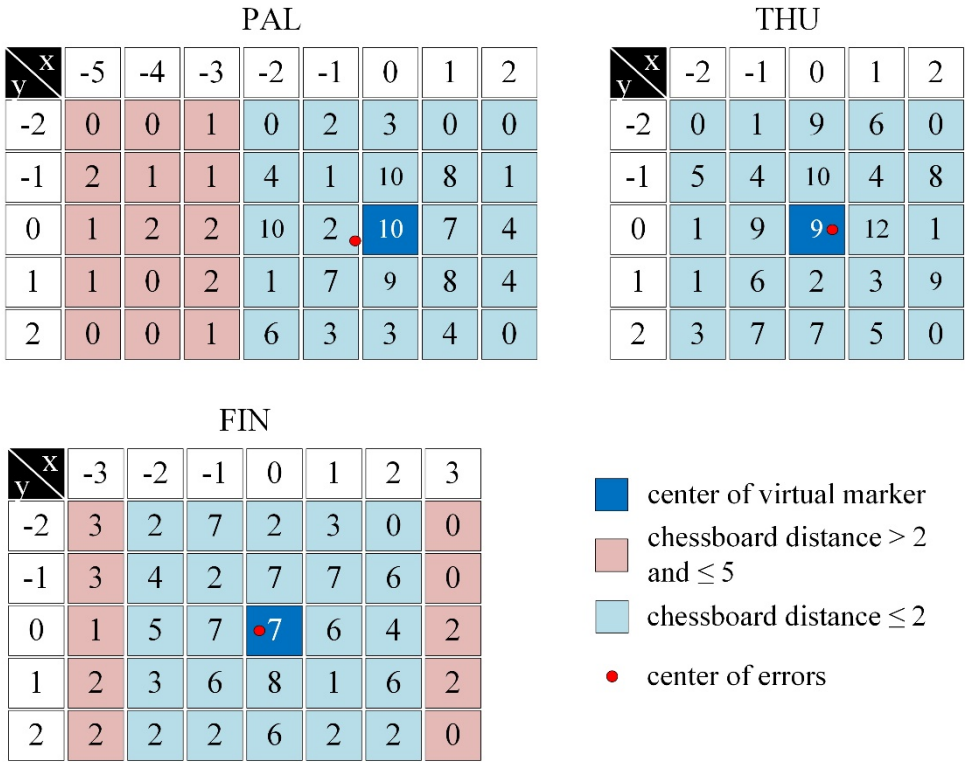

Figure 8.15 The distance between P_V and P_R and their normalized frequency

As can be seen in Figure 8.15, a bias can exist towards the negative errors along x-axis where the errors are more than 2. To investigate, the center of the errors was calculated as the sum of the weighted errors along an axis over the totaled weights; the weights were the frequency. Referring to the results, the center in PAL had a bias of 0.53 pixels towards the left side (to the wrist in Figure 8.14). This can be attributed to the fluctuation of the estimated *P* tending to move to get closer to the wrist. As the future work, we aim to reduce the estimation error of the corners, especially *P*, on the silhouette.

Chapter 9 An interactive digital prototyping tool for concept selection

This chapter introduces an interactive digital prototyping tool to allow users produce design solutions by setting the values of the parameters of SDS. It comprises a virtual table on which users can produce a solution and a virtual menu by which they can navigate between the parameters and set their values. To build the interactions with users, the tool requires an A4 size paper on which a certain drawing is printed, a web-camera, and a 2D digital screen (Figure 7.3).

9.1 The setup of the tool

The tool records the environment including the paper by using the web-camera, analyzes the scenes of the paper to extract 3D geometrical information of the paper, augments DP on the paper in the environment, and projects the augmented environment on the screen. To extract the geometrical information, a sketch is drawn on the paper (Figure 9.1-a). The sketch consists of a blank square and a solid circle that is inside the square and close to one of its corners. The sketch is in blue color, i.e. (0,0,255) in RGB color system, and printed on a white paper. To record the scenes of the environment, the web-camera is placed at the height of 300-500 mm, with orientation >45º with respect to the horizontal plane X"Y" (Figure 9.1-b).

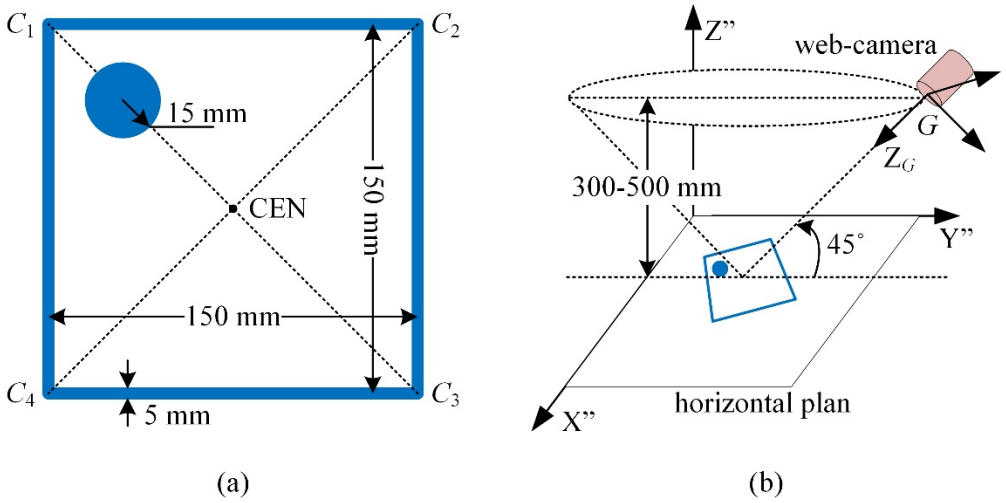

Figure 9.1 (a) the sketch on the A4 paper and (b) the constraints to the location of the web-camera in the space

The constraints are based on MoD Std 00-25-17 [160] defining the minimum comfortable distance and preferred angular lines of sight for viewing a console (table). Therefore, the scenes recorded by the web-camera can be in the same scale and perspective view as the scenes that the users see when working behind the console. Such projection of the scenes can help users to immerse in the environment and have the feeling of viewing the console.

9.2 User interaction with the digital prototype

DP is augmented in the environment on the paper, at the center of the square (Figure 9.2). DP is attached to the paper, and can be translated in X"Y" plane and rotated about Z" by moving the paper in X"Y". It is projected with the same scale and perspective view as its physical realization on the paper. Therefore, it can be imagined that a real object is placed on the paper, and this improves user immersion into the environment. To do this, first, location of the center (CEN) of the square and orientation (ORI) of the square are measured on the recorded scenes. CEN and ORI are measured with respect to the coordinate system *G* attached to the pinhole of the web-camera (Figure 9.1-b). DP is placed in front of a virtual camera at CEN with ORI. The virtual camera has the properties of the web-camera and was modelled in OpenGL. Third, the virtual image of DP is taken and projected on the recorded scenes. In the following, estimation of CEN and ORI is described.

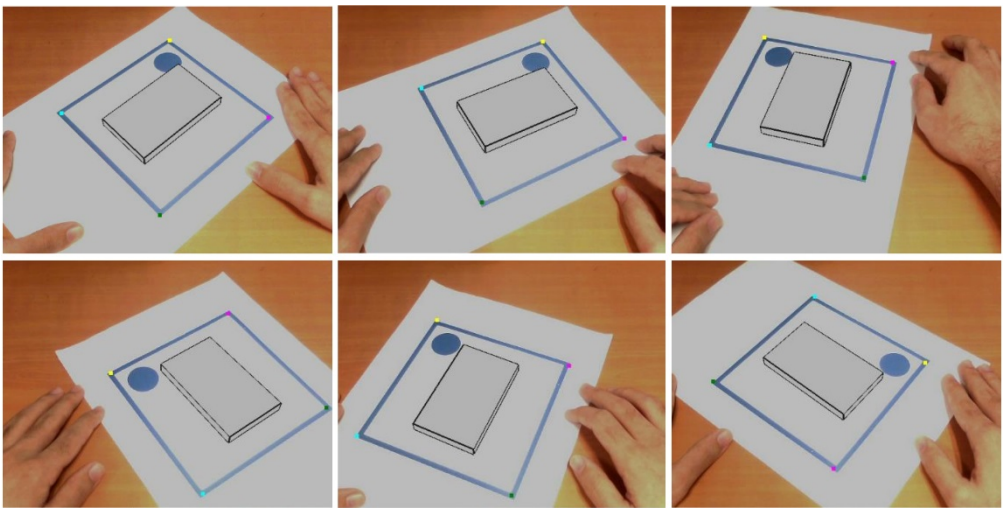

Figure 9.2 Screenshots of the scenes on the 2D screen when moving the paper

In Section 8.3.1, it was shown that the position and orientation of a tingle with known side lengths can be obtained by using its 2D image. Using the same method, four quadratic equations (8.4) can be obtained by four corners of the square. By referring to Section 8.3.1, the intersection of the elliptical cylinders defined by the equations gives the depth of the corners. There is at least one intersection because the quadratic equations are resulted from a square. The number of intersections cannot be more than two because the four corners cannot be collinear in the image plane according to the constraints to the location of the web-camera. It cannot be two as well because the vector of the square plane is upward (Sections 8.3 and 8.5). Therefore, the four equations intersect at only one point giving the depth of the corners. In Section 8.4, each corner of the triangle could be corresponded to a point on the hand, whereas, here, there are 4 possible orientations for the square because when rotating it by 90º, its geometry remains unchanged. The choices for the retrieved points can be $C_1C_2C_3C_4$, $C_2C_3C_4C_1$, $C_3C_4C_1C_2$, and/or $C_4C_1C_2C_3$ (Figure 9.1-a). To choose the correct orientation, the circle is added to the sketch. Its center is closer to C_1 than the other corners, and thus, the retrieved point closest to it, is labelled by C_1, and the other points are labelled in the clockwise direction. CEN (9.1) is obtained by intersecting the diagonals of the square, i.e. C_1C_3 and C_2C_4. ORI is calculated as (roll,pitch,yaw) by using (8.8). To do this, P and W are set to 0. T and F are replaced by C_1-CEN and C_2-CEN respectively, and L_{PF}=L_{TP}=10.61 mm.

$$\text{CEN}=\begin{pmatrix} \dfrac{X_{C_1}X_{C_4}-X_{C_2}X_{C_3}}{(X_{C_1}+X_{C_4})-(X_{C_2}+X_{C_3})} \\ \dfrac{Y_{C_1}Y_{C_4}-Y_{C_2}Y_{C_3}}{(Y_{C_1}+Y_{C_4})-(Y_{C_2}+Y_{C_3})} \\ \dfrac{Z_{C_1}Z_{C_4}-Z_{C_2}Z_{C_3}}{(Z_{C_1}+Z_{C_4})-(Z_{C_2}+Z_{C_3})} \end{pmatrix} \tag{9.1}$$

Our approach to localization of the corners in the image plane is based on the notion that the corners are the intersections of the sides of the square. Thus, first, the sides are detected. To do this, Hough transform [161, 162] , a feature extraction technique, is utilized. This technique, first, finds all the pixels that can be on the sides. They can be the blue pixels (Γ); blue is fuzzy here, i.e. those pixels that can be blue more than red and green in RGB color system. Then, each Γ is considered as a point on a straight line represented by Hesse normal form [163], i.e. $\rho= \Gamma_x\cdot\cos(\phi)+ \Gamma_y\cdot\sin(\phi)$,

where ρ is the distance from the origin to the closest point on the line, and ϕ is the angle between x-axis and that closest point (Figure 9.3-a). Thus, a pair (ρ,ϕ) is associated with a blue line in $\rho\phi$ plane (Figure 9.3-b). Given a Γ, the set of all lines, going through it, corresponds to a sinusoidal curve in $\rho\phi$ plane, which is unique to Γ. A set of Γ forming a line produces sinusoids intersecting at (ρ,ϕ) of that line. Thus, to detect collinear points, the concurrent sinusoids should be found. To do this, a two-dimensional array, or accumulator, is defined whose bins correspond to a pair (ρ,ϕ); ρ and ϕ are quantized (Figure 9.3-b). For each Γ, (ρ,ϕ) are calculated, and then, the value of the accumulator's bin associated with the calculated (ρ,ϕ), is incremented. At the end, each bin has a value equal to the number of Γ positioned on a line. As such, the bins with the highest values indicate the lines that are most represented by the blue pixels. Four bins with the highest values are chosen to identify the sides.

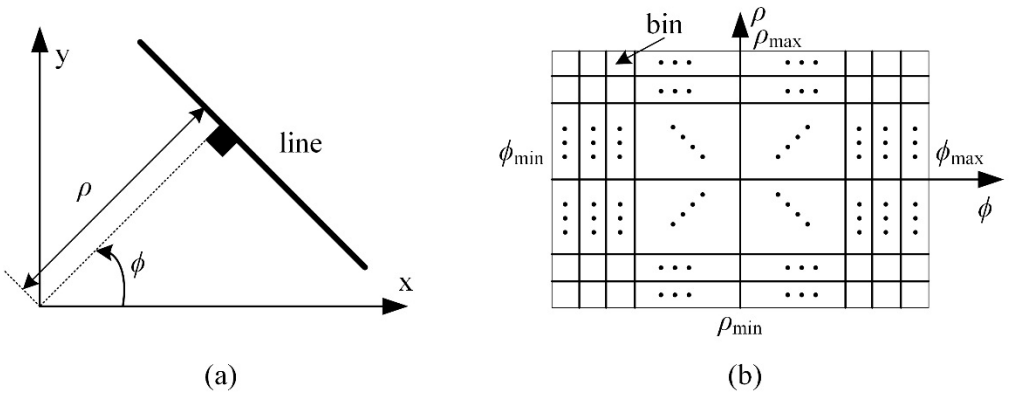

Figure 9.3 (a) the straight line represented by Hesse normal form and (b) Hough space for the set of straight lines in 2D space

The circle is detected to find C_1 among the identified corners in order to label the corners. Its center is located on a diagonal of the square and at the distance of 35 mm from C_1. Therefore, the center can be at 4 positions given by (9.2). To find the circle, the amount of blue in the color of the pixels around these positions is measured. That amount is the sum of the blue component of the RGB color of the pixels. The pixels with the distance (L^∞-norm) of less than 7 from the positions are considered. The position with the larger amount corresponds to C_1 because it is the closest point to the circle among the positions (9.2). The other corners are labelled by C_2, C_3, and C_4 in the clockwise direction.

$$(x,y)=\lambda\cdot\left(\frac{X_C+\left(35/150\sqrt{2}=0.1650\right)(X_{C'}-X_C)}{Z_C+0.1650(Z_{C'}-Z_C)}\quad\frac{Y_C+0.1650(Y_{C'}-Y_C)}{Z_C+0.1650(Z_{C'}-Z_C)}\right) \tag{9.2}$$

Where, (x,y) gives the positions of the center in the image plane. *C* and *C'* represent a corner and its opposite corner respectively. λ is the focal length of the camera.

9.3 User-tool interactions

To set the values of the parameters of solutions, a virtual menu is augmented on the table (Figure 9.4).

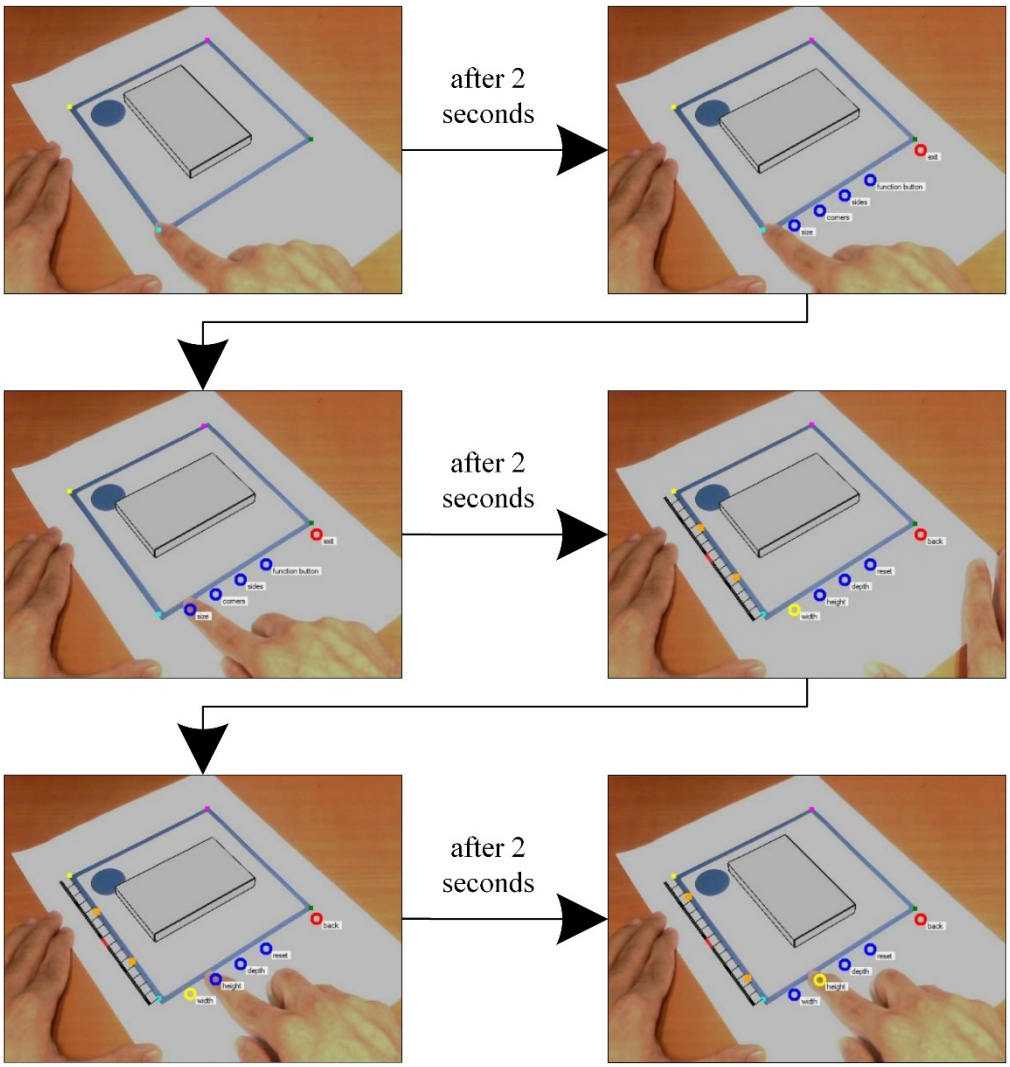

Figure 9.4 (a) activating the menu and (b) navigating between the items

To pop up the menu, user can point any corner by his/her finger for 2 seconds (Figure 9.4-a), and the menu is augmented next to the adjacent sides of that corner. Users can navigate between the items in the menu and change the values by pointing with their fingers at them. To navigate, the finger should remain on the item for 2 seconds (Figure 9.4-b). To change the value, the finger should move along a side of the square, and the length that the finger is pointing at is used to set the value (Figure 9.5). The hierarchical diagram of the menu is shown in Figure 9.6. According to the menu, user can change the value of the parameters p_1 to p_8 (Figure 7.2).

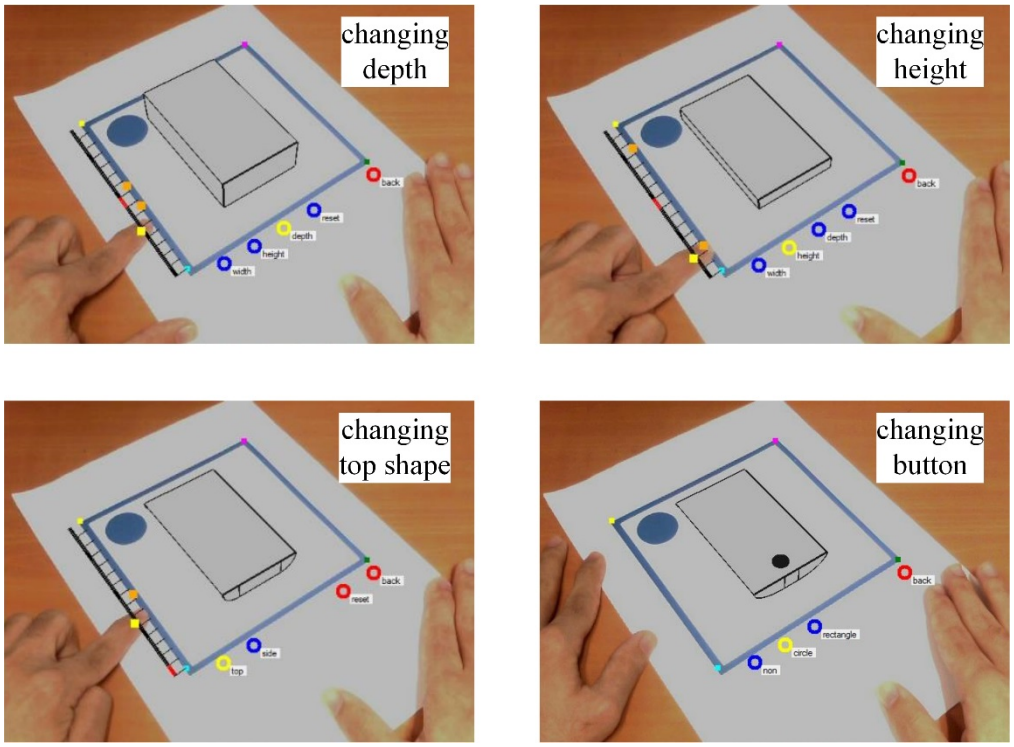

Figure 9.5 Setting the values of the parameters (a) width and (b) p_5 in Figure 7.2

To recognize whether a finger is pointing at a corner, the hue of an area of ±2 pixels around the corners is monitored in each frame. The hue is considered because the hue of fingers is quite different from white and blue (the color of the paper and sketch respectively). When the change in hue is more than 25% for 2 seconds, the menu is activated. The same procedure is followed for navigating between the items of the menu. When setting the values, the 25% change leads to immediate action (Figure 9.5).

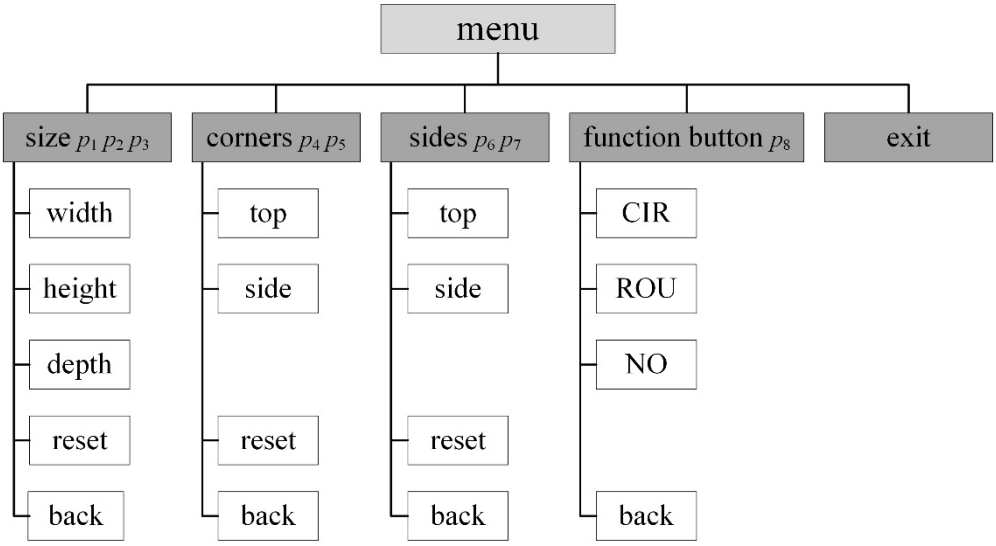

Figure 9.6 The hierarchical diagram of the menu

9.4 Proof-of-concept: experimental study

An experiment was performed to verify the method. An almost 2-minute video (1820 frames of 640-by-480 pixel) was recorded by putting markers (red color and 5 mm diameter) on the corners. The Hough space was $-640 \leq r \leq 640$ pixel and $-90 \leq \theta \leq 90^{\circ}$. For each frame, CEN and ORI were obtained by using the method as well as the data of the markers. The position of a marker was calculated as the center of pixels found for it. The difference between CEN was 0.07±1.39 and -0.19±1.54 pixel along x and y respectively (Figure 9.7), and for ORI, was 1.68±2.31˚; this difference was the angle (9.3) between the vectors representing ORI, and was positive. These small errors can show that the method can place DP similar to its physical realization on the table. In addition, referring to the user evaluations of the tool in Section 7.6.2, the high scores (3.20±2.09) given to the tool on 'distracting-immersive' dimension, can show that the projection of DP on the paper is close to reality. These can imply that the tool can be valid for rendeirng the form and size of design solutions to users.

$$\mathrm{ANG} = \cos^{-1} \frac{\left(\overrightarrow{C_1C_2} \times \overrightarrow{C_1C_3}\right) \cdot \left(\overrightarrow{C_1C_2} \times \overrightarrow{C_1C_3}\right)}{\left\|\overrightarrow{C_1C_2} \times \overrightarrow{C_1C_3}\right\| \left\|\overrightarrow{C_1C_2} \times \overrightarrow{C_1C_3}\right\|} \tag{9.3}$$

Where, · denotes the dot product, and non-italic characters refer to the positions obtained by using the markers.

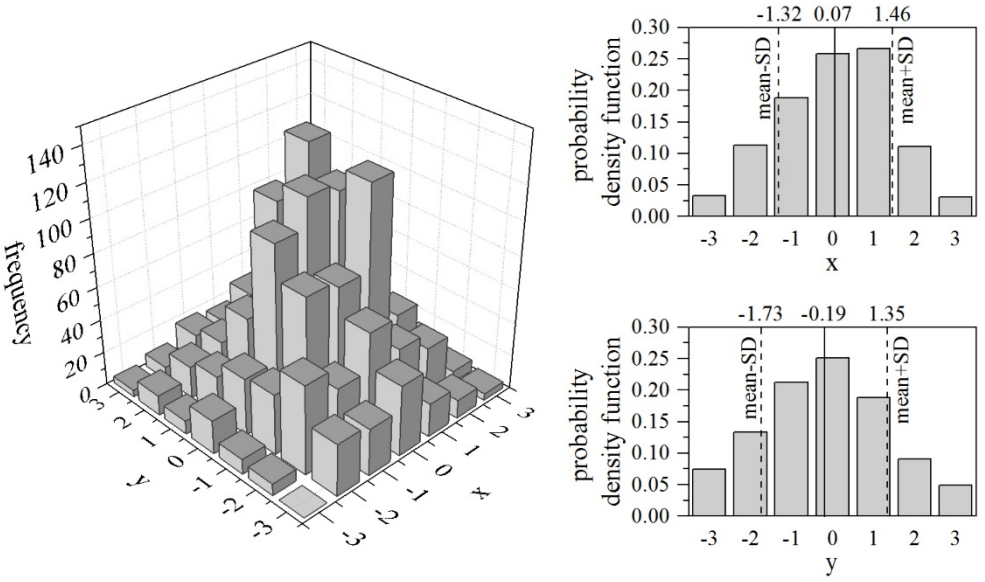

(a) (b)

Figure 9.7 The estimation error of CEN (a) frequency of the distance in xy plane, (b) the probability density function along x and y

9.5 Evaluation of the tool

To evaluate the tool on 'degree-of-correctness' and 'time-to-estimate', after the hands-on training in EXP-M (Section 7.6), the subjects were asked to reproduce the solution shown in Figure 9.8.

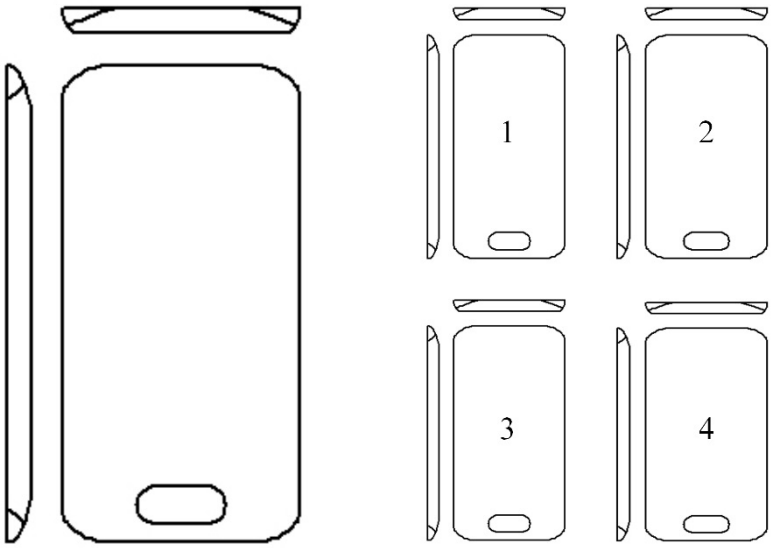

Figure 9.8 The single solution and the four solutions

The solution was rendered by the tool, and each subject was given 15 seconds to interact with it in order to estimate its parameters. Then, they had 2 minutes for the reproduction. After reproduction, the distance (*D*) between the solutions was measured. *D* was the distance defined for the clustering in Section 7.5. To evaluate on 'handling-of-variations', 4 solutions (Figure 9.8) were chosen with *D* of less than 10% from each other, and randomly augmented in the 4 viewports of EXP-M. In total, there were 24 cases (permutation without repetition, 4!/(4-4)!) for putting the solutions in the viewports. In each case, the user was asked to choose his/her highest quality solution in less than 5 seconds. At the end, the high quality solution was the one chosen more than the others. Dd was measured as the frequency of not choosing the highest quality solution. Table 9.1 gives *F*.

Table 9.1 The specification of the parameters of *F* (Table 4.1)

F			the output
F_{DC}	F_{TE} (10)	F_{HV} (∞ & 4)	$DCET_{DC}$ $DCET_{TE}$ $DCET_{HV}$
[0,5]	[0, 15]	[0, 2]	1.00
(5,10]	---	(2, 4]	0.67
(10,15]	---	(4, 6]	0.33
(15,∞)	(t_{max}=15, ∞)	(Dd_{max}=6, 17]	0.00

The effectiveness of the tool was obtained for only 1 stage, and DCET was 0.65±0.25. According to Table 4.3, this DCET shows that the tool delivers great performance, and is effective in communicating design solutions to users. The evaluation results on each assessment dimension are demonstrated in Figure 9.9. As can be seen, the tool can deliver high performance on all the dimensions. It is also immersive as shown in Section 7.6.2, indicating that users can focus on their tasks to produce higher quality solutions. Overall, it can be said that the tool is valid for its intended uses defined by concept selection (Chapter 7).

Overall, this chapter developed a simple test bed for concept selection. It is not ready for commercial product design. The computation time for the DP generation and display was around 0.1 s (was run on a 64-bit operating system on a personal computer with CPU of Core i5 3.30 GHz and RAM of 8 GB). The short time of 0.1 s shows that the real-time interactive performance was achieved with 10 fps.

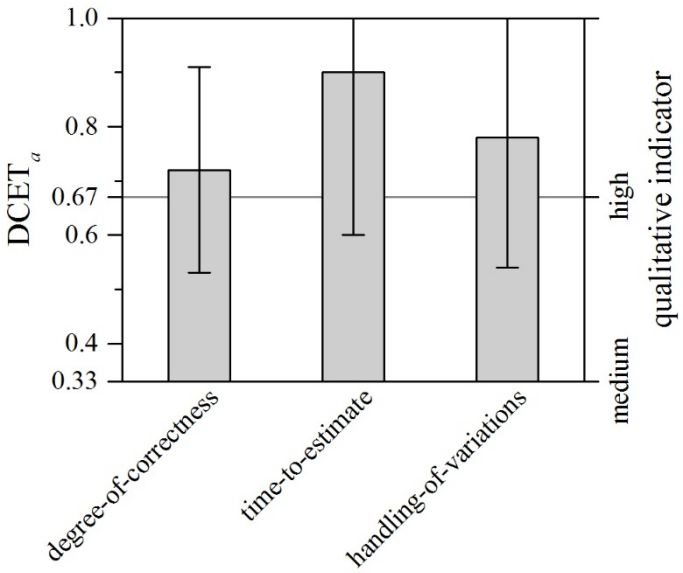

Figure 9.9 DCET of the tool on the assessment dimensions

Chapter 10 Conclusions and recommendations

This thesis developed a framework for concept validation by using digital prototyping and quantitative feedback. The framework aimed to identify the best product concept by using user feedback on the specification values and design solutions. The framework involves users at two stages before concept generation and at concept selection. For these two stages, two methodologies, namely specification solicitation and concept selection, were devised to deal with the large number of specification values and the big space of design solutions respectively. Both methodologies utilized adaptive sampling to represent the specification values and design solutions to users, and statistical hypothesis test to analyze user feedback. To implement the methodologies, a tool based on digital prototyping was created. A novel method was developed to build real-time virtual grasping and manipulation of DPs with the hand. To validate the proposed system, hand-held electronic consumer products, such as smartphones were considered for the case studies. We focused on the form, size, weight, and talk-time of the smartphones because of their impacts on the users' purchasing decisions.

The framework defined the general functionality of the concept validation using digital prototyping and quantitative feedback. In a case study on the size of the front face of smartphones, we showed that the framework could identify the best size. The identified best size was also evaluated by users, and it scored eight out of ten points. This shows the capability of the framework in identification of the best specification values. Besides, this score was 1.41 times higher than the score of the best size identified by utilizing physical prototyping and qualitative feedback (Figure 3.5-c, Section 3.5.3). Thus, digital prototyping and quantitative feedback are the better choices for the framework.

Specification solicitation was one of the major contributions of this thesis. It identifies the highest quality values of technical specifications before concept generation. This can be an interesting topic because the majority of the existing studies targeted 'setting final specification' stage to optimize the values, while we attempted to perform it at the early conceptual design to pass the highest quality values to concept generation. Specification solicitation can be essentially influential to the development of a quality product concept, and has not been done on large number of specifications. A case study was done on the values of width, height, depth, weight, and talk-time of smartphones. The results provided clear evidence that

the methodology could successfully determine the highest quality values of these five specifications. It was shown that the methodology could deal with five technical specifications while reducing the user fatigue (Section 6.4), whereas, the existing studies have not generally gone beyond two specifications because of encountering the fatigue [35, 36]. By specification solicitation, designers can focus on the highest quality specification values and put in more efforts to generating design solutions with these specification values. This boosts the productivity at concept generation, and results in a space of higher quality design solutions. To prevent user fatigue, the methodology considers user feedback on the values of single and paired technical specifications. However, it is possible that the correlation between more than two specifications be influential to the quality. Further study is needed to incorporate larger combinations of specifications into the methodology, and we plan to start with three-combinations.

Concept selection is based on a novel approach that allows a user to produce a solution complying with his/her expectation of a quality solution. In contrast, the traditional approach allows a user to choose a solution from a set of produced ones. Our methodology decomposes the generated solutions into several parameters and allows users to set the values of the parameters. In a case study, we attempted to identify the highest quality smartphone with respect to the form, size, weight, and talk-time by using our methodology and an IGA method [20], which was one of the recently-revealed methods and utilized by the French carmaker Renault. Our methodology and IGA method identified almost similar clusters of the best design solutions. In comparison with IGA, our methodology achieved 42% greater similarity in the solutions of each cluster, and 16% greater dissimilarity between the solutions of the clusters (Figure 7.6 and Figure 7.7). The centroid of each cluster was considered as the selected design solution. The centroids by our methodology scored 1.55 more points than those by the IGA method (Figure 7.9). Besides, the methodology helped users produce their quality solutions about four times faster, and prevented fatigue more effectively. Overall, our methodology outperformed the IGA method in terms of identification of the highest quality solutions. Aggregation of the users' quality solutions (the centroid method was used in our case study) to develop a quality one is a critical task. Although our methodology led to much more similar solutions in each cluster, the aggregation can still be critical. As a future work, we aim to work towards the aggregation.

The proposed methodologies were tested in the case studies of enhancing the existing designs. It was shown that the methodologies were effective in helping to generate the designs that evoke users' satisfaction. For new designs quite different from old ones, we did not perform any study. We think that for these new designs, the proposed methodologies can be utilized when physical characteristics of the new designs and range of their values are set. Then, the methodologies help to identify the best values of the characteristics for the new designs. It should be noted that this could be achieved if involved users are able to understand the new designs through interactions with digital prototypes since the methodologies utilize digital prototyping to render a design to users.

Incorporation of the variance into the feedback analysis was the other significant contribution of this thesis. A process was proposed for the analysis. In a case study (Section 5.2), we compared the results of our process and methods considering the mean values as the quality of solutions. User feedback on 16 samples of the size of the front face of the smartphones was collected, and by using the data of 12 samples, the quality of the other four samples were estimated. By using the paired *t*-test, strong evidence was found to support that the mean values cannot provide sufficient information to estimate the quality. In contrast, it was supported that our process successfully estimated the quality. However, when the number of the samples grows, the process becomes computationally expensive and time-consuming. As a future work, we aim to cluster the samples according to the mean values of their feedback, and go through the process for each cluster.

A tool based on digital prototyping was created to implement the methodologies. A novel method was pioneered to build virtual grasping and manipulation in virtual environment. It was shown that the method is valid for building the interactions. It was also demonstrated that the tool immerses users in the environment and helps users understand the design solutions and estimate the specification values correctly and quickly. The tool has the potential to incorporate digital models of the visual properties of color and texture. As a future work, we aim to incorporate these models in the tool. Moreover, for building the user-DP interactions, the devised method only requires a web-camera and a 2D digital screen, which are offered by personal machines such as laptops, tablets, and smartphones. Another future work can focus on reducing the computation cycles of the method so as to build the interactions on the users' machines. Thus, users can be involved in concept validation through the networks, leading to more user feedback for concept validation. Therefore, digital

prototyping is superior to 3D printing and physical prototyping for implementation of the methodologies since more user feedback can be collected. More feedback helps to identify better design solution.

Overall, conclusive evidence was provided that the framework can deal with large number of specifications and solutions, and yields the product concepts that effectively fulfill the user needs. Before concept generation, the framework identified the best targets for a large number of specifications. At concept selection, the framework identified the best solutions from the big space of design solutions. Besides, it prevented user fatigue by using the developed methodologies and tool.

Bibliography

[1] Ulrich, K.T. and S.D. Eppinger. (5th ed). Product Design and Development. pp. 415, New York: McGraw-Hill/Irwin. 2012.

[2] Arastehfar, S., Y. Liu, and W.F. Lu. On Design Concept Validation through Prototyping: Challenges and Opportunities. In Proc. 19th International Conference on Engineering Design (ICED13), Design for Harmonies, Vol. 6: Design Information and Knowledge, August 2013, Seoul, Korea, pp. 119-128.

[3] Kurakawa, K. A Scenario-Driven Conceptual Design Information Model and Its Formation, Research in Engineering Design, *15*(2), pp. 122-137. 2004.

[4] Reid, T.N., E.F. MacDonald, and P. Du. Impact of Product Design Representation on Customer Judgment, Journal of Mechanical Design, *135*(9), pp. 091008-091020. 2013.

[5] Maropoulos, P.G. and D. Ceglarek. Design Verification and Validation in Product Lifecycle, CIRP Annals - Manufacturing Technology, *59*(2), pp. 740-759. 2010.

[6] Kortler, S., A. Kohn, and U. Lindemann. Validation of Product Properties Considering a High Variety of Complex Products. In Proc. International Design Conference - Design, May 2012, Dubrovnik, Croatia, pp. 1731-1740.

[7] Tseng, K.C. and I.-T. Pu. A Novel Integrated Model to Increase Customer Satisfaction, Journal of Industrial and Production Engineering, *30*(6), pp. 373-380. 2013.

[8] Arastehfar, S., Y. Liu, and W.F. Lu. A Framework for Concept Validation in Product Design Using Digital Prototyping, Journal of Industrial and Production Engineering, *31*(5), pp. 286-302. 2014.

[9] Tseng, M.M. and X. Du. Design by Customers for Mass Customization Products, CIRP Annals - Manufacturing Technology, *47*(1), pp. 103-106. 1998.

[10] Ninan, J.A. and Z. Siddique. Internet-Based Framework to Support Integration of Customer in the Design of Customizable Products, Concurrent Engineering Research and Applications, *14*(3), pp. 245-256. 2006.

[11] Curtis, S.K., B.J. Hancock, and C.A. Mattson. Usage Scenarios for Design Space Exploration with a Dynamic Multiobjective Optimization Formulation, Research in Engineering Design, *24*(4), pp. 395-409. 2013.

[12] Piela, P., B. Katzenberg, and R. McKelvey. Integrating the User into Research on Engineering Design Systems, Research in Engineering Design, *3*(4), pp. 211-221. 1992.

[13] Tian, Y.Q., D.L. Thurston, and J.V. Carnahan. Incorporating End-User's Attitudes Towards Uncertainty into an Expert System, Journal of Mechanical Design, *116*(2), pp. 493-500. 1994.

[14] Campbell, R., et al. Design Evolution through Customer Interaction with Functional Prototypes, Journal of Engineering Design, *18*(6), pp. 617-635. 2007.

[15] Hsu, S.H., M.C. Chuang, and C.C. Chang. A Semantic Differential Study of Designers' and Users' Product Form Perception, International Journal of Industrial Ergonomics, *25*(4), pp. 375-391. 2000.

[16] Reid, T.N., B.D. Frischknecht, and P.Y. Papalambros. Perceptual Attributes in Product Design: Fuel Economy and Silhouette-Based Perceived Environmental Friendliness Tradeoffs in Automotive Vehicle Design, Journal of Mechanical Design, *134*(4), pp. 041006-041015. 2012.

[17] Chen, C.-H. and W. Yan. An in-Process Customer Utility Prediction System for Product Conceptualisation, Expert Systems with Applications, *34*(4), pp. 2555-2567. 2008.

[18] Ren, Y. and P.Y. Papalambros. A Design Preference Elicitation Query as an Optimization Process, Journal of Mechanical Design, *133*(11), pp. 111004-111013. 2011.

[19] Tovares, N., P. Boatwright, and J. Cagan. Experiential Conjoint Analysis: An Experience-Based Method for Eliciting, Capturing, and Modeling Consumer Preference, Journal of Mechanical Design, *136*(10), pp. 101404-101416. 2014.

[20] Poirson, E., et al. Eliciting User Perceptions Using Assessment Tests Based on an Interactive Genetic Algorithm, Journal of Mechanical Design, *135*(3), pp. 031004-031020. 2013.

[21] Li, H. The Role of Virtual Experience in Consumer Learning. PhD Thesis, Michigan State University. 2002.

[22] Stark, R., et al. Competing in Engineering Design—the Role of Virtual Product Creation, CIRP Journal of Manufacturing Science and Technology, *3*(3), pp. 175-184. 2010.

[23] Kan, H., V.G. Duffy, and C.-J. Su. An Internet Virtual Reality Collaborative Environment for Effective Product Design, Computers in Industry, *45*(2), pp. 197-213. 2001.

[24] Gironimo, G.D., A. Lanzotti, and A. Vanacore. Concept Design for Quality in Virtual Environment, Computers & Graphics, *30*(6), pp. 1011-1019. 2006.

[25] Crilly, N., J. Moultrie, and P.J. Clarkson. Shaping Things: Intended Consumer Response and the Other Determinants of Product Form, Design Studies, *30*(3), pp. 224-254. 2009.

[26] Ford, D.N. and D.K. Sobek. Adapting Real Options to New Product Development by Modeling the Second Toyota Paradox, Engineering Management, IEEE Transactions on, *52*(2), pp. 175-185. 2005.

[27] Zhang, Q., M.A. Vonderembse, and M. Cao. Product Concept and Prototype Flexibility in Manufacturing: Implications for Customer Satisfaction, European Journal of Operational Research, *194*(1), pp. 143-154. 2009.

[28] Choi, S.H. and H.H. Cheung. A Versatile Virtual Prototyping System for Rapid Product Development, Computers in Industry, *59*(5), pp. 477-488. 2008.

[29] Lu, S.-Y., M. Shpitalni, and R. Gadh. Virtual and Augmented Reality Technologies for Product Realization, CIRP Annals-Manufacturing Technology, *48*(2), pp. 471-495. 1999.

[30] Petiot, J.-F. and S. Grognet. Product Design: A Vectors Field-Based Approach for Preference Modelling, Journal of Engineering Design, *17*(03), pp. 217-233. 2006.

[31] Kulok, M. and K. Lewis. A Method to Ensure Preference Consistency in Multi-Attribute Selection Decisions, Journal of Mechanical Design, *129*(10), pp. 1002-1011. 2006.

[32] Maddulapalli, A.K. and S. Azarm. Product Design Selection with Preference and Attribute Variability for an Implicit Value Function, Journal of Mechanical Design, *128*(5), pp. 1027-1037. 2005.

[33] Artacho, M.A., A. Ballester, and E. Alcántara. Analysis of the Impact of Slight Changes in Product Formal Attributes on User's Emotions and Configuration of an Emotional Space for Successful Design, Journal of Engineering Design, *21*(6), pp. 693-705. 2009.

[34] Takagi, H. Interactive Evolutionary Computation: Fusion of the Capabilities of Ec Optimization and Human Evaluation, Proceedings of the IEEE, *89*(9), pp. 1275-1296. 2001.

[35] Villa, C. and R. Labayrade. Solving Complex Design Problems through Multiobjective Optimisation Taking into Account Judgements of Users, Research in Engineering Design, *25*(3), pp. 223-239. 2014.

[36] Kelly, J.C., et al. Incorporating User Shape Preference in Engineering Design Optimisation, Journal of Engineering Design, *22*(9), pp. 627-650. 2011.

[37] Artacho-Ramirez, M., J. Diego-Mas, and J. Alcaide-Marzal. Influence of the Mode of Graphical Representation on the Perception of Product Aesthetic and Emotional Features: An Exploratory Study, International Journal of Industrial Ergonomics, *38*(11), pp. 942-952. 2008.

[38] Kang, J., et al. Instant 3d Design Concept Generation and Visualization by Real-Time Hand Gesture Recognition, Computers in Industry, *64*(7), pp. 785-797. 2013.

[39] Lee, C.-S., S. Chun, and S.W. Park. Tracking Hand Rotation and Various Grasping Gestures from an Ir Camera Using Extended Cylindrical Manifold Embedding, Computer Vision and Image Understanding, *117*(12), pp. 1711-1723. 2013.

[40] Dominio, F., M. Donadeo, and P. Zanuttigh. Combining Multiple Depth-Based Descriptors for Hand Gesture Recognition, Pattern Recognition Letters, *50*, pp. 101-111. 2014.

[41] de La Gorce, M., D.J. Fleet, and N. Paragios. Model-Based 3d Hand Pose Estimation from Monocular Video, Pattern Analysis and Machine Intelligence, IEEE Transactions on, *33*(9), pp. 1793-1805. 2011.

[42] Yun, M.H., et al. Incorporating User Satisfaction into the Look-and-Feel of Mobile Phone Design, Ergonomics, *46*(13-14), pp. 1423-1440. 2003.

[43] Yoon, J., K. Kim, and T. Yoon. Are Lighter Smartphones Ergonomically Better?, 대한인간공학회지, *34*(1), pp. 11-18. 2015.

[44] Nanda, P., et al. Effect of Smartphone Aesthetic Design on Users' Emotional Reaction: An Empirical Study, The TQM Journal, *20*(4), pp. 348-355. 2008.

[45] Ling, M. and P. Yuan. An Empirical Research: Consumer Intention to Use Smartphone Based on Consumer Innovativeness. In Proc. Consumer Electronics, Communications and Networks (CECNet), 2012 2nd International Conference on, 2012, pp. 2368-2371.

[46] Arastehfar, S., Y. Liu, and W.F. Lu. An Evaluation Methodology for Design Concept Communication Using Digital Prototypes, Journal of Mechanical Design. Accepted to.

[47] Okazaki, S. and F. Mendez. Exploring Convenience in Mobile Commerce: Moderating Effects of Gender, Computers in Human Behavior, *29*(3), pp. 1234-1242. 2013.

[48] Wu, C.-M., Portable Wireless Charging Apparatus and System, 2014, Google Patents.

[49] Sylcott, B., J. Cagan, and G. Tabibnia. Understanding Consumer Tradeoffs between Form and Function through Metaconjoint and Cognitive Neuroscience Analyses, Journal of Mechanical Design, *135*(10), pp. 101002-101015. 2013.

[50] Arastehfar, S., Y. Liu, and W.F. Lu. On Design Concept Validation through Prototyping: Challenges and Opportunities. In Proc. DS 75-6: Proceedings of the 19th International Conference on Engineering Design (ICED13), Design for Harmonies, Vol. 6: Design Information and Knowledge, Seoul, Korea, 19-22.08. 2013, 2013,

[51] Virzi, R.A., J.L. Sokolov, and D. Karis. Usability Problem Identification Using Both Low-and High-Fidelity Prototypes. In Proc. Proceedings of the SIGCHI Conference on Human Factors in Computing Systems, 1996, pp. 236-243.

[52] Thomke, S.H. The Role of Flexibility in the Development of New Products: An Empirical Study, Research Policy, *26*(1), pp. 105-119. 1997.

[53] Sauer, J. and A. Sonderegger. The Influence of Prototype Fidelity and Aesthetics of Design in Usability Tests: Effects on User Behaviour, Subjective Evaluation and Emotion, Applied Ergonomics, *40*(4), pp. 670-677. 2009.

[54] Fontana, M., C. Rizzi, and U. Cugini. 3d Virtual Apparel Design for Industrial Applications, Computer-Aided Design, *37*(6), pp. 609-622. 2005.

[55] Gyi, D., R. Cain, and I. Campbell. The Value of Computer-Based Product Representations in Co-Designing with Older Users, Journal of Engineering Design, *21*(2-3), pp. 305-313. 2009.

[56] Söderman, M. Virtual Reality in Product Evaluations with Potential Customers: An Exploratory Study Comparing Virtual Reality with Conventional Product Representations, Journal of Engineering Design, *16*(3), pp. 311-328. 2005.

[57] Iansiti, M. and A. MacCormack. Developing Products on Internet Time, Harvard Business Review, *75*(5), pp. 108-117. 1996.

[58] Eisenhardt, K.M. and B.N. Tabrizi. Accelerating Adaptive Processes: Product Innovation in the Global Computer Industry, Administrative Science Quarterly, pp. 84-110. 1995.

[59] Takala, R. Product Demonstrator: A System for up-Front Testing of User-Related Product Features, Journal of Engineering Design, *16*(3), pp. 329-336. 2005.

[60] Barbieri, L., et al. Mixed Prototyping with Configurable Physical Archetype for Usability Evaluation of Product Interfaces, Computers in Industry, *64*(3), pp. 310-323. 2013.

[61] Kim, D.B. and K.H. Lee. Computer-Aided Appearance Design Based on Brdf Measurements, Computer-Aided Design, *43*(9), pp. 1181-1193. 2011.

[62] Orzechowski, M., et al. Alternate Methods of Conjoint Analysis for Estimating Housing Preference Functions: Effects of Presentation Style, Journal of Housing and the Built Environment, *20*(4), pp. 349-362. 2005.

[63] Kelly, J., P. Papalambros, and G. Wakefield. The Development of a Tool for the Preference Assessment of the Visual Aesthetics of an Object Using Interactive Genetic Algorithms. In Proc. 9th Generative Art Conference, GA, 2005,

[64] Qian, L. and D. Ben-Arieh. Joint Pricing and Platform Configuration in Product Family Design with Genetic Algorithm. In Proc. ASME International Design Engineering Technical Conferences and Computers and Information in Engineering Conference, August 2009, San Diego, California, USA, pp. 49-58.

[65] Kelly, J. and P. Papalambros. Use of Shape Preference Information in Product Design. In Proc. International Conference on Engineering Design (ICED07), August 2007, Paris, France, pp. 803-814.

[66] Machwe, A.T., I.C. Parmee, and J.C. Miles. Integrating Aesthetic Criteria with a User-Centric Evolutionary System Via a Component-Based Design Representation. In Proc. International Conference on Engineering Design (ICED05), 2005,

[67] Stewart, T.J. A Critical Survey on the Status of Multiple Criteria Decision Making Theory and Practice, Omega, *20*(5), pp. 569-586. 1992.

[68] Lim, J. Hedonic Scaling: A Review of Methods and Theory, Food Quality and Preference, *22*(8), pp. 733-747. 2011.

[69] Fukuda, S. and Y. Matsuura. Prioritizing the Customer's Requirements by Ahp for Concurrent Design, ASME DES ENG DIV PUBL DE., ASME, NEW YORK, NY(USA), 1993, *52*, pp. 13-19. 1993.

[70] Beynon, M., B. Curry, and P. Morgan. The Dempster–Shafer Theory of Evidence: An Alternative Approach to Multicriteria Decision Modelling, Omega, *28*(1), pp. 37-50. 2000.

[71] Davis, L. and G. Williams. Evaluating and Selecting Simulation Software Using the Analytic Hierarchy Process, Integrated Manufacturing Systems, *5*(1), pp. 23-32. 1994.

[72] Scott, M.J. and I. Zivkovic. On Rank Reversals in the Borda Count. In Proc. ASME International Design Engineering Technical Conferences and Computers and Information in Engineering Conference, September 2003, pp. 795-803.

[73] See, T.-K., A. Gurnani, and K. Lewis. Multi-Attribute Decision Making Using Hypothetical Equivalents and Inequivalents, Journal of Mechanical Design, *126*(6), pp. 950-958. 2004.

[74] Yan, W., C.-H. Chen, and M.-D. Shieh. Product Concept Generation and Selection Using Sorting Technique and Fuzzy C-Means Algorithm, Computers & Industrial Engineering, *50*(3), pp. 273-285. 2006.

[75] Hsiao, S.-W., F.-Y. Chiu, and S.-H. Lu. Product-Form Design Model Based on Genetic Algorithms, International Journal of Industrial Ergonomics, *40*(3), pp. 237-246. 2010.

[76] Orsborn, S., J. Cagan, and P. Boatwright. Quantifying Aesthetic Form Preference in a Utility Function, Journal of Mechanical Design, *131*(6), pp. 061001-061011. 2009.

[77] Green, P.E. and V. Srinivasan. Conjoint Analysis in Marketing: New Developments with Implications for Research and Practice, The Journal of Marketing, *54*(4), pp. 3-19. 1990.

[78] Wassenaar, H.J. and W. Chen. An Approach to Decision-Based Design with Discrete Choice Analysis for Demand Modeling, Journal of Mechanical Design, *125*(3), pp. 490-497. 2003.

[79] Michalek, J.J., F.M. Feinberg, and P.Y. Papalambros. Linking Marketing and Engineering Product Design Decisions Via Analytical Target Cascading*, Journal of Product Innovation Management, *22*(1), pp. 42-62. 2005.

[80] Chang, J.J. and J.D. Carroll. How to Use Prefmap and Prefmap-2 {Programs Which Relate Preference Data to Multidimensional Scaling Solutions, Unpublished manuscript, Bell Telephone Labs, Murray Hill, NJ. 1972.

[81] Huber, J. Ideal Point Models of Preference, Advances in Consumer Research, Jg, *3*(1), pp. 138-142. 1976.

[82] Coello, C.C., G.B. Lamont, and D.A. Van Veldhuizen. Evolutionary Algorithms for Solving Multi-Objective Problems: Springer Science & Business Media. 2007.

[83] Scott, M.J. and E.K. Antonsson. Aggregation Functions for Engineering Design Trade-Offs, Fuzzy sets and systems, *99*(3), pp. 253-264. 1998.

[84] Otto, K.N. and E.K. Antonsson. Trade-Off Strategies in Engineering Design, Research in Engineering Design, *3*(2), pp. 87-103. 1991.

[85] Eschnauer, H., J. Koski, and A. Osyczka. Multicriteria Design Optimization: Procedures and Application, Berlin: Springer-Verlag Berlin. 1990.

[86] Scott, M.J. and E.K. Antonsson. Compensation and Weights for Trade-Offs in Engineering Design: Beyond the Weighted Sum, Journal of Mechanical Design, *127*(6), pp. 1045-1055. 2005.

[87] Keeney, R.L. and H. Raiffa. Decisions with Multiple Objectives: Preferences and Value Trade-Offs. pp. 569, UK: Cambridge university press. 1993.

[88] Tsai, H.-C., S.-W. Hsiao, and F.-K. Hung. An Image Evaluation Approach for Parameter-Based Product Form and Color Design, Computer-Aided Design, *38*(2), pp. 157-171. 2006.

[89] Wenfeng, L., W. Zhenyu, and C. Dingfang. Modeling and Simulation of Product's Surface Design, Computers & Industrial Engineering, *46*(2), pp. 267-273. 2004.
[90] Huang, S.-H., Y.-I. Yang, and C.-H. Chu. Human-Centric Design Personalization of 3d Glasses Frame in Markerless Augmented Reality, Advanced Engineering Informatics, *26*(1), pp. 35-45. 2012.
[91] Bruno, F. and M. Muzzupappa. Product Interface Design: A Participatory Approach Based on Virtual Reality, International Journal of Human-Computer Studies, *68*(5), pp. 254-269. 2010.
[92] Bordegoni, M., G. Colombo, and L. Formentini. Haptic Technologies for the Conceptual and Validation Phases of Product Design, Computers & Graphics, *30*(3), pp. 377-390. 2006.
[93] emercedesbenz. Design of the 2007 Mercedes S-Class. 2007; Available from: http://www.emercedesbenz.com/Apr06/18DesignOfThe2007MercedesSClass.html.
[94] Bao, J.S., et al. Immersive Virtual Product Development, Journal of Materials Processing Technology, *129*(1–3), pp. 592-596. 2002.
[95] Nee, A.Y.C., et al. Augmented Reality Applications in Design and Manufacturing, CIRP Annals - Manufacturing Technology, *61*(2), pp. 657-679. 2012.
[96] Bogaert, L., et al. Stereoscopic Projector for Polarized Viewing with Extended Color Gamut, Displays, *31*(2), pp. 73-81. 2010.
[97] Ng, L.X., et al. Garde: A Gesture-Based Augmented Reality Design Evaluation System, International Journal on Interactive Design and Manufacturing, *5*(2), pp. 85-94. 2011.
[98] Stark, R., J.H. Israel, and T. Wöhler. Towards Hybrid Modelling Environments—Merging Desktop-Cad and Virtual Reality-Technologies, CIRP Annals - Manufacturing Technology, *59*(1), pp. 179-182. 2010.
[99] Israel, J.H., et al. Investigating Three-Dimensional Sketching for Early Conceptual Design—Results from Expert Discussions and User Studies, Computers & Graphics, *33*(4), pp. 462-473. 2009.
[100] Dorman, J. and A. Rockwood. Surface Design Using Hand Motion with Smoothing, Computer-Aided Design, *33*(5), pp. 389-402. 2001.
[101] Fuge, M., et al. Conceptual Design and Modification of Freeform Surfaces Using Dual Shape Representations in Augmented Reality Environments, Computer-Aided Design, *44*(10), pp. 1020-1032. 2012.
[102] Leu, M.C., et al. Creation of Freeform Solid Models in Virtual Reality, CIRP Annals - Manufacturing Technology, *50*(1), pp. 73-76. 2001.
[103] Ho, M.-F., et al. A Multi-View Vision-Based Hand Motion Capturing System, Pattern Recognition, *44*(2), pp. 443-453. 2011.
[104] Erol, A., et al. Vision-Based Hand Pose Estimation: A Review, Computer Vision and Image Understanding, *108*(1–2), pp. 52-73. 2007.
[105] Allen, N.A., C.A. Shaffer, and L.T. Watson. Building Modeling Tools That Support Verification, Validation, and Testing for the Domain Expert. In Proc. 37th conference on Winter simulation, December 2005, Orlando, FL, pp. 419-426.
[106] Babuska, I. and J.T. Oden. Verification and Validation in Computational Engineering and Science: Basic Concepts, Computer Methods in Applied Mechanics and Engineering, *193*(36), pp. 4057-4066. 2004.
[107] Sargent, R.G. Verification and Validation of Simulation Models. In Proc. 37th conference on Winter simulation, December 2005, Orlando, FL, pp. 130-143.
[108] ISO. 9000: Quality Management Systems. Fundamentals and Vocabulary, British Standards Institution. 2005.

[109] Geraci, A., et al. Ieee Standard Computer Dictionary: Compilation of Ieee Standard Computer Glossaries: IEEE Press. 1991.
[110] JCGM. The International Vocabulary of Metrology—Basic and General Concepts and Associated Terms (Vim), 3rd Edn., Joint Committee for Guides in Metrology. 2008.
[111] Global Harmonization Task Force, Quality Management System–Process Validation Guidance, 2nd Ed., 2004.
[112] ARPa SAE Aerospace. Aerospace Recommended Practice. 2009.
[113] Cross, N., Design and Designing, 2006, Milton Keynes: The Open University.
[114] Manufacture Materials Design, 2001, Milton Keynes: The Open University.
[115] Sarkar, P. and A. Chakrabarti. Ideas Generated in Conceptual Design and Their Effects on Creativity, Research in Engineering Design, *25*(3), pp. 185-201. 2014.
[116] Woodbury, R., S. Datta, and A. Burrow, Erasure in Design Space Exploration, in Artificial Intelligence in Design'00521-543, Springer, 2000.
[117] Dyn, N., D. Levin, and S. Rippa. Data Dependent Triangulations for Piecewise Linear Interpolation, IMA journal of numerical analysis, *10*(1), pp. 137-154. 1990.
[118] Henderson, M.R., Representing Functionality and Design Intent in Product Models, in 2nd ACM symposium on Solid modeling and applications1993, ACM: Montreal, Quebec, Canada. p. 387-396.
[119] Desmet, P.M. and P. Hekkert. Framework of Product Experience, International Journal of Design, *1*(1), pp. 57-66. 2007.
[120] Maier, A.M. A Grid-Based Assessment Method of Communication in Engineering Design, Unpublished doctoral dissertation, University of Cambridge, Cambridge, UK. 2007.
[121] Crilly, N., A.M. Maier, and P.J. Clarkson. Representing Artefacts as Media: Modelling the Relationship between Designer Intent and Consumer Experience, International Journal of Design, *2*(3), pp. 15-27. 2008.
[122] Maier, A.M. and M. Kleinsmann. Studying and Supporting Design Communication, Artificial Intelligence for Engineering Design, Analysis and Manufacturing, *27*(02), pp. 87-90. 2013.
[123] Agost, M.-J. and M. Vergara. Relationship between Meanings, Emotions, Product Preferences and Personal Values. Application to Ceramic Tile Floorings, Applied Ergonomics, *45*(4), pp. 1076-1086. 2014.
[124] Crilly, N., J. Moultrie, and P.J. Clarkson. Seeing Things: Consumer Response to the Visual Domain in Product Design, Design studies, *25*(6), pp. 547-577. 2004.
[125] Gonzales, R.C. and R. Woods. Digital Image Processing. pp. 681. 2002.
[126] Nilsson, J. and J. Siponen. Challenging the Hci Concept of Fidelity by Positioning Ozlab Prototypes. In Proc. 2006, pp. 349-360.
[127] Kuhfeld, W.F. Conjoint Analysis, SAS Tech. Pap., pp. 681-801. 2010.
[128] Kalish, S. and P. Nelson. A Comparison of Ranking, Rating and Reservation Price Measurement in Conjoint Analysis, Marketing Letters, *2*(4), pp. 327-335. 1991.
[129] Allenby, G.M., N. Arora, and J.L. Ginter. Incorporating Prior Knowledge into the Analysis of Conjoint Studies, Journal of Marketing Research, pp. 152-162. 1995.
[130] Louviere, J.J. Conjoint Analysis Modelling of Stated Preferences: A Review of Theory, Methods, Recent Developments and External Validity, Journal of Transport Economics and Policy, pp. 93-119. 1988.

[131] Hsee, C.K., et al. Specification Seeking: How Product Specifications Influence Consumer Preference, Journal of Consumer Research, *35*(6), pp. 952-966. 2009.
[132] Jiang, H., et al. A Methodology of Integrating Affective Design with Defining Engineering Specifications for Product Design, International Journal of Production Research, *53*(8), pp. 2472-2488. 2015.
[133] Pál, L., R. Oláh-Gál, and Z. Makó. Shepard Interpolation with Stationary Points, Acta Univ Sapientiae, Informatica, *1*(1), pp. 5-13. 2009.
[134] Guyon, H. and J.-F. Petiot. Market Share Predictions: A New Model with Rating-Based Conjoint Analysis, International Journal of Market Research, *53*(6), pp. 831-857. 2011.
[135] Wassenaar, H.J., et al. Enhancing Discrete Choice Demand Modeling for Decision-Based Design, Journal of Mechanical Design, *127*(4), pp. 514-523. 2005.
[136] Hooley, G. Multidimensional Scaling of Consumer Perceptions and Preferences, European Journal of Marketing, *14*(7), pp. 436-448. 1980.
[137] SANTA, C., et al. Descriptive Analysis, Consumer Clusters and Preference Mapping of Commercial Mayonnaise in Argentina, Journal of sensory studies, *17*(4), pp. 309-325. 2002.
[138] Toubia, O., J.R. Hauser, and D.I. Simester. Polyhedral Methods for Adaptive Choice-Based Conjoint Analysis, Journal of Marketing Research, *41*(1), pp. 116-131. 2004.
[139] Swait, J. and W. Adamowicz. The Influence of Task Complexity on Consumer Choice: A Latent Class Model of Decision Strategy Switching, Journal of Consumer Research, *28*(1), pp. 135-148. 2001.
[140] Tseng, I., J. Cagan, and K. Kotovsky. Learning Stylistic Desires and Generating Preferred Designs of Consumers Using Neural Networks and Genetic Algorithms. In Proc. ASME International Design Engineering Technical Conferences and Computers and Information in Engineering Conference (IDETC/CIE), January 2011, Washington, DC, pp. 601-607.
[141] Gong, D., Y. Zhou, and T. Li. Cooperative Interactive Genetic Algorithm Based on User's Preference, International Journal of Information Technology, *11*(10), pp. 1-10. 2005.
[142] Hair, J.F., et al. Multivariate Data Analysis: Pearson Prentice Hall Upper Saddle River, NJ. 2006.
[143] Gu, Z., M. Xi Tang, and J.H. Frazer. Capturing Aesthetic Intention During Interactive Evolution, Computer-Aided Design, *38*(3), pp. 224-237. 2006.
[144] Yannou, B., M. Dihlmann, and R. Awedikian. Evolutive Design of Car Silhouettes. In Proc. ASME International Design Engineering Technical Conferences and Computers and Information in Engineering Conference, August 2008, Brooklyn, New York, USA, pp. 15-24.
[145] Kelly, J.C. Interactive Genetic Algorithms for Shape Preference Assessment in Engineering Design. PhD Thesis, University of Michigan. 2008.
[146] Feng, Z., et al. Real-Time Oriented Behavior-Driven 3d Freehand Tracking for Direct Interaction, Pattern Recognition, *46*(2), pp. 590-608. 2013.
[147] Romero, J., et al. Non-Parametric Hand Pose Estimation with Object Context, Image and Vision Computing, *31*(8), pp. 555-564. 2013.
[148] Prisacariu, V.A. and I. Reid. 3d Hand Tracking for Human Computer Interaction, Image and Vision Computing, *30*(3), pp. 236-250. 2012.
[149] Lu, S., et al. Using Multiple Cues for Hand Tracking and Model Refinement. In Proc. Computer Vision and Pattern Recognition, IEEE Computer Society Conference on, June 2003, pp. II-443-50.
[150] Morshidi, M. and T. Tjahjadi. Gravity Optimised Particle Filter for Hand Tracking, Pattern Recognition, *47*(1), pp. 194-207. 2014.

[151] Kirac, F., Y.E. Kara, and L. Akarun. Hierarchically Constrained 3d Hand Pose Estimation Using Regression Forests from Single Frame Depth Data, Pattern Recognition Letters, *50*, pp. 91-100. 2013.
[152] Ge, S.S., Y. Yang, and T.H. Lee. Hand Gesture Recognition and Tracking Based on Distributed Locally Linear Embedding, Image and Vision Computing, *26*(12), pp. 1607-1620. 2008.
[153] Shen, X., et al. Dynamic Hand Gesture Recognition: An Exemplar-Based Approach from Motion Divergence Fields, Image and Vision Computing, *30*(3), pp. 227-235. 2012.
[154] Li, Y.-T. and J.P. Wachs. Hegm: A Hierarchical Elastic Graph Matching for Hand Gesture Recognition, Pattern Recognition, *47*(1), pp. 80-88. 2014.
[155] Bray, M., E. Koller-Meier, and L. Van Gool. Smart Particle Filtering for High-Dimensional Tracking, Computer Vision and Image Understanding, *106*(1), pp. 116-129. 2007.
[156] Premaratne, P., S. Ajaz, and M. Premaratne. Hand Gesture Tracking and Recognition System Using Lucas–Kanade Algorithms for Control of Consumer Electronics, Neurocomputing, *116*(0), pp. 242-249. 2013.
[157] Chen, F.-S., C.-M. Fu, and C.-L. Huang. Hand Gesture Recognition Using a Real-Time Tracking Method and Hidden Markov Models, Image and Vision Computing, *21*(8), pp. 745-758. 2003.
[158] Li, Y.-T. and J.P. Wachs. Recognizing Hand Gestures Using the Weighted Elastic Graph Matching (Wegm) Method, Image and Vision Computing, *31*(9), pp. 649-657. 2013.
[159] Padam Priyal, S. and P.K. Bora. A Robust Static Hand Gesture Recognition System Using Geometry Based Normalizations and Krawtchouk Moments, Pattern Recognition, *46*(8), pp. 2202-2219. 2013.
[160] MoD Std 00-25-17, Human Factors for Designers of Systems: Personnel Domain -Technical Guidance and Data, in Defence Standard 00-25 Part 17, Issue 12004, UK Ministry of Defence.
[161] Illingworth, J. and J. Kittler. A Survey of the Hough Transform, Computer vision, graphics, and image processing, *44*(1), pp. 87-116. 1988.
[162] Leavers, V.F. Shape Detection in Computer Vision Using the Hough Transform: Springer. 1992.
[163] Duda, R.O. and P.E. Hart. Use of the Hough Transformation to Detect Lines and Curves in Pictures, Communications of the ACM, *15*(1), pp. 11-15. 1972.

Appendix A The aggregation function *F*

The first differential of the aggregation function F is obtained, (A.1). The partial differentials of F_{DC}, F_{TE}, and F_{HV} with respect to D are less than zero because they are strictly monotonically decreasing. Besides, their coefficients are greater than zero. Thus, the summation of the weighted partial differentials is less than zero. Therefore, F is strictly monotonically decreasing with respect to D.

$$\begin{aligned}\frac{\partial F(D,t)}{\partial D} &= \left(w_{DC}\cdot w_{TE}\cdot F_{TE} + w_{HV}\cdot w_{DC}\cdot F_{HV}\right)\frac{\partial F_{DC}}{\partial D} \\ &+ \left(w_{TE}\cdot w_{HV}\cdot F_{HV} + w_{DC}\cdot w_{TE}\cdot F_{DC}\right)\frac{\partial F_{TE}}{\partial D} \\ &+ \left(w_{HV}\cdot w_{DC}\cdot F_{DC} + w_{TE}\cdot w_{HV}\cdot F_{TE}\right)\frac{\partial F_{HV}}{\partial D} < 0\end{aligned} \tag{A.1}$$

According to (A.1), the higher $DCET_a$ at t results in the greater coefficients of the differentials. As such, to reach a specific DCET at $t+\Delta t$, the smaller increase in $DCET_a$ from t to $t+\Delta t$ will be required if the coefficients of the differentials become greater. Therefore, (4.2) indicates that the enhancement of user estimates at $t+\Delta t$ ($\Delta t>0$) can be larger if the user estimates are more correct at t.

Appendix B Relationships of smartphone parameters

A study was done on the values of p_1, p_2, p_3, p_9, and p_{10} of 15 smartphones in the market by the 3rd quarter of 2014 (Table B.1). A linear relationship was identified between p_9 and $p_1 \cdot p_2$ (Figure B.1). The line fits the data with R^2=0.8332.

Table B.1 The parameters and their values

smartphone	p_1 (mm)	p_2 (mm)	p_3 (mm)	p_9 (h)	p_{10} (g)
iPhone 6+	77.8	158.1	7.1	24	172
iPhone 6	67.0	138.1	6.9	14	129
iPhone 5S	58.6	123.8	7.6	10	112
iPhone 5C	59.2	124.4	9.0	10	132
Grand Prime	72.1	144.8	8.6	17	156
Galaxy S5	72.5	142.0	8.1	21	145
Grand 2	75.3	146.8	8.9	17	163
Galaxy S4	70.1	142.0	7.1	17	132
Lumia 1520	85.4	162.8	8.7	25	209
Lumia 1320	85.9	164.2	9.8	21	220
Lumia 1020	71.4	130.4	10.4	13.5	158
Xperia Z3	72.0	152.0	7.3	16	152
Xperia Z2	73.3	146.8	8.2	19	163
HTC One M8	70.6	146.4	9.4	20	160
HTC One	68.2	137.4	9.3	18	143

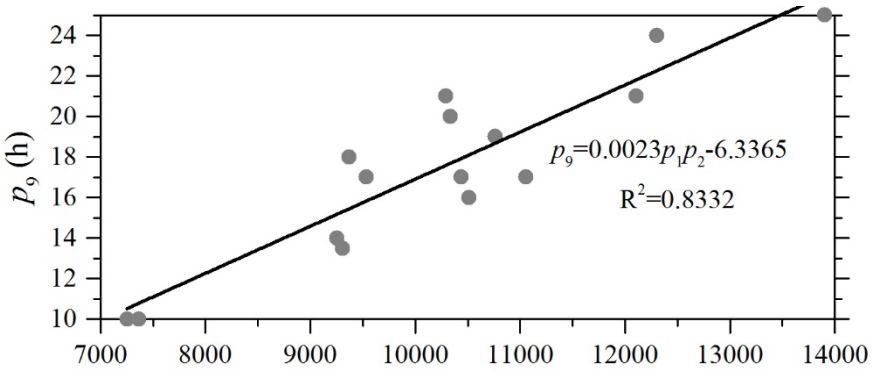

Figure B.1 The relationships between P_9 (talk-time) and P_1P_2

Regarding the weight, it was found that p_{10} and $p_1 \cdot p_2 \cdot p_3$ are also lying on a line (Figure B.2). The line fits the data with R^2=0.9094. These large R^2 show that the points are almost collinear, and the lines give the relationship.

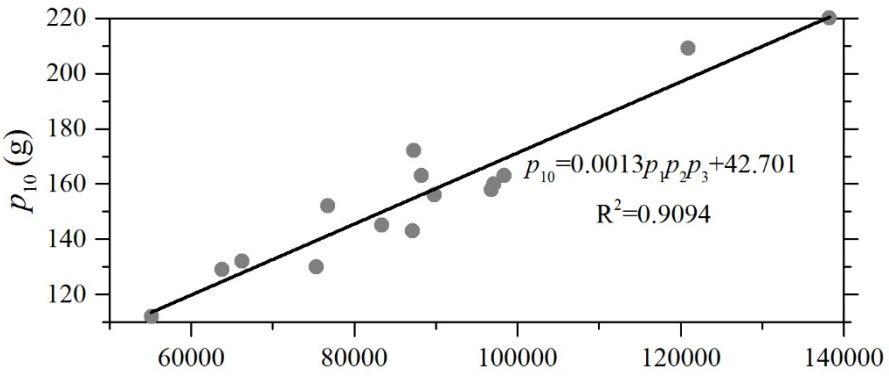

Figure B.2 The relationships between P_{10} (weight) and $P_1P_2P_3$

Appendix C Relationships between joint variables of the hand in grasping

We studied the movements of the joints at Z_1, Z_2, and Z_3 for grasping objects. Ten subjects participated in the study. They were asked to grasp 5 objects with L_{PF} equals to 50, 65, 80, 95, and 110 mm. The joints angles θ_1, θ_2, and θ_3 were measured. It was found that the joints are moving dependently, and there is a relationship between the joints angles (θ_1, θ_2, θ_3) when the hand grasps an object (Figure C.1). We considered $\theta_2 \approx 0.6\theta_1$ and $\theta_3 \approx 0.5\theta_1$.

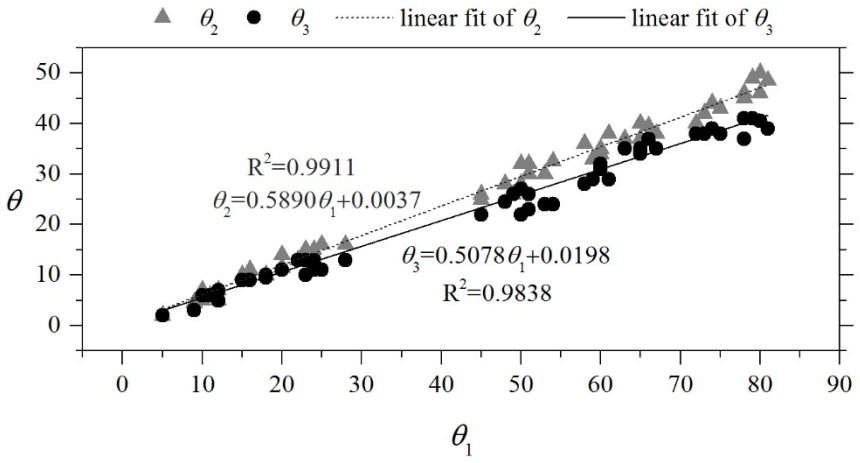

Figure C.1 The relationships between the joint variables

Appendix D Derivation of L_{PF} and proof of its one-to-one property

According to Denavit-Hartenberg convention, X, Y, and Z components of the point F is given by the transformation matrices in (D.1). The matrices are obtained based on the configuration in Figure 8.1. Table D.1 shows Denavit-Hartenberg parameters.

Table D.1 The Denavit-Hartenberg parameters

Link	theta (^{o})	offset (mm)	length of normal (mm)	alpha (^{o})
1	0	0	L	90
2	θ_1	0	L_1	0
3	θ_2	0	L_2	0
4	θ_3	0	L_3	0

$$
\begin{aligned}
{}^{XYZ}F &= {}^{XYZ}_{4}\mathbf{T}\ {}^{4}F = {}^{XYZ}_{1}\mathbf{T}\,{}^{1}_{2}\mathbf{T}\,{}^{2}_{3}\mathbf{T}\,{}^{3}_{4}\mathbf{T}\ {}^{4}F \\
&= \begin{bmatrix} 1 & 0 & 0 & L \\ 0 & 0 & -1 & 0 \\ 0 & 1 & 0 & 0 \\ 0 & 0 & 0 & 1 \end{bmatrix} \cdot \begin{bmatrix} \cos(\theta_1) & -\sin(\theta_1) & 0 & L_1\cos(\theta_1) \\ \sin(\theta_1) & \cos(\theta_1) & 0 & L_1\sin(\theta_1) \\ 0 & 0 & 1 & 0 \\ 0 & 0 & 0 & 1 \end{bmatrix} \\
&\cdot \begin{bmatrix} \cos(\theta_2) & -\sin(\theta_2) & 0 & L_2\cos(\theta_2) \\ \sin(\theta_2) & \cos(\theta_2) & 0 & L_2\sin(\theta_2) \\ 0 & 0 & 1 & 0 \\ 0 & 0 & 0 & 1 \end{bmatrix} \\
&\cdot \begin{bmatrix} \cos(\theta_3) & -\sin(\theta_3) & 0 & L_3\cos(\theta_3) \\ \sin(\theta_3) & \cos(\theta_3) & 0 & L_3\sin(\theta_3) \\ 0 & 0 & 1 & 0 \\ 0 & 0 & 0 & 1 \end{bmatrix} \cdot \begin{bmatrix} 0 \\ 0 \\ 0 \\ 1 \end{bmatrix} \\
&= \begin{bmatrix} L + L_1\cos(\theta_1) + L_2\cos(1.6\theta_1) + L_3\cos(2.1\theta_1) \\ 0 \\ L_1\sin(\theta_1) + L_2\sin(1.6\theta_1) + L_3\sin(2.1\theta_1) \\ 1 \end{bmatrix} = \begin{bmatrix} X_{PF} \\ 0 \\ Z_{PF} \\ 1 \end{bmatrix}
\end{aligned}
\tag{D.1}
$$

Therefore, L_{PF} is given by:

$$L_{PF}(\theta_1) = \sqrt{{X_{PF}}^2 + {Z_{PF}}^2} \tag{D.2}$$

The proof of the one-to-one property is given below:

$$
\begin{aligned}
L_{PF}(\varphi) &= \sqrt{X_{PF}{}^2 + Z_{PF}{}^2} \\
&= L^2 + L_1^2 + L_2^2 + L_3^2 \\
&\quad + 2L(L_1\cos(\varphi) + L_2\cos(1.6\varphi) + L_3\cos(2.1\varphi)) \\
&\quad + 2L_1L_2\cos(0.6\varphi) + 2L_2L_3\cos(0.5\varphi) + 2L_3L_1\cos(1.1\varphi)
\end{aligned}
\tag{D.3}
$$

Suppose: $L_{PF}(\varphi)=L_{PF}(\omega)$. Then:

$$
\begin{aligned}
\rightarrow\ & 2L(L_1\cos(\varphi) + L_2\cos(1.6\varphi) + L_3\cos(2.1\varphi)) + 2L_2L_3\cos(0.5\varphi) \\
& + 2L_1L_2\cos(0.6\varphi) + 2L_3L_1\cos(1.1\varphi) \\
& = \\
& 2L(L_1\cos(\omega) + L_2\cos(1.6\omega) + L_3\cos(2.1\omega)) + 2L_2L_3\cos(0.5\omega) \\
& + 2L_1L_2\cos(0.6\omega) + 2L_3L_1\cos(1.1\omega)
\end{aligned}
$$

$$
\begin{aligned}
\rightarrow\ & -4LL_1\sin\big(0.5(\varphi+\omega)\big)\sin\big(0.5(\varphi-\omega)\big) \\
& -4LL_2\sin\big(0.8(\varphi+\omega)\big)\sin\big(0.8(\varphi-\omega)\big) \\
& -4LL_3\sin\big(1.05(\varphi+\omega)\big)\sin\big(1.05(\varphi-\omega)\big) \\
& -4L_1L_2\sin\big(0.6(\varphi+\omega)\big)\sin\big(0.6(\varphi-\omega)\big) \\
& -4L_2L_3\sin\big(0.5(\varphi+\omega)\big)\sin\big(0.5(\varphi-\omega)\big) \\
& -4L_3L_1\sin\big(1.1(\varphi+\omega)\big)\sin\big(1.1(\varphi-\omega)\big) \\
& =0
\end{aligned}
\tag{D.4}
$$

Note that $0\le\varphi,\omega\le 80^{\circ}$. Then, if:

$$
\begin{cases}
\varphi=\omega \rightarrow \text{the above expression is zero} \\
\qquad\quad \text{the above expression cannot be zero} \\
\varphi\neq\omega \rightarrow \text{since all the sinus has the same sign and non-zero} \\
\qquad\quad \text{(one of the angles } (\varphi \text{ or } \omega) \text{ is non-zero).}
\end{cases}
\tag{D.5}
$$

Consequently, $L_{PF}(\varphi)=L_{PF}(\omega)$ if and only if $\varphi=\omega$. Therefore, the relationship between L_{PF} and θ_1 is one-to-one.

List of Publications

[1] **Arastehfar, S.**, W.F. Lu, and Y. Liu. An Evaluation Methodology for Design Concept Communication Using Digital Prototypes, accepted to Journal of Mechanical Design.

[2] **Arastehfar, S.**, Y. Liu, and W.F. Lu. A Framework for Concept Validation in Product Design Using Digital Prototyping, Journal of Industrial and Production Engineering, 31(5), pp. 286-302. 2014.

[3] **Arastehfar, S.**, Y. Liu, and W.F. Lu. On Design Concept Validation through Prototyping: Challenges and Opportunities. Proceeding of the 19th International Conference on Engineering Design (ICED13), Design for Harmonies, Vol. 6: Design Information and Knowledge, August 2013, Seoul, Korea, pp. 119-128.

[4] **Arastehfar, S.**, Y. Liu, and W.F. Lu. A New Discrete Event System Model for Supervising and Controlling Robotic Arm Path Tacking Tasks Based on Adaptive Masking. In Proc. ASME 2012 International Design Engineering Technical Conferences and Computers and Information in Engineering Conference, August 2012, Chicago, Illinois, USA, pp. 1217-1226.